2007

Assessment and Analysis of QuikSCAT and COAMPS Model Vector Wind Products for the Gulf of Mexico: A Long-Term and Hurricane Perspective

Neha Sharma
Louisiana State University and Agricultural and Mechanical College

ASSESSMENT AND ANALYSIS OF QUIKSCAT AND COAMPS MODEL VECTOR WIND PRODUCTS FOR THE GULF OF MEXICO: A LONG-TERM AND HURRICANE PERSPECTIVE

A Thesis

Submitted to the Graduate Faculty of the
Louisiana State University and
Agricultural and Mechanical College
in partial fulfillment of the
requirements for the degree of
Master in Science

in

The Department of Oceanography and Coastal Sciences

by
Neha Sharma
B.E., Pune University, 2005
December 2007

Acknowledgments

I would like to acknowledge the faculty, staff and graduate students of the Department of Oceanography and Coastal Sciences at Louisiana State University for contributing towards the success of this project. This project has been conducted as part of a NASA Decision Support through Earth Science Results funded project no. N06-4913. Partial funding is also acknowledged from a CMI-MMS service contract 1435-0104 CA 32806 to E. J. D'Sa.

I would like to thank Dr. Eurico J. D'Sa, my major professor, for giving me the opportunity to work on this project. His help and support has been invaluable throughout the course of this thesis. I would also like to thank my committee members Dr. Lawrence J. Rouse and Dr. Mark Benfield for their insights and advice towards the progress and ultimate completion of the study.

I would also like to acknowledge Dr. Dong S. Ko from the Naval Research Laboratory for providing the COAMPS dataset.

I am very grateful to Dr. Nan Walker for the GOES-12 SST maps she provided to aid in the hurricane analysis. I would like to acknowledge Dr. Mitsuko Korobkina for providing the SSHA and MODIS SST datasets for analysis. These data are being processed as part of a NASA project validation study. I would also like to thank Ganesh Sundarraj and Padmanava Dash for their help towards the programming aspect of this project.

I would especially like to thank my parents, Mr. V.K. Sharma and Mrs. Sudha Sharma, my brother, Mr. Ritesh Sharma, and all my friends for their love, motivation and encouragement throughout the project and especially during the final stages.

Table of Contents

List of Tables

List of Figures

Abstract

Global weather changes have become a matter of grave concern in hurricane prone areas as intensities of hurricanes are observed to be increasing every year, necessitating improved monitoring capabilities. NASA's QuikSCAT satellite sensor has provided significant support in analyzing and forecasting winds for the past 8 years. In this study, the performance of QuikSCAT products, including JPL's latest L2B 12.5km swath winds, was evaluated against buoy-measured winds in the Gulf of Mexico. The long-term study period was 1/2005 – 2/2007. The Coupled Ocean/Atmospheric Mesoscale Prediction System (COAMPS) was also assessed. The regression analyses showed very good results for QuikSCAT products, with the best results obtained from L2B winds. R^2 values for moderate wind speeds were 0.75 and 0.89, 0.88 and 0.93, 0.66 and 0.77 for speed and direction and for L3, L2B and COAMPS respectively. The National Weather Product (NWP) model winds provided in the L2B dataset were also studied. Hurricanes that took place from 2002 to 2006 were studied individually to obtain regressions of QuikSCAT and COAMPS versus buoys for those events. The correlations were very high indicating that QuikSCAT is at par with buoys during hurricanes. These measurements were compared with the NHC best track analyses to determine the accuracy and found to be almost half those obtained by NHC, possibly due to rain contamination. Sea Surface Height Anomaly (SSHA) measurements by Jason-1 and sea surface temperature (SST) measurements by the Moderate Resolution Imaging Spectroradiometer (MODIS) Aqua and GOES-12 (Geostationary) were compared with wind fields during hurricanes to study the effects of the Loop Current and Warm Core Rings on the intensification of the hurricanes. A preliminary study was conducted in which the regions of enhanced wind

speeds were observed by studying the longitudinal and latitudinal transects across the hurricane for two hurricanes, namely Hurricanes Ivan and Katrina. This study would act as a precursor to further analysis of the radius of maximum wind and critical wind radii.

Chapter 1. Introduction

1.1. Purpose of Study

The NASA Quick Scatterometer (QuikSCAT) satellite, which was launched on 19th June 1999, carries the SeaWinds instrument, the first satellite-borne scanning radar Ku-band scatterometer which can measure vector winds over 90% of the global ocean under clear and cloudy conditions in 24hr (Callahan, 2006). This study was conducted to evaluate the performance of QuikSCAT in the Gulf of Mexico (GOM) and to ascertain its reliability for accurate measurements during extreme conditions required for emergency preparedness. Although many studies (Freilich and Dunbar, 1999; Atlas et al., 1999; Ebuchi et al., 2002) have been conducted on the same lines, they have mostly concentrated on the performance of QuikSCAT in offshore locations, far from land. The complexity of coastal winds and the various processes taking place in the Gulf of Mexico make it even more important to study this region in depth and ascertain how well prepared we are for emergencies. The latest QuikSCAT product by the Jet Propulsion Laboratory (JPL), i.e. the Level 2B 12.5 km swath wind product is one of the datasets evaluated in this study. Correlation analyses of QuikSCAT's wind retrievals against buoy wind measurements, obtained from National Data Buoy Center (NDBC) buoys (Fig. 1), are performed. The time period under consideration is from January 2005 to February 2007. The Coupled Ocean/Atmospheric Mesoscale Prediction System (COAMPS), a regional model actively used by the Naval Research Laboratory (NRL), is also evaluated against buoy measurements for the same time period.

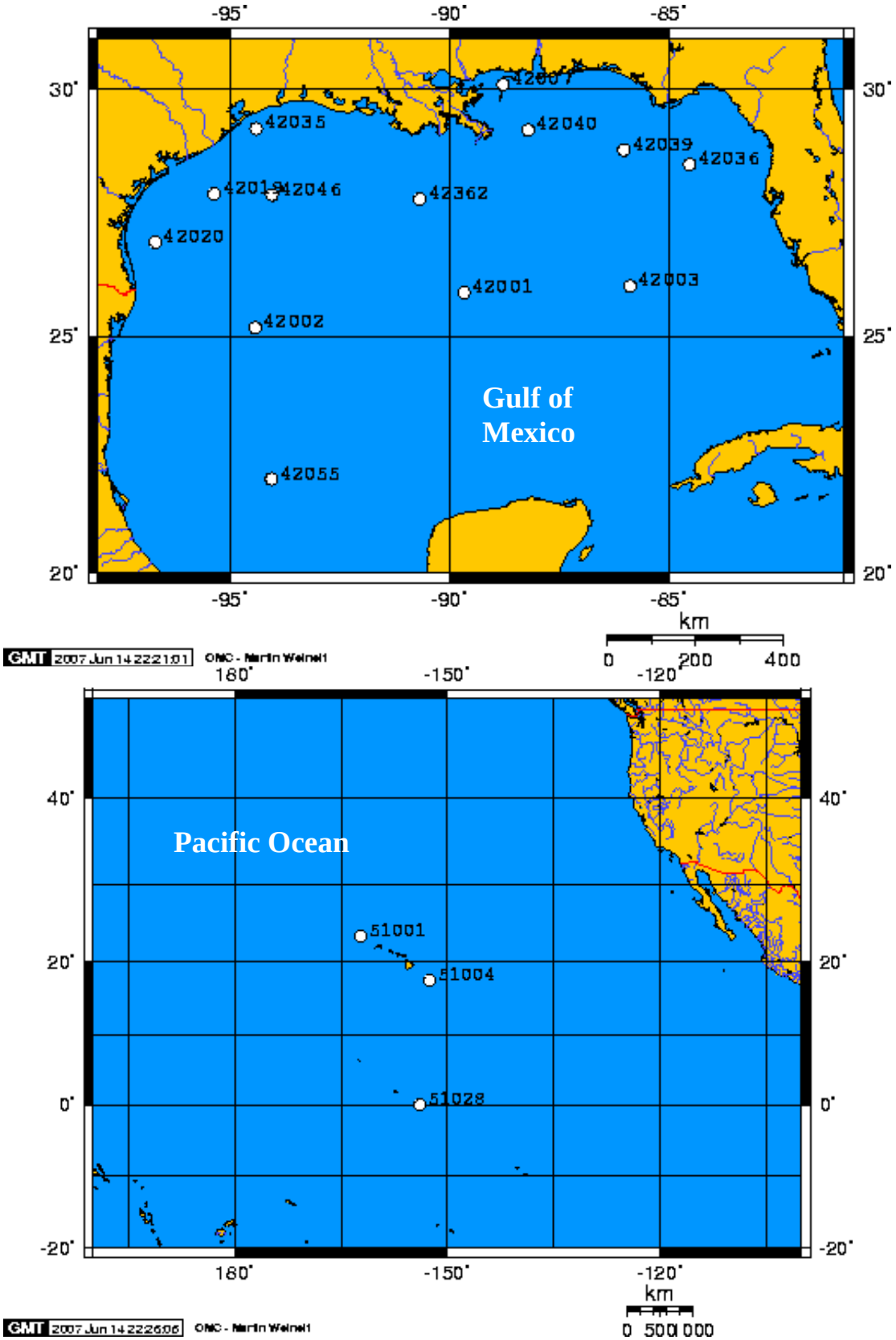

Figure 1. Study area (upper panel) in the Gulf of Mexico, and buoys used in the study. Pacific reference buoys shown in lower panel. Maps obtained from http://www.aquarius.geomar.de/omc/.

Hurricanes that occurred in the last 5 years from 2002 to 2006 are used to compare the performance of QuikSCAT and COAMPS with that of buoys present in the GOM. It is rather intuitive to perform the evaluation of QuikSCAT particularly during extreme conditions and, hence, many studies have been conducted for the same purpose (Cione and Uhlhorn, 2003; Chelton et al. 2004; Emanuel 2005; Elsner et al., 2006; Chelton et al., 2006). However, they have concentrated on comparing it with model or other satellite outputs. In this study, the comparison is done directly with buoys to establish bounds on QuikSCAT's reliability.

Vector maps of the QuikSCAT dataset provided a clear picture of the closed circulation of the storm and location of the eye. Changes in intensity of the storm can also be discerned. Sea surface height anomaly (SSHA) images from Jason-1, Sea surface temperature (SST) measurements from the Moderate Resolution Imaging Spectroradiometer (MODIS) Aqua satellite and SST maps from GOES -12 (Geostationary) satellite are used to estimate a possible cause for the same. The two datasets (SSHA and MODIS SST) were obtained from pre-processed NASA products available on the Jet Propulsion Laboratory website http://podaac-www.jpl.nasa.gov/ and the Ocean Color website http://oceancolor.gsfc.nasa.gov/ respectively. The GOES-12 SST maps also depict SSH contours computed from data obtained from Jason-1, TOPEX/POSEIDON and Geosat Follow-on (Leben et al., 2002) and were obtained from Walker et al. (2005) and Walker et al. (2006a,b). The Jason-1 and MODIS datasets were mapped and helped in identifying the location of the Loop Current and presence of warm core rings to understand the causes of increase in intensity of the hurricanes. Longitudinal and latitudinal transects across the eyes of the Hurricanes Ivan and Katrina were studied to estimate the regions of enhanced winds as a preliminary study.

1.2. QuikSCAT

Scatterometers measure the surface roughness of the ocean, affected by the wind magnitude and direction, by transmitting microwave pulses and receiving the backscatter. Centimeter-scale gravity or capillary waves on the ocean surface reflect or backscatter the radar power primarily by means of the Bragg resonance process (Callahan, 2006; M. H. Freilich, SeaWinds Algorithm Document). These waves are usually in equilibrium with the wind. The crests and troughs of the small-scale waves tend to be aligned perpendicularly to the wind direction. This results in a modulation of the observed backscatter with the wind direction. Thus, backscatter cross section varies with both wind speed and wind direction at moderate incidence angles. The normalized radar cross section (σ_o) is determined from the backscatter power. Multiple and simultaneous σ_o measurements obtained from different directions can thus be used to simultaneously solve for wind speed and direction (Callahan, 2006; M. H. Freilich, SeaWinds Algorithm Document).

QuikSCAT data are exceptional in providing high-quality and accurate ocean surface wind analyses. The QuikSCAT satellite was launched into a sun-synchronous, 98.6° inclination, 803 km circular orbit with a local equator crossing time at the ascending node of 6:00am ± 30 min and a swath width of 1800 km (Fig. 2). The recurrent and orbital periods of the orbit are 4 days and 101 min, respectively (Callahan, 2006).

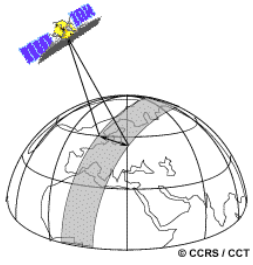

Figure 2. QuikSCAT's orbit and view.

The SeaWinds instrument on QuikSCAT is a microwave scatterometer that measures near-surface wind speed and direction (10 m neutral winds) under all weather and cloud conditions over the global oceans. It uses a rotating dish antenna with two pencil beams that sweep in a circular pattern at incidence angles of 46° (horizontally polarized) and 52° (vertically polarized) (Fig. 3 & 4). The antenna radiates microwave pulses (13.4 GHz) across broad regions on the earth's surface (Callahan, 2006).

The vector wind is determined by combining several backscatter observations made from multiple viewing geometries as the scatterometer passes overhead. At each geographical location or wind vector cell (WVC), usually two, three or four wind solutions are found to be consistent with the observed backscatter, all with approximately the same wind speed but different wind directions. These wind solutions characterize the goodness-of-fit between the σ_o measurements and the model function. For QuikSCAT, the model function is cast in a tabular form. Each radar backscatter observation samples a patch of ocean about 25 km x 37 km which is the ellipsoidal instantaneous antenna footprint (or 'egg'). Wind speed and direction are retrieved from σ_o measurements through a geophysical model function (GMF) (Callahan, 2006). In addition to wind speed and direction, other factors can influence backscatter observations and thereby affect the retrieved winds. The most important of these is rain. Rain changes the ocean surface roughness, and attenuates and scatters the radar energy. This is the combined effect of high incidence angles (46° and 54°) and the operating frequency (13.4 GHz). QuikSCAT provides accurate ocean surface winds in all conditions except for moderate to heavy rain, defined as a vertically integrated rain rate >2 mm km^{-2} hr^{-1}. This value of rain rate and estimates from collocated Special Sensor Microwave Imager (SSM/I) observations were used to tune the SeaWinds rain flag. Besides rain, light winds are troublesome,

since the ocean surface acts more like a smooth reflector than a scatterer. The measurement geometry of SeaWinds results in error characteristics that vary across the satellite swath. Errors are smaller in an optimum region of the swath, termed the mid-swath, "sweet spot", away from the nadir and the far edges of the swath (Callahan, 2006).

One major drawback with the SeaWinds backscatter measurements is that they are highly affected by land contamination. If any part of the swath falls over land, the backscatter measurements are greatly altered and rendered invalid. Hence, all such swaths are completely eliminated. This is a cause of serious concern for coastal regions. With the complexity of wind fields and physical processes in coastal regions, it becomes necessary to have as much information as possible and with maximum resolution. However, with QuikSCAT, no wind measurements are available until about 30 km from the shoreline, as in the 25 km products, and 20 km for the 12.5 km product.

The NASA Jet Propulsion Laboratory (JPL) Physical Oceanography Distributed Active Archive Center (PO.DAAC) distributes standard wind products from QuikSCAT at three levels from their website http://podaac-www.jpl.nasa.gov/. Level 1B has the time-ordered Earth-located Sigma-0 swath measurements. Level 2A (swath) has the surface flagged sigma-0 measurements and attenuations at 25 km and 12.5 km resolutions. Level 2B (swath) is derived from Level 2A sigma-0 measurements and has the ocean wind vectors at 25 km and 12.5 km resolutions. Level 3 is evenly distributed gridded global data at 25 km resolution which is intended for large-scale analysis. The GMF function utilized for this product is the QSCAT-1, which is inherently limited for high wind speeds. This product is supplied with separate ascending node and descending node measurements. The latest product by JPL is an improvement on the Level 2B wind measurements in that the spatial resolution is 12.5 km, i.e. double its initial accuracy.

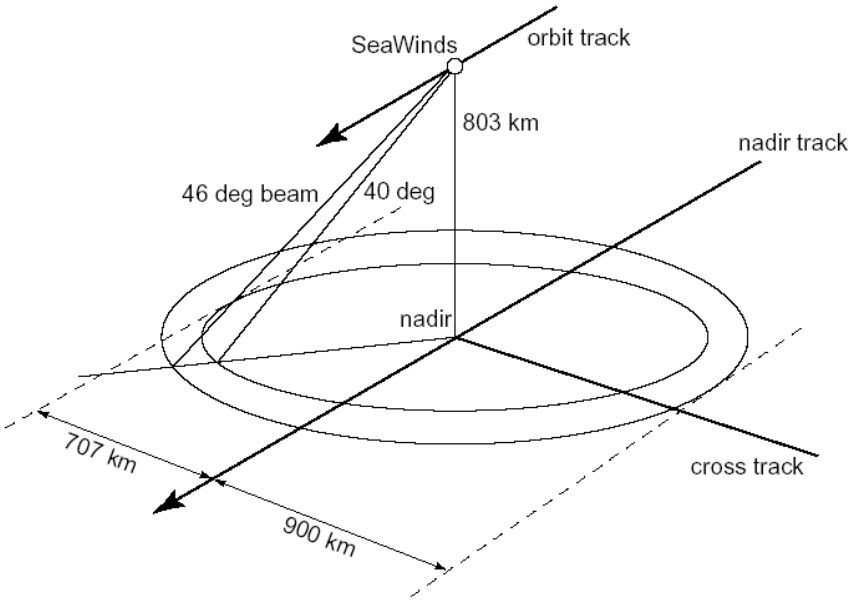

Figure 3. Details of QuikSCAT's track and swath with inner beam. (Taken from SeaWinds Algorithm Document by M.H. Freilich)

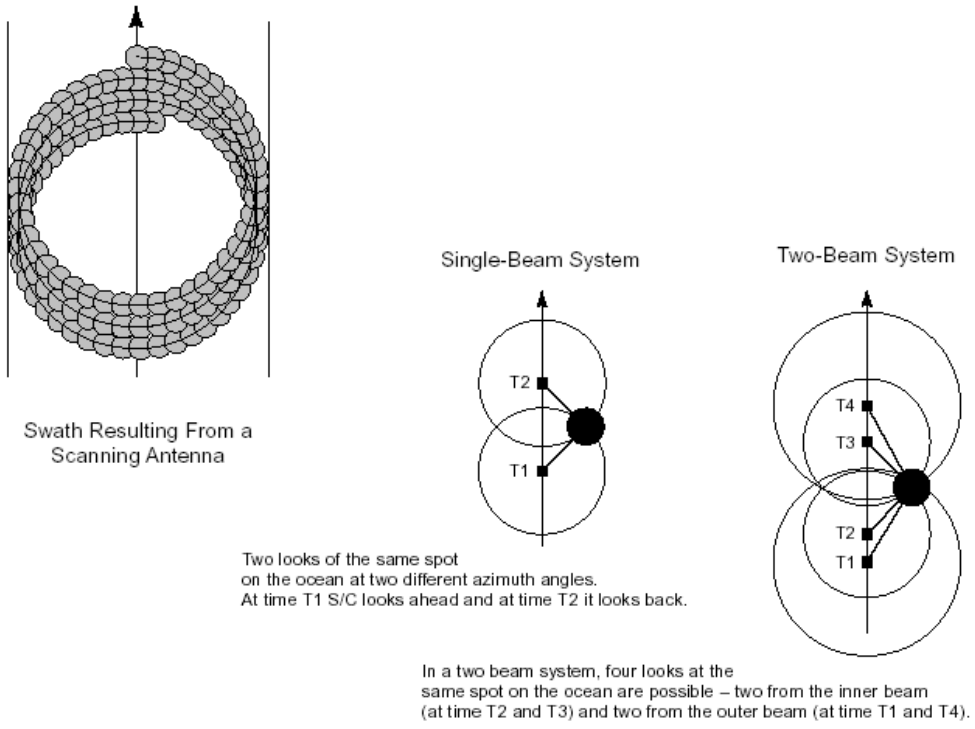

Figure 4. Inner beam and outer beam measurement technique and coverage. (Taken from SeaWinds Algorithm Document by M.H. Freilich)

The GMF function utilized for this product is the QSCAT-1/F13, in which wind retrievals higher than 16m/s were recalibrated to winds derived from SSM/I F13, but even for this function, measurements above 20 m/s are not very accurate. Level 2B data is supplied as each file containing information on one revolution of the satellite. Overall, there are 14-15 files per day. This product contains three datasets. The first dataset is the wind speed and direction obtained using the ambiguity removal algorithm, i.e. the Maximum Likelihood Estimator (MLE), to estimate the most likely wind direction measurement out of four ambiguities obtained at each wind vector cell. The baseline ambiguity removal algorithm for SeaWinds incorporates the Numerical Weather Product (NWP) initialization technique, or 'first guess', developed by Dunbar and Freilich, used for ERS-1, NSCAT-1 and NSCAT-2 processing (Fig. 5). The NWP wind field is the NCEP 2.5° resolution 1000mb, or 100m, global data analysis model outputs closest in time to the QuikSCAT pass. This is a nudging technique in which the median filter algorithm is initialized with an initial field of wind vector solutions which is any ambiguity with probability above a threshold and closest to the direction of the NWP analysis field (Callahan, 2006). The median filter then generates the final wind vector selections (Callahan, 2006). The second dataset is the wind speed and direction measurement obtained from the Direction Interval Retrieval with Threshold Nudging (DIRTH) algorithm and is the enhancement of the ambiguity selected by the MLE. It is obtained by the combination of two separate algorithms. Direction Interval Retrieval (DIR) algorithm is used to correct for near-nadir wind direction errors due to the positions of the two beams resulting in non-optimal measurement geometry. Threshold Nudging (TN) algorithm is used to account for far-swath errors which occur due to the absence of measurements from the inner beam. Both DIR and TN algorithms are utilized to obtain

DIRTH that calculates a range of wind directions that is representative of the selected ambiguity in each wind vector cell. DIR then applies a median filter over the entire swath to determine the optimal wind direction within the calculated range for each wind vector cell (WVC) (Callahan, 2006). The third dataset contains nudge field, i.e. NWP wind field, wind speed and direction estimates for each WVC. They represent spatially interpolated measurements and reflect weather conditions at or near the location of the WVC.

Both the DIRTH and NWP (NCEP) datasets are considered in this study and are also compared to each other. Since the measurements are not at the same level, i.e. DIRTH at 10m neutral winds and NWP at representative 100m wind measurements, the correlation between the two is likely to be relatively crude. The mission requirements of QuikSCAT for wind measurements are an accuracy of 2m/s in wind speed for the range 3-20m/s and 10% for the range 20-30m/s and 20° rms in wind direction for wind speeds ranging from 3m/s to 30m/s (Callahan, 2006).

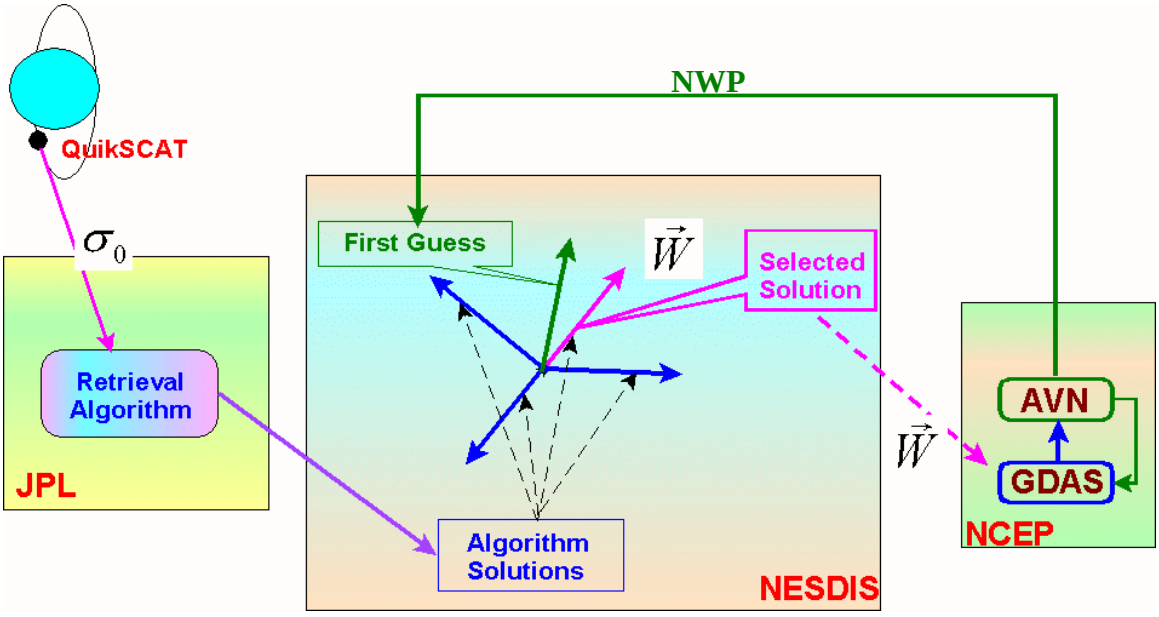

Figure 5. Processing algorithm for Level 2B products. Ambiguity removal and wind direction selection based on initialization from NWP (NCEP) wind fields.

Tang et al. (2004) conducted a study and produced a product that would improve the resolution of QuikSCAT winds to 12.5 km by converting its "egg" swath into "slices". The objective of this product is to aid in coastal measurements so that crucial wind retrievals closer to the shore can be obtained. The strict criterion of the 25 km product to screen out any swath if even a part of it touches land, was relaxed for this product such that all those "slices" whose centers were over water were used. They observed that the high resolution product is not as accurate as the low resolution product due to the detection of more noise. Also, it displayed the same trend of giving better results for offshore measurements as compared to nearshore measurements. However, the accuracy of the high resolution (12.5 km) product falls within or at least very close to the design specifications of the instrument. Offshore, the bias and the RMSD for wind speed are 0.42 and 1.14 m/s and for wind direction they are 3.98° and 22.83° respectively. For nearshore, the bias and the RMSD for wind speed are 0.93 and 1.83 m/s and for wind direction they are 4.71° and 31.15° respectively. Hence, the speed specifications are met for the instrument, but the direction specifications are not. The logical follow up of these results would be to rethink the relaxation on the land contamination criterion. Tang et al. again applied the criterion to discard data within 25 km of the shoreline. However, the difference in the results was negligible; hence that was not the problem. It was also observed that the ambiguity removal skill degraded by about 2% to 6% with the high resolution algorithm. Overall, they concluded that the performance of the high resolution product is satisfactory for offshore measurements and could be useful for medium to high winds in coastal regions. This product, Level 2B (12.5 km) is now being distributed from July 2006 as a standard product by JPL and that is what is used in this study for validation against buoy data in the Gulf of Mexico.

1.3. COAMPS

The Coupled Ocean/Atmospheric Mesoscale Prediction System (COAMPS) is an analysis-nowcast and short-term forecast tool applicable for various physical parameters over any region of the Earth. It was developed by the Marine Meteorology Division (MMD) of the Naval Research Laboratory (NRL) and is run operationally by the Fleet Numerical Meteorology and Oceanography Center.

Observations from aircrafts, rawinsondes, ships, buoys and satellites are blended with the first-guess fields, which are either the global fields from the Navy Operational Global Atmospheric Prediction System (NOGAPS) or the most recent COAMPS forecast, to generate the current analysis. The analysis is run first to prepare the initial and boundary files used in the forecast model. The forecast executable performs time integration of the model numeric and physics. COAMPS forecasts parameters up to 48 hours at 1 to 3 hour increments. The data used in this study was obtained from the latest version, i.e. the MM5.

The Fifth-Generation National Center of Atmospheric Research (NCAR)/Penn State University Mesoscale Model (MM5) is a limited-area, non-hydrostatic, terrain-following sigma-coordinate model designed to simulate or predict mesoscale and regional scale atmospheric circulation. The atmospheric model uses nested grids to achieve high resolution for a given area. It also uses non-hydrostatic dynamics which allows the model to be used a few-kilometer scale that helps resolve small scale weather features such as thunderstorms. It has a multitasking capability on shared and distributed memory machines along with a four-dimensional data assimilation capability.

Chapter 2. Regression Analysis and Evaluation Studies

2.1. Introduction

QuikSCAT was launched in 1999 after the early termination of the NASA Scatterometer (NSCAT), on the Japanese ADEOS-1 satellite, due to power loss in 1997. SeaWinds on QuikSCAT employs a compact, higher resolution "pencil-beam" design compared to the "fan-beam" design used by NSCAT. QuikSCAT continues to provide high quality data till date, even when a second attempt (ADEOS-II) ended due to subsystem failure. Hence, QuikSCAT proved to be a reliable and accurate source for remote sensing of the global winds. Numerous studies have been conducted to evaluate the performance of QuikSCAT against in-situ observations made by buoys for its potential importance for wind measurements and weather forecasting over the world oceans.

2.2. Literature Review of QuikSCAT Evaluation Studies

Ebuchi et al. (2002) conducted a study similar to this study using buoys located in the Pacific Ocean, Atlantic Ocean, Gulf of Mexico and along the east coast of the United States. In their study, the Level 2B (25 km) wind product, which gives two wind measurement outputs, was used for evaluation. One is produced using the Maximum Likelihood Estimator (MLE) (Long and Mendel 1991) and the median filter ambiguity removal algorithm. The other is produced using the Direction Interval Retrieval with Threshold Nudging (DIRTH) algorithm (JPL 2001). Both these wind products were evaluated against corresponding buoy measurements. However, only offshore buoys were used. They maintained a time difference between the satellite and buoy measurements of

less than 30 min and a spatial difference between the two of less than 25 km, so as to allow maximum concurrence of the two measurements. Ebuchi et al. concluded that rms differences for wind speed and wind direction were within the bounds of the mission requirements and, hence, the measurements made by QuikSCAT are satisfactory for moderate winds. On studying the effects of oceanographic and atmospheric parameters on the wind measurements, they concluded that there was no significant effect due to sea surface temperature variation and air-sea temperature difference. However, there was some correlation between the wind and significant wave height measurements.

Pickett et al. (2003) performed the validation of QuikSCAT measurements against buoys along the west coast of the U.S. As opposed to Ebuchi et al., they concentrated on nearshore winds. They used the swath data, gridded near-real-time data and gridded science datasets for the comparisons allowing a mean temporal and spatial difference between the satellite and buoy measurements of 16 min and 25 km respectively. They encountered large wind direction errors which could be removed to some extent by ignoring light winds. Their conclusion for fixing this problem was just simple editing, i.e. removing these data points manually or using band pass filtering. They also came across some large wind speed spikes that they concluded to be due to the inaccurate rain-flagging algorithm used for the satellite processing. Overall, they still found large errors in the measurements. Using spectral analysis, Pickett et al. deduced that this is due to the high-frequency energy of coastal winds and the overall complexity of nearshore wind fields. More such evaluation studies were conducted even before the above two, such as Freilich and Dunbar (1999) and Atlas et al. (1999), employing different tolerance intervals for temporal and spatial difference. Similar results were obtained by them as well.

A few studies have also been conducted to improve the resolution of SeaWinds' measurements to finer than 25 km. Long et al. (2001, 2003) have developed the scatterometer image reconstruction (SIR) algorithm for enhancing the resolution. They were able to reconstruct the finer scale backscatter measurements to obtain a higher resolution of spatial sampling and so, have the capacity to retrieve mesoscale coastal wind features. They were able to improve the resolution up to 2.5 km (Long et al., 2003), however, the accuracy was reduced and the noise levels were quite high, rendering the measurements invalid for many applications. Upon validation, their wind estimates were encouraging. Further studies and comparisons are underway.

Chao et al. (2003) conducted a study to create a high resolution wind product for coastal regions by blending QuikSCAT measurements with regional mesoscale atmospheric model (COAMPS) simulations. QuikSCAT displays inaccuracy in nearshore measurements, on the other hand, COAMPS displays inaccuracy in offshore measurements. Their study was carried out to overcome these characteristics thereby creating a product that would give higher accuracy than either of them alone. They evaluated the performance of their product using three moored locations off the coast of central California. Their results showed significant improvement in the correlation and RMS when the blended product was used as opposed to both QuikSCAT and COAMPS individually.

2.3. Data and Methods

My study is based on the same lines as those discussed above. A thorough examination of QuikSCAT's performance in the Gulf of Mexico is conducted using NDBC buoys. Three buoys in the Pacific Ocean, near the Hawaiian Islands, are also considered for referencing

and comparison. QuikSCAT has been observed by previous studies, as mentioned in the previous section, to be highly affected by land contamination and give satisfactory results for measurements far from the coast. The wind measurements by COAMPS model are also evaluated against the same NDBC buoys to establish a better understanding of QuikSCAT's standing among the various data assimilation methods for this complex coastal region. Two datasets from QuikSCAT are used for the evaluation process, namely Level 3 gridded data at 25 km resolution and Level 2B swath data at 12.5 km resolution, the latter being the latest product supplied by JPL. The time interval under consideration is from January 2005 to February 2007. For the COAMPS data, the time interval is from January 2005 to December 2006. In the QuikSCAT dataset, a rain flag is also provided to ascertain the reliability of each measurement. This rain flag has been found to be far too conservative, hence, it is not taken into consideration and all the data are used. However, for the sake of comparison, regression analysis for the L2B DIRTH dataset, using moderate winds, is also conducted after consideration of the rain flag.

The HDF files obtained from the PO.DAAC website (http://podaac-www.jpl.nasa.gov/) were converted into ASCII files using an IDL program (© 2007 ITT Corporation). These were then compared with ASCII files containing buoy measurements using a C program. For this comparison, it was necessary to ensure that the QuikSCAT measurements were as close as possible to the buoy measurements in space and also in time for a fair analysis. Once the corresponding measurements, coinciding with respect to time and distance, were obtained, they were plotted in Sigma Plot (© 2002 SYSTAT Software Inc.). Statistical analysis on the data was performed using SAS (© 2007 SAS Institute Inc.).

The sea surface temperature data used is the Level 2 product from MODIS. This dataset has already been processed for various atmospheric and cloud corrections and is distributed as a NASA product. Averaging was performed on the data to obtain composites and then mapped using Seadas. Sea surface height data from Jason-1 is also available directly off the website in 10-day cycles and here the files are converted to ASCII format and mapped using IDL.

2.4. Results

2.4.1. Time Series

Before plotting the regressions, a time series over the two years of the QuikSCAT L2B wind measurement was plotted (Figure 6) along with the difference between that and the buoy data (QS – buoy). This was done to determine the performance of QuikSCAT at each of the buoy locations over time and also to evaluate the performance of the buoys. QuikSCAT wind speed is plotted as the upper line while the speed difference is the lower line. For buoys 42001, 42002, 42019, 42020 and 42040 a definite cycle of increase and decrease of wind speed can be observed, with increase taking place starting fall, through winter and ending near spring and decrease in spring, summer and fall. This cycle is not so apparent for buoys 42035, 42040, 42046 and 42362. Large variations of the QuikSCAT-buoy difference can be seen about the zero line. This is because of the discrepancy in measurement accuracy at these buoys. Table 1 provides details of the mean and standard deviations of all the measurements, i.e. the QuikSCAT speed and direction and the difference between QuikSCAT and buoy measurements.

For buoys 42035 and 42040, this is an expected outcome because of their proximity to land and the diminished performance of QuikSCAT in view of that.

However, buoys 42046 and 42362 display such large differences because their measurement accuracy levels are not as high as the remaining buoys. The measurements for these buoys are obtained in integer values. Also, buoy 42046 takes measurements every half an hour and buoy 42362 takes measurements every hour. All the other buoys have wind measurements at 10-min intervals. For this reason, it would be advisable to avoid using buoys 42046 and 42362 in this evaluation so as to perform a fair analysis. Buoys 42001 and 42002 are relatively offshore and display almost zero variation throughout. Buoys 42019 and 42020 are closer to the coast and illustrate that QuikSCAT tends to overestimate the speed. Overall, performance is good at most of the buoys with increase in variance with decrease in distance from the coast.

For the regression analysis, various conditions are applied to the QuikSCAT and then compared with buoy data to see how the results vary. At first, all the data is taken as is and compared directly with buoy data keeping a maximum time interval of 20 min and spatial interval of 0.1˚ (~10km). As it has been demonstrated earlier (Freilich and Dunbar, 1999; Ebuchi et al., 2002; Chao et al., 2003; Pickett et al., 2003), QuikSCAT's performance at very light winds (< 3m/s) and strong winds (> 20m/s) is highly diminished. Hence, here such conditions are also considered and the corresponding correlations are plotted. The buoys being used in this study are scattered over the Gulf of Mexico. Some of the buoys are offshore while others are much closer to the coast. As a result, measurements made at different buoy locations by QuikSCAT are of differing accuracies. Hence, variations of measurements at each buoy location are plotted. The measurements are the differences between QuikSCAT and buoys, obtained by directly subtracting buoy values from the QuikSCAT values for both wind speed and direction.

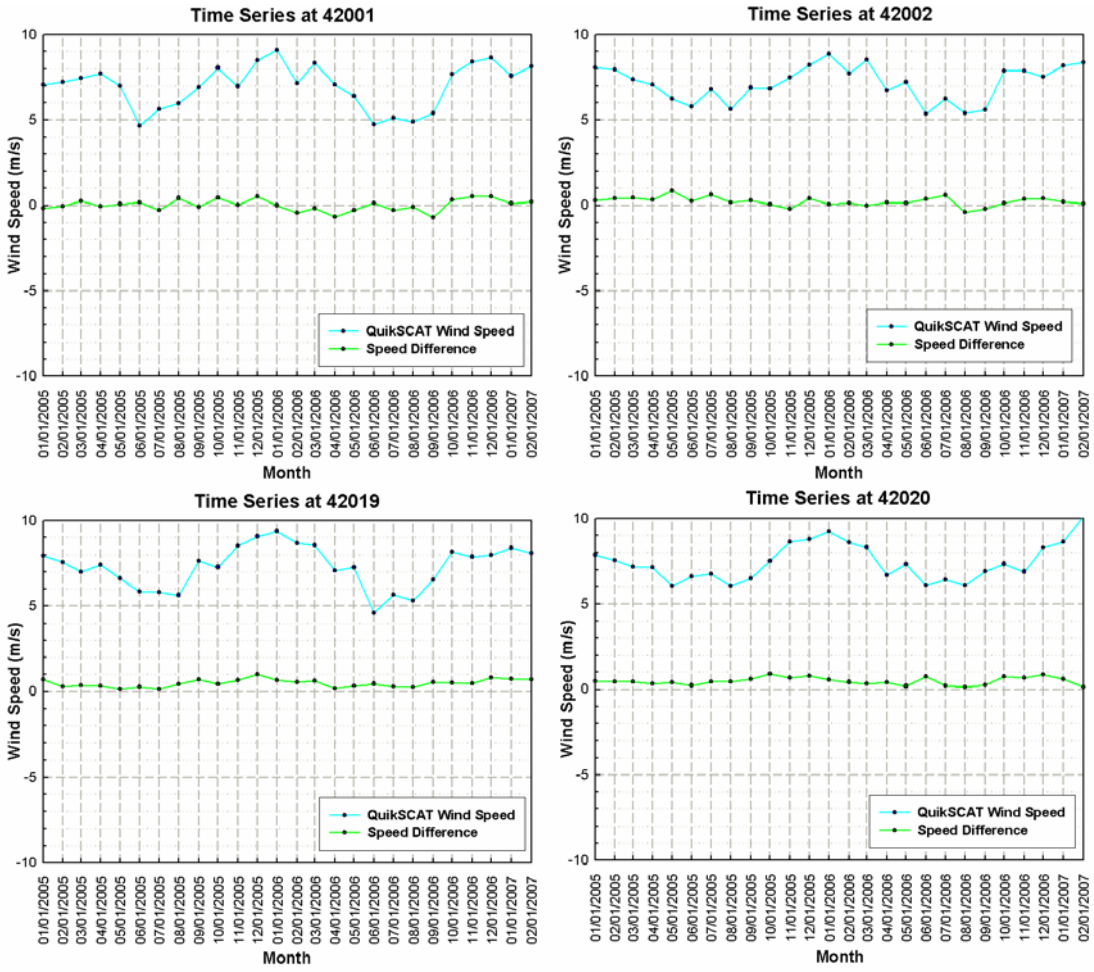

Figure 6. Time Series of monthly averaged QuikSCAT wind speed for buoys 42001, 42002, 42019 and 42020 is shown as a line plot to depict seasonal variations. Also shown is the difference in speed between QuikSCAT and buoy measurements (QS - Buoy).

Figure 7. Time Series of monthly averaged QuikSCAT wind speed for buoys 42035, 42040, 42046 and 42362 is shown as a line plot to depict seasonal variations. Also shown is the difference in speed between QuikSCAT and buoy measurements (QS - Buoy).

Table 1. Buoy locations and their distances from shore are given along with the means and standard deviations of the QuikSCAT speed and direction measurements and differences (QS - buoy).

Buoys	Geographic Location	Distance from Coast (km)	Speed		Direction		Speed Difference		Direction Difference	
			Mean	Std Dev	Mean	Std Dev	Mean	Std Dev	Mean	Std Dev
42001	25.9° N, -89.67° W	364.88	6.98	1.29	135.91	31.51	0.008	0.34	-1.76	6.31
42002	25.17° N, -94.42° W	293.48	7.14	1.03	130.96	20.28	0.22	0.27	2.34	6.78
42019	27.91° N, -95.36° W	127.13	7.29	1.24	144.31	25.08	0.48	0.23	6.52	5.37
42020	26.94° N, -96.7° W	100.19	7.44	1.10	143.39	21.64	0.47	0.22	7.89	3.42
42035	29.25° N, -94.41° W	54.547	7.79	0.73	141.48	39.68	1.52	0.80	8.45	10.00
42040	29.18° N, -88.21° W	87.94	7.61	1.30	155.08	52.52	0.76	0.32	3.91	7.47
42046	27.89° N, -94.04° W	167.3	7.17	1.36	146.31	33.15	1.03	0.88	-3.31	6.24
42362	27.8° N, -90.67° W	154.8	6.84	1.37	147.85	38.80	-1.05	0.67	20.01	10.75

Similar graphs for COAMPS, depicting the variations at the various buoy locations, are also plotted.

The Level 3 regression plots exhibited a reasonably high coefficient of determination when all the data are used. For the wind direction plots, the data at the upper left and lower right corners are also considered to be correlated due to the 0° and 360° discrepancies. However, it adversely affects the calculation of the coefficient of determination (R^2), hence, for the calculation of R^2, the range was elongated to higher than 360° and the data were adjusted such that it continues to increase beyond 360° instead of starting over from 0°, keeping a margin of ±20°. For example, for a buoy measurement of 10° and a QS measurement of 355°, the difference is not 345°, but 15°. In the plots, however, the original format of the data is maintained. Figures 8 and 9 display results for the GOM and Pacific respectively.

For moderate winds, i.e. speeds ranging from 3 m/s to 20 m/s, the correlation for the wind appears to increase slightly (from 0.72 to 0.75 for speed and 0.82 to 0.89 for direction). Wind measurements appear to be adversely affected by light and strong winds. Overall, wind direction correlation is actually higher than wind speed correlation. In the lower panels of Figures 8 and 9, both moderate and light/strong winds, in different colors, are shown for illustrating this point. It can be observed that the wind direction data points are more scattered for the light/strong winds.

For the same regression analysis conducted on the data in the Pacific Ocean (Figure 9), the data are better correlated. There is not much difference between the correlations for wind speed and direction and there isn't a big impact of light or strong winds on the regression, possibly because the dataset for the Pacific was smaller. In the lower panels of Figure 9, the scattered data points in the wind direction plot primarily

belong to the light/strong winds. Also, the correlation is not much higher than that in the Gulf of Mexico, especially for wind direction.

To understand how the accuracy of QuikSCAT varied with increase in wind speed, the differences between QuikSCAT measurements and buoy measurements, obtained by subtracting buoy winds from QuikSCAT winds, were plotted against the buoy wind speed. These are shown in Figures 10 and 11 for the Gulf of Mexico and Pacific, respectively. The lines in the plots are regression lines (for observing bias) and not zero lines. For wind direction, the accuracy of measurement increases with wind speed with largest variations at light winds. For moderate wind plots, the measurements involving light winds are removed and so the correlation for wind direction improves. For the Pacific, the data is evenly spread out about zero, but again, there is higher variance in wind direction for lower wind speeds.

When the performance at the individual buoys was analyzed (Figure 12), the measurement differences at the buoys 42046 and 42362 was also included to emphasize the inappropriateness of using these buoys for the evaluation. Variances for both speed and direction are much higher for these buoys compared to the rest. The three Pacific buoys show uniform and good accuracy. Although most of the buoys in the Gulf of Mexico appear to be fairly well correlated with QuikSCAT, two buoys in particular were problematic. These are buoys 42035 and 42040. The speed measurements at these buoys are reasonable, however, for the direction, they show higher variance compared to the rest. This is probably due to their proximity to land. Buoy 42035 is closest to the coast and buoy 42040 is directly to the east of the Mississippi River delta. QuikSCAT's performance is highly degraded due to land contamination. Measurements made very close to the coast have to be used with extreme caution, as indicated by these results.

2.4.2. Level 3 Gridded Data

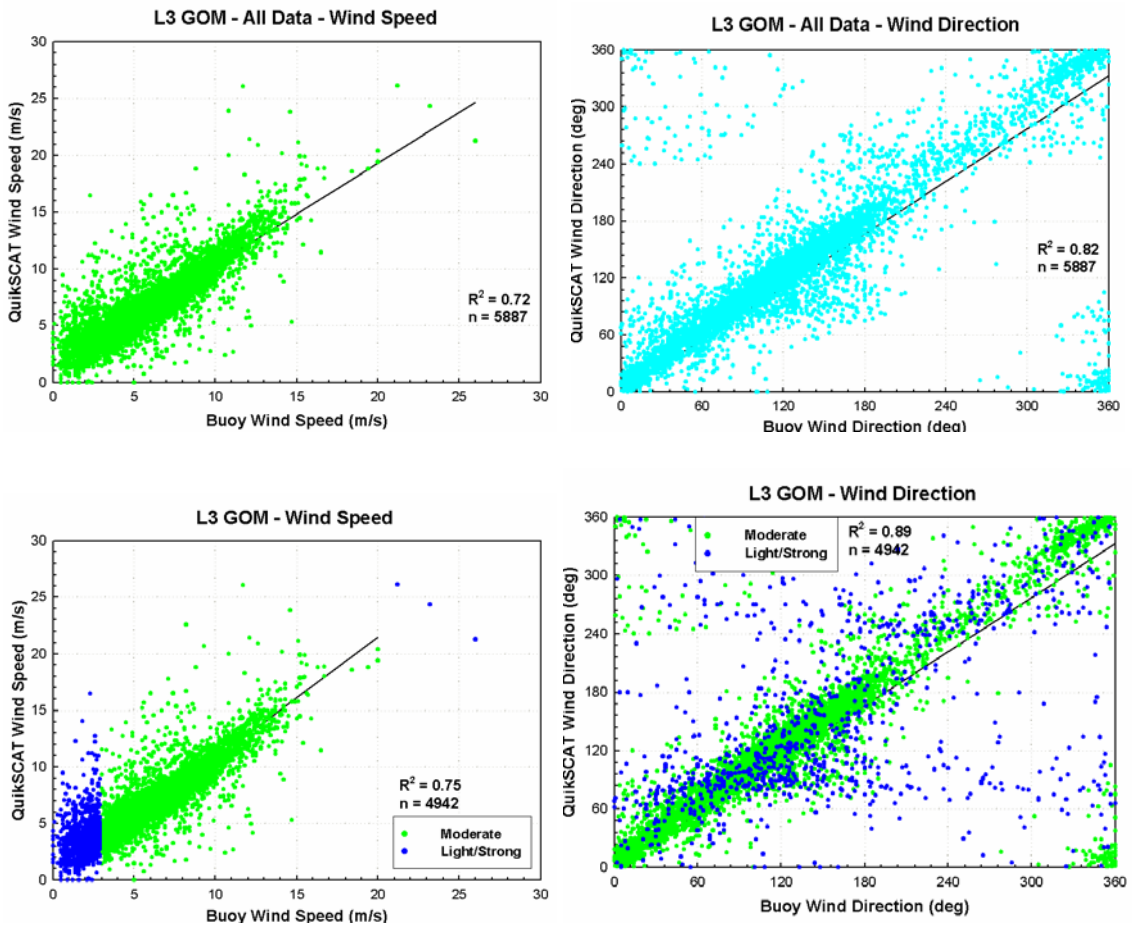

Figure 8. QuikSCAT L3 vs. buoys for wind speed (left panels) and direction (right panels) in the Gulf of Mexico. Upper panels depict regression for all the data using all the buoys. Lower panels depict regression for moderate winds ranging from 3m/s to 20m/s, light and strong winds are also shown in color-coded format. 'R^2' is the coefficient of determination and 'n' is the number of datapoints.

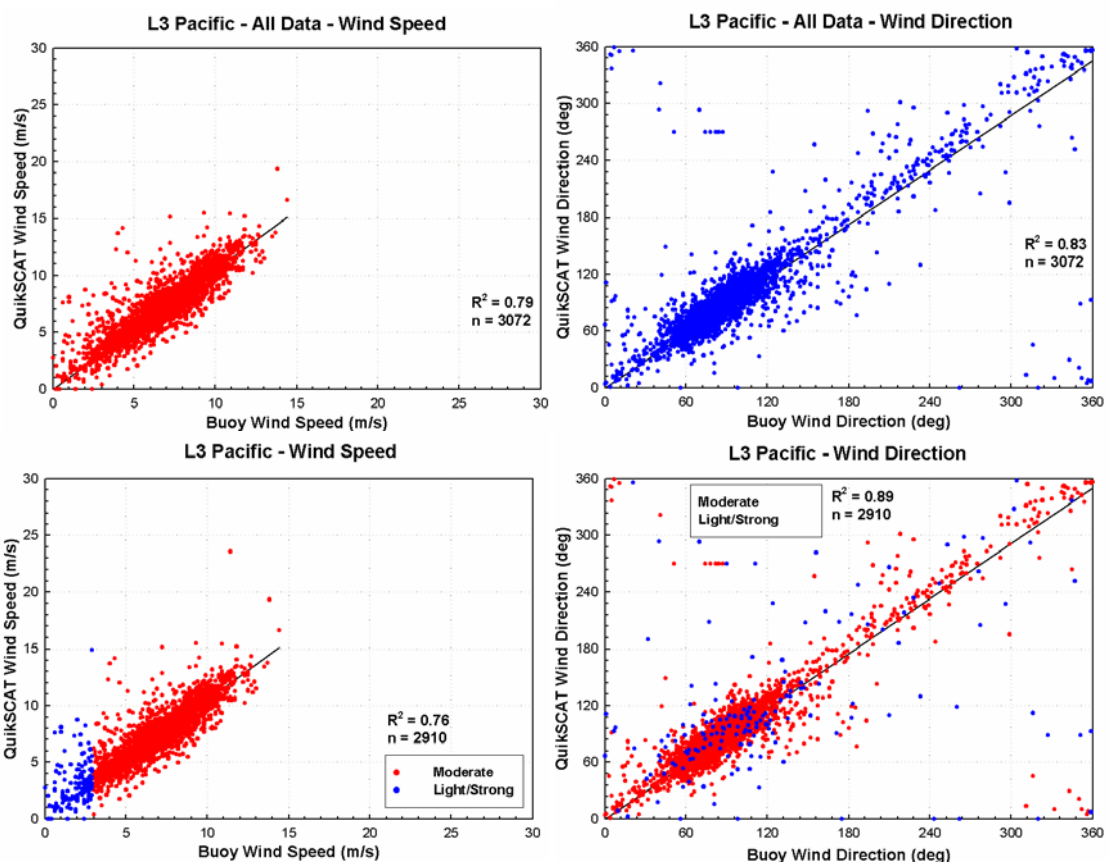

Figure 9. QuikSCAT L3 vs. buoys for wind speed (left panels) and direction (right panels) in the Pacific Ocean. Upper panels depict regression for all the data using all the buoys. Lower panels depict regression for moderate winds ranging from 3m/s to 20m/s, light and strong winds are also shown in color-coded format. 'R^2' is the coefficient of determination and 'n' is the number of datapoints.

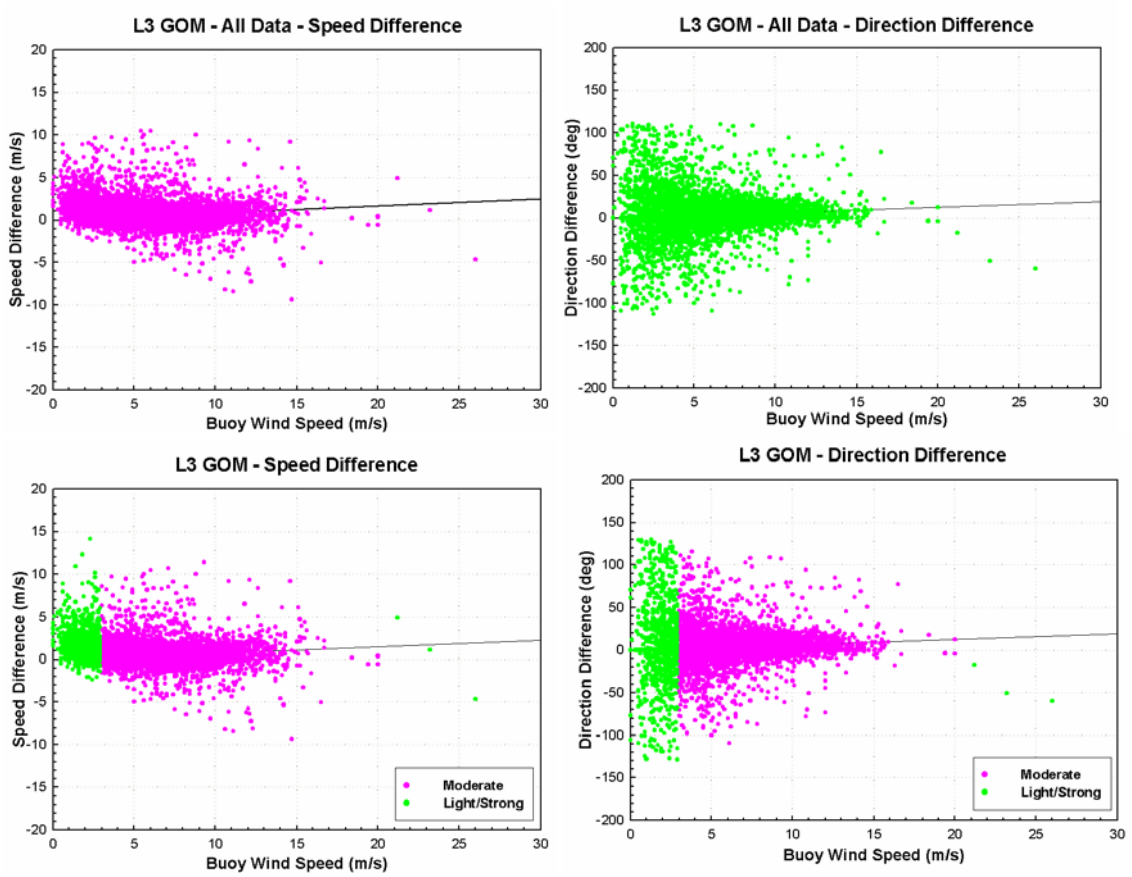

Figure 10. Difference between QuikSCAT L3 and buoy retrievals (QS-Buoy) are plotted against buoy wind speed to illustrate the variation of accuracy of QuikSCAT as wind speed increases for the Gulf of Mexico. Upper panels depict measurements for all the data. Lower panels depict measurements for moderate wind speeds (i.e. ranging from 3m/s to 20 m/s); light and strong winds are also shown distinguished by color. Line shown is the regression line depicting bias and not the zero line.

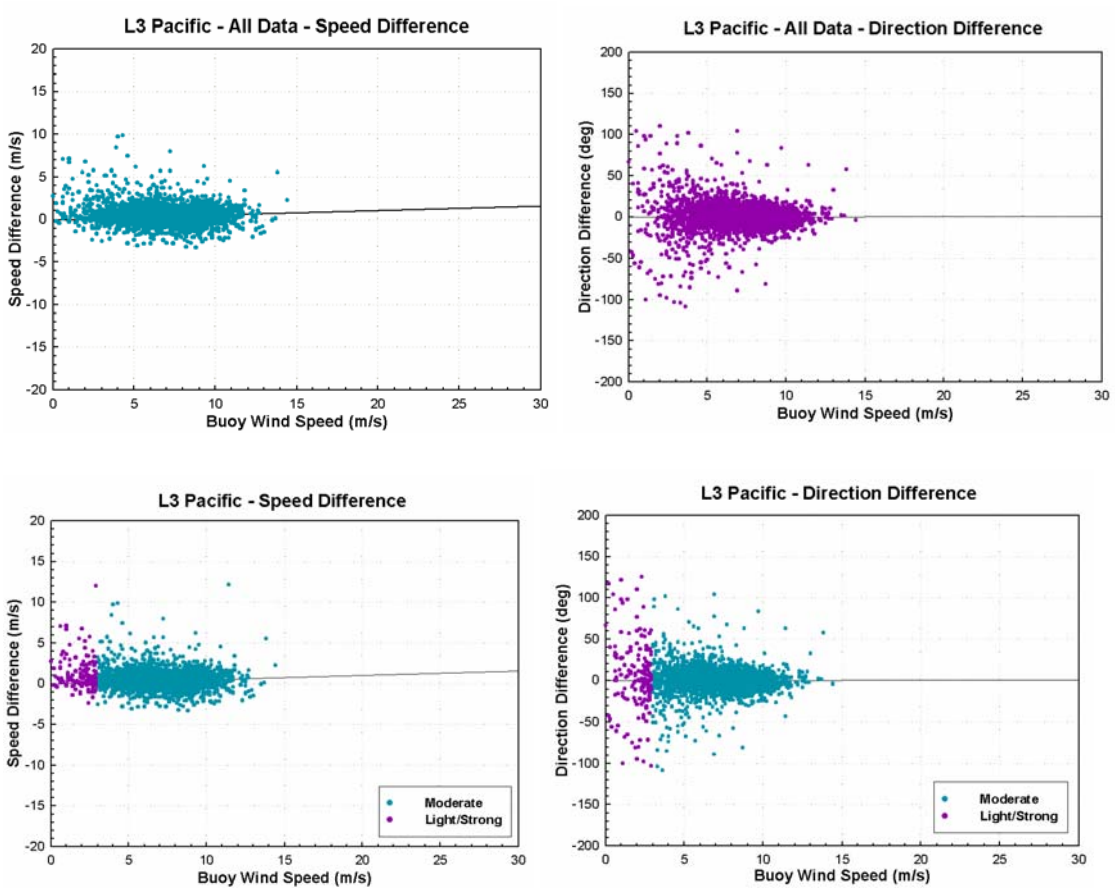

Figure 11. Difference between QuikSCAT L3 and buoy retrievals (QS-Buoy) are plotted against buoy wind speed to illustrate the variation of accuracy of QuikSCAT as wind speed increases for the Pacific Ocean. Upper panels depict measurements for all the data. Lower panels depict measurements for moderate wind speeds (i.e. ranging from 3m/s to 20 m/s); light and strong winds are also shown distinguished by color. Line shown is the regression line depicting bias and not the zero line.

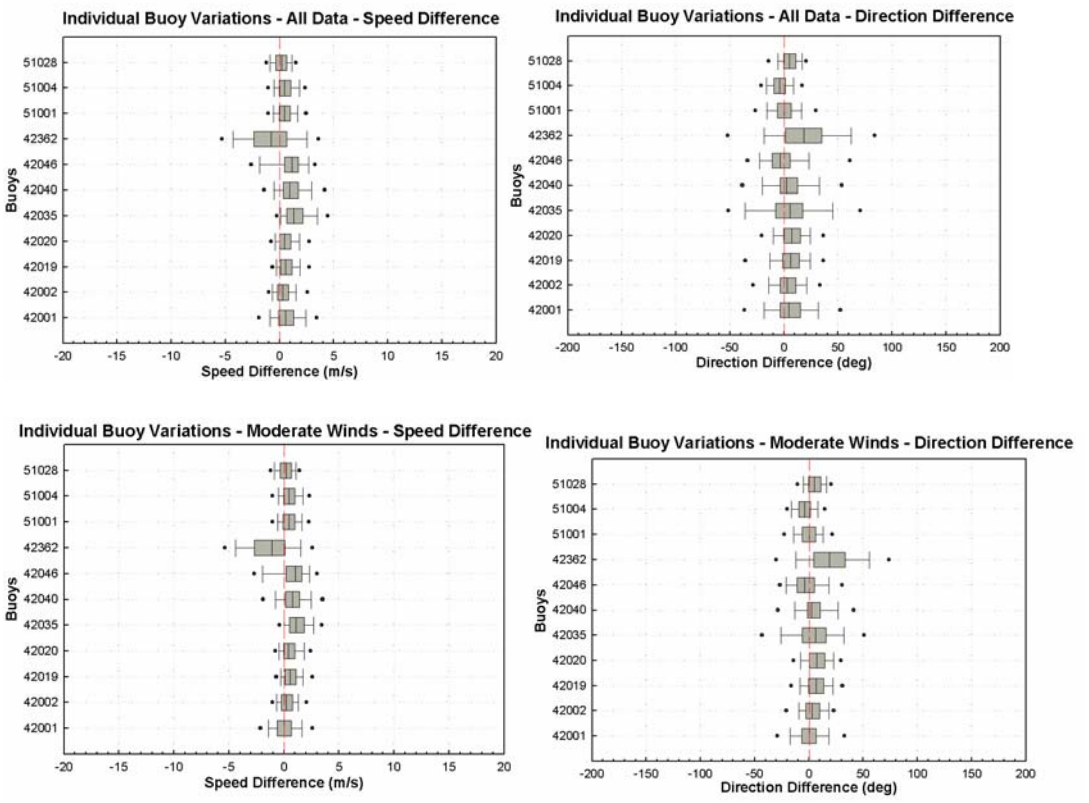

Figure 12. Individual buoy variations for all the buoys under consideration (GOM and Pacific) are shown. The x-axis is the difference between QuikSCAT L3 and buoy measurements (QS-Buoy). The edges of the boxes depict the 25th and 75th percentile. The central line denotes the median. The error bars beyond the box depict the 10th and 90th percentile and the points depict the 5th and 95th percentile.

2.4.3. Level 2B Swath Data

For the Level 2B data, both DIRTH and NWP products are plotted together in the same plot in different colors for comparison (Figure 13). DIRTH appears to show better correlation for wind speed than NWP. This is because the NWP winds are at 1000mb, i.e. approximately 100m above the sea surface, not 10 m neutral winds, whereas, DIRTH dataset is direct 10 m neutral wind measurements by QuikSCAT. Hence, they are not directly equivalent. The regression plots for the L2B data shows better correlation than the L3 data. The wind direction correlates very well as can be observed from the R^2 values (R^2=0.89, Figure13). Wind direction measurements have improved results when light and strong winds are removed. The lower panel in Figure 13 shows Pacific data which has a slightly better correlation than the GOM data.

For showing the regression for moderate winds, the DIRTH and NWP were plotted separately (Figures 14 and 15) for clarity and to illustrate the effect of light winds on the accuracy of measurement. The coefficient of determination is higher in this case and the regression for wind direction is quite satisfactory. As can be observed, the discrepancy in direction measurement occurs at light and strong winds for both DIRTH and NWP with DIRTH being more adversely affected. In the Pacific, the correlation is very similar to the Gulf of Mexico as is obvious from the R^2 values. Hence, there is not a measurable difference between accuracy of measurement for offshore and coastal regions when only moderate winds are considered for the evaluation.

For determining the effect of wind speed on the accuracy of QuikSCAT, the difference between DIRTH and buoys and NWP and buoys was plotted against the buoy wind speed (Figures 16 and 17). For both DIRTH and NWP, the data is slightly positively biased, more so for NWP.

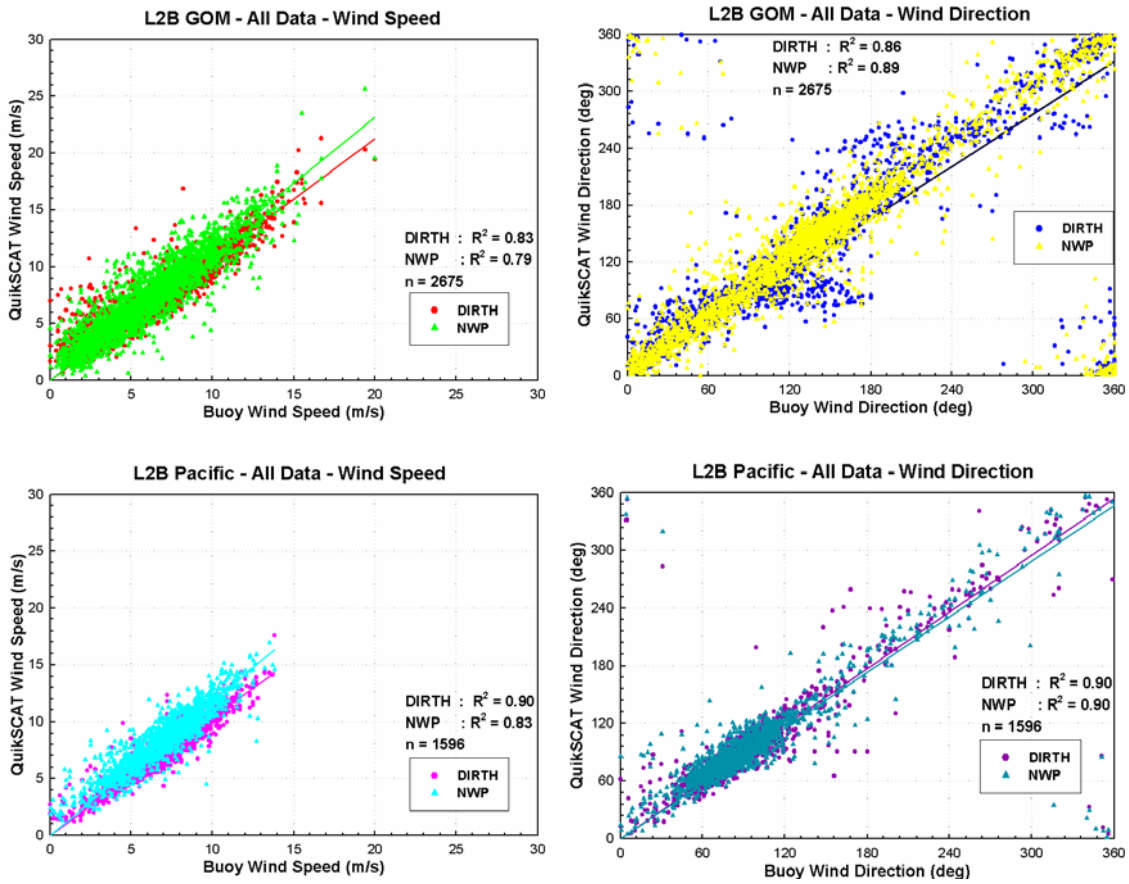

Figure 13. QuikSCAT vs. buoys for wind speed (left panels) and direction (right panels). Upper panels depict correlation for all the data for the buoys in the Gulf of Mexico. Lower panels depict correlation for all the data for the buoys in the Pacific. Each plot displays both DIRTH and NWP datasets with their corresponding coefficient of determinations (R^2) and number of datapoints (n).

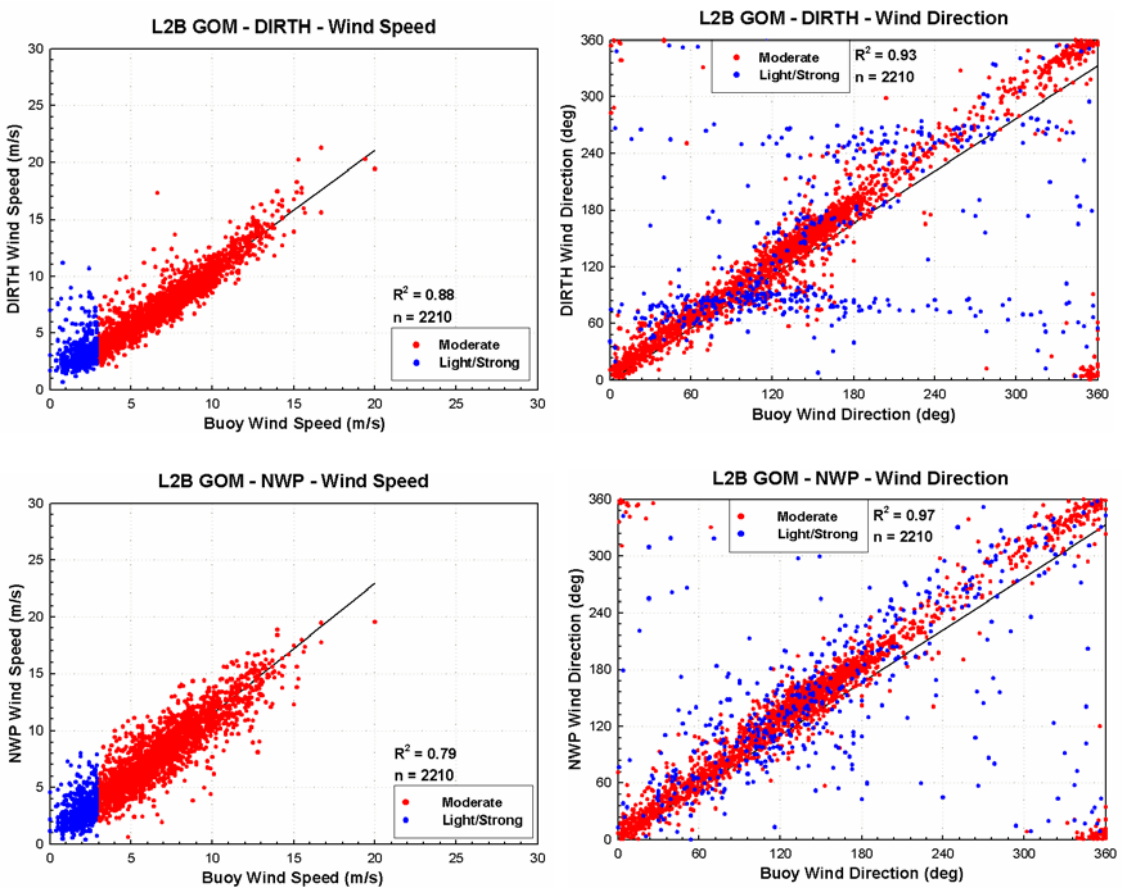

Figure 14. Correlations in the Gulf of Mexico for DIRTH (upper) and NWP (lower) are shown separately for the moderate (3m/s to 20m/s) and light/strong winds. The R^2 is only for the moderate winds. 'n' is the number of data points.

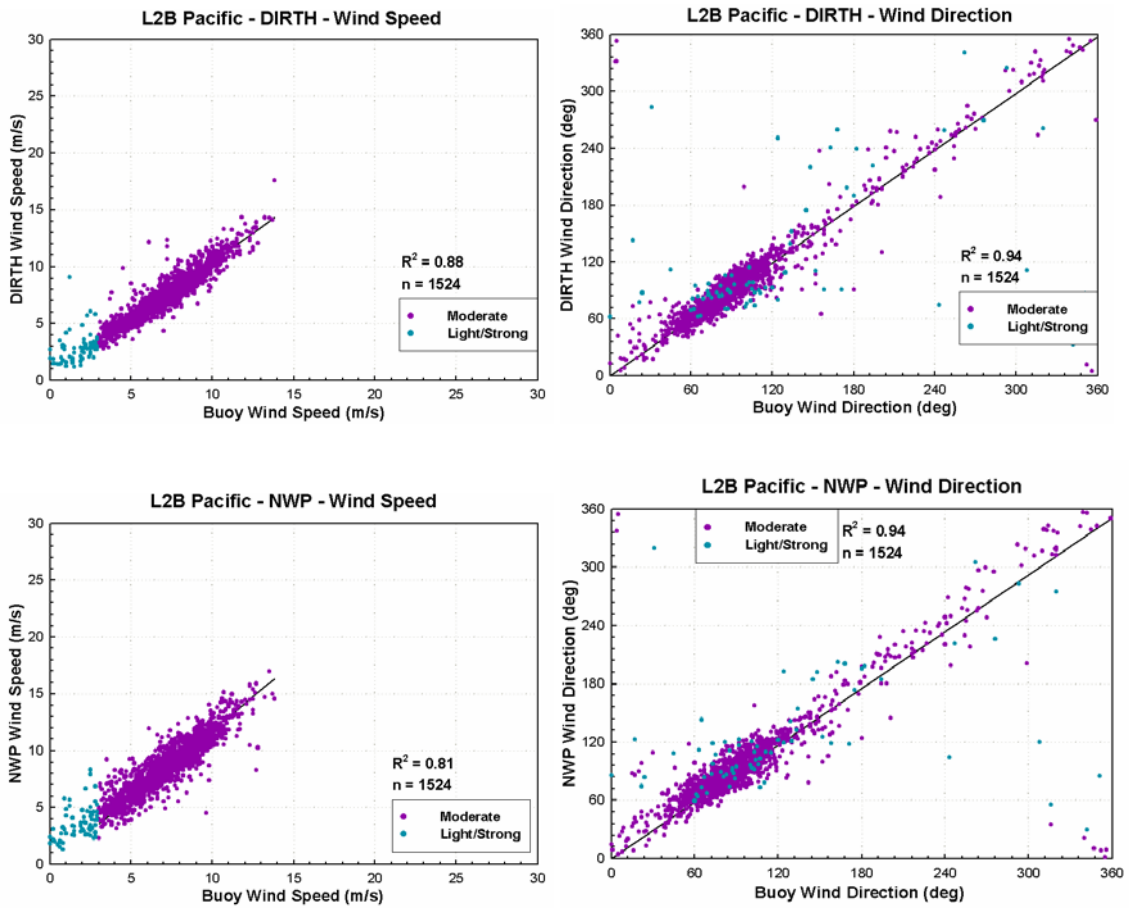

Figure 15. Correlations in the Pacific for DIRTH (upper) and NWP (lower) are shown separately for the moderate (3m/s to 20m/s) and light/strong winds. The R^2 is only for the moderate winds. 'n' is the number of data points.

Again, for wind direction, greatest discrepancy occurs at low wind speeds and the accuracy increases with wind speed. The obvious question that arises after this analysis is how well DIRTH and NWP relate to each other. Hence, regression analysis of these two datasets is also performed (Figures 18 and 19). As indicated by JPL, the methods of measurement for these two datasets are so different that any comparison between them would be very coarse. The results obtained by the regression indicate the same. The correlations are reasonably good and improvements for wind direction when light/strong winds are not considered. In the Pacific, again the correlations are good but not as good as they were when the QuikSCAT datasets were compared to buoys.

To compare the results for each buoy, box plots are plotted (Figures 20 and 21) depicting the variation of the difference in QuikSCAT and buoy measurements. The buoys 42035 and 42040 show maximum variance due to their proximity to land. The variance for all buoys is comparatively lesser for moderate winds. These results are similar to those obtained for the L3 dataset.

2.4.4. COAMPS Data

Analysis and prediction data by COAMPS were evaluated against buoys in the GOM (Figure 22). For this part of the study, the Pacific reference buoys were not used. While not as good as QuikSCAT, COAMPS data seem to be reasonably well correlated with buoy data. The extremely high number of data points tends to create a clutter in the graph; however, a linear trend can be observed. Although the regression line appears to be negatively biased, above 10 m/s, the COAMPS data is observed to be slightly above the trend. Hence, the regression line may be influenced by the extremely high number of datapoints in the low wind speed range.

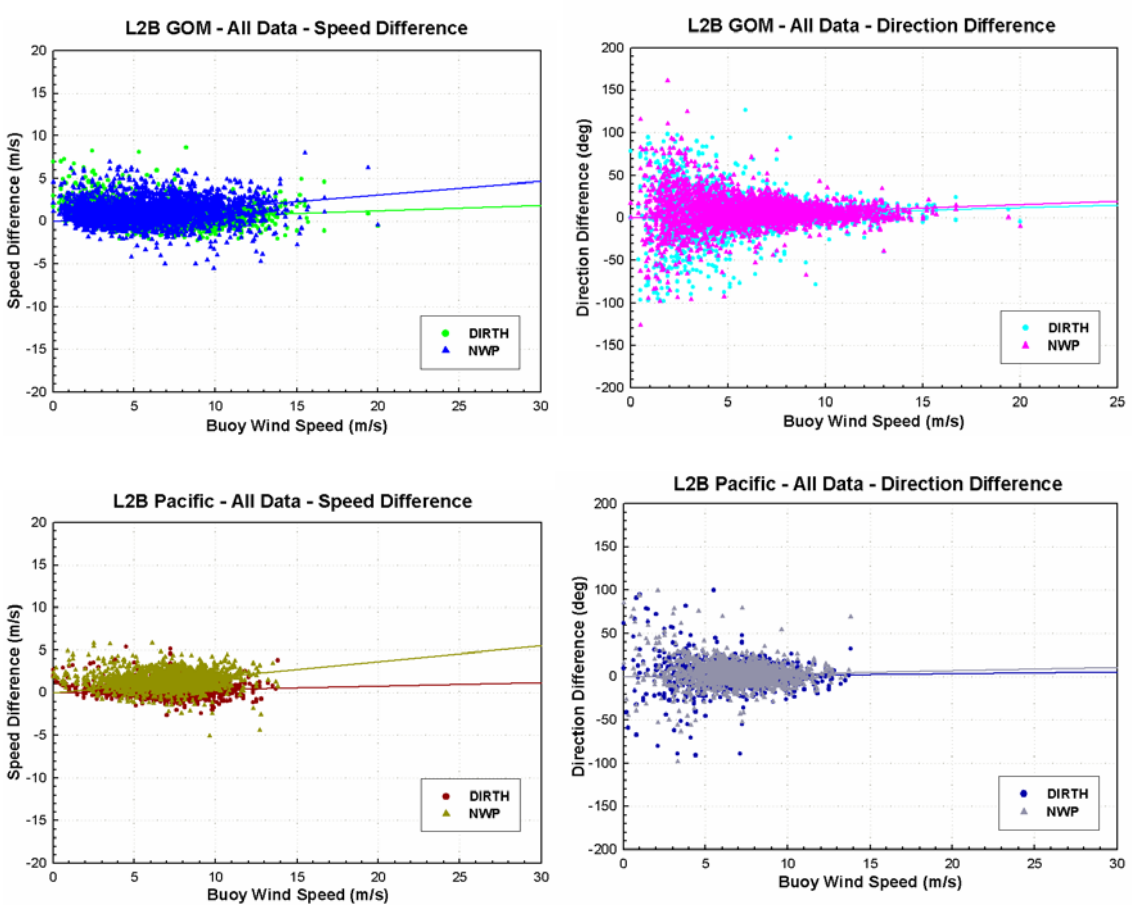

Figure 16. Difference between QuikSCAT (DIRTH and NWP) and buoy retrievals (QS-Buoy) are plotted against buoy wind speed to illustrate the variation of accuracy of QuikSCAT as wind speed increases for the Gulf of Mexico (upper) and Pacific Ocean (lower). Lines shown are the regression lines.

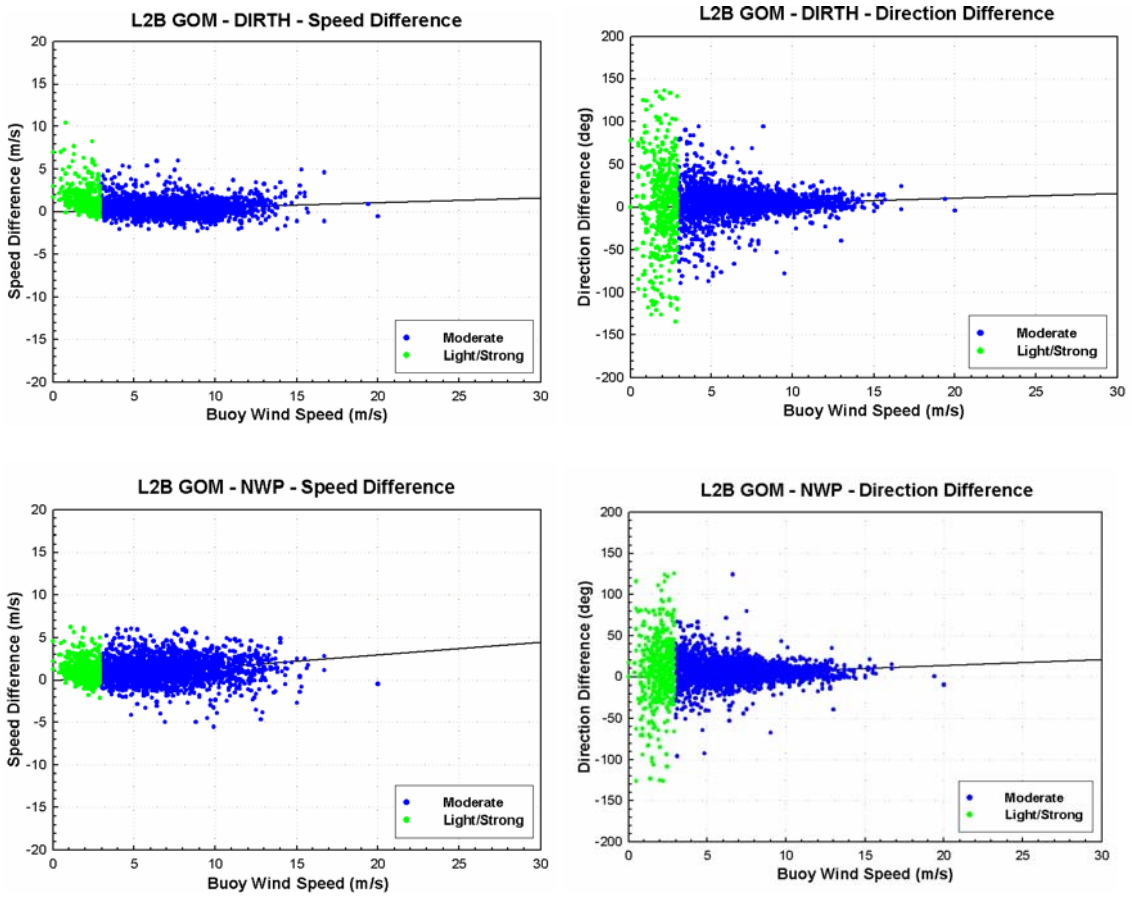

Figure 17. Difference in DIRTH - buoy and NWP - buoy measurements are plotted against the buoy wind speed to illustrate the effect of wind speed on the accuracy of QuikSCAT measurements. The moderate (3m/s to 20m/s) winds and the light/strong winds are shown in different colors for identification. Lines shown are the regression lines.

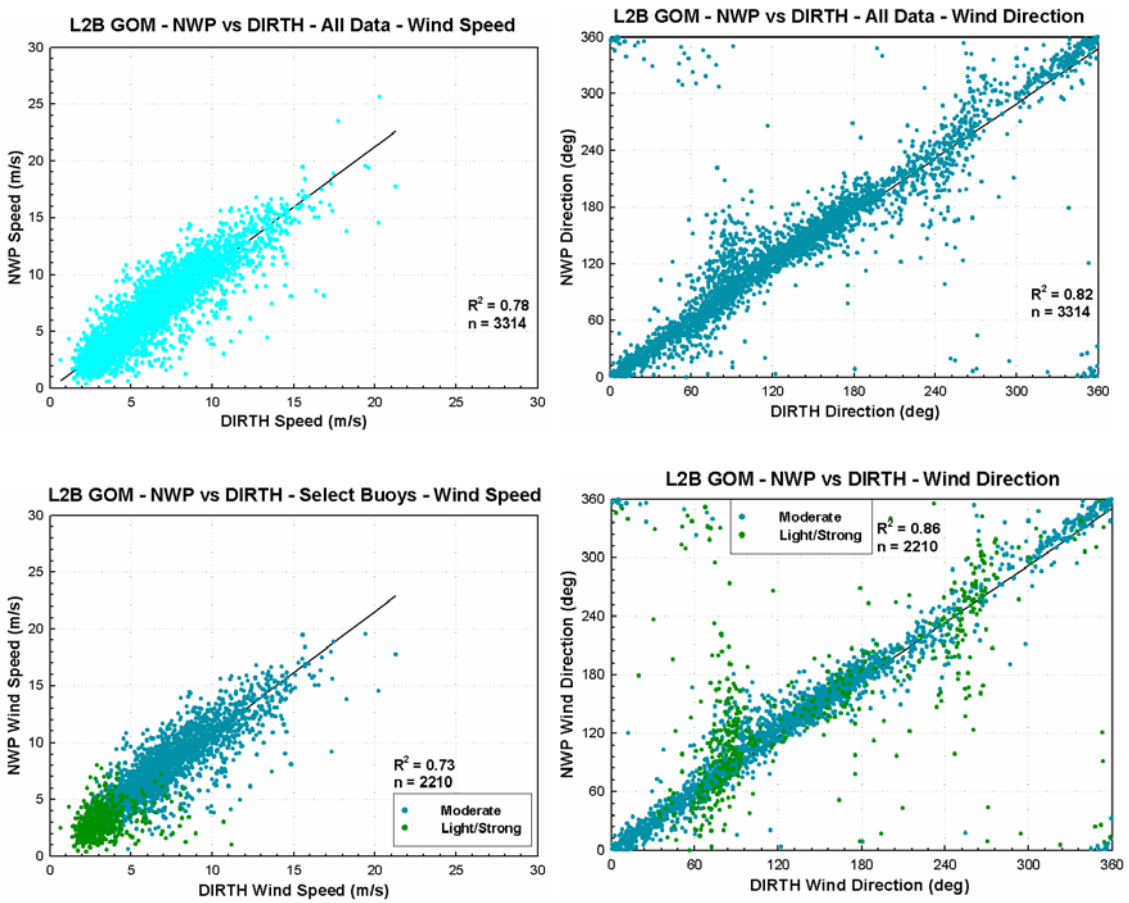

Figure 18. NWP vs. DIRTH measurements from the L2B dataset for wind speed (left panels) and direction (right panels). Upper panels depict all the data for all the buoys in the Gulf of Mexico. Lower panels depict both moderate (3 to 20m/s) and light/strong winds. The R^2 corresponds only to the moderate winds. 'n' is the number of data points.

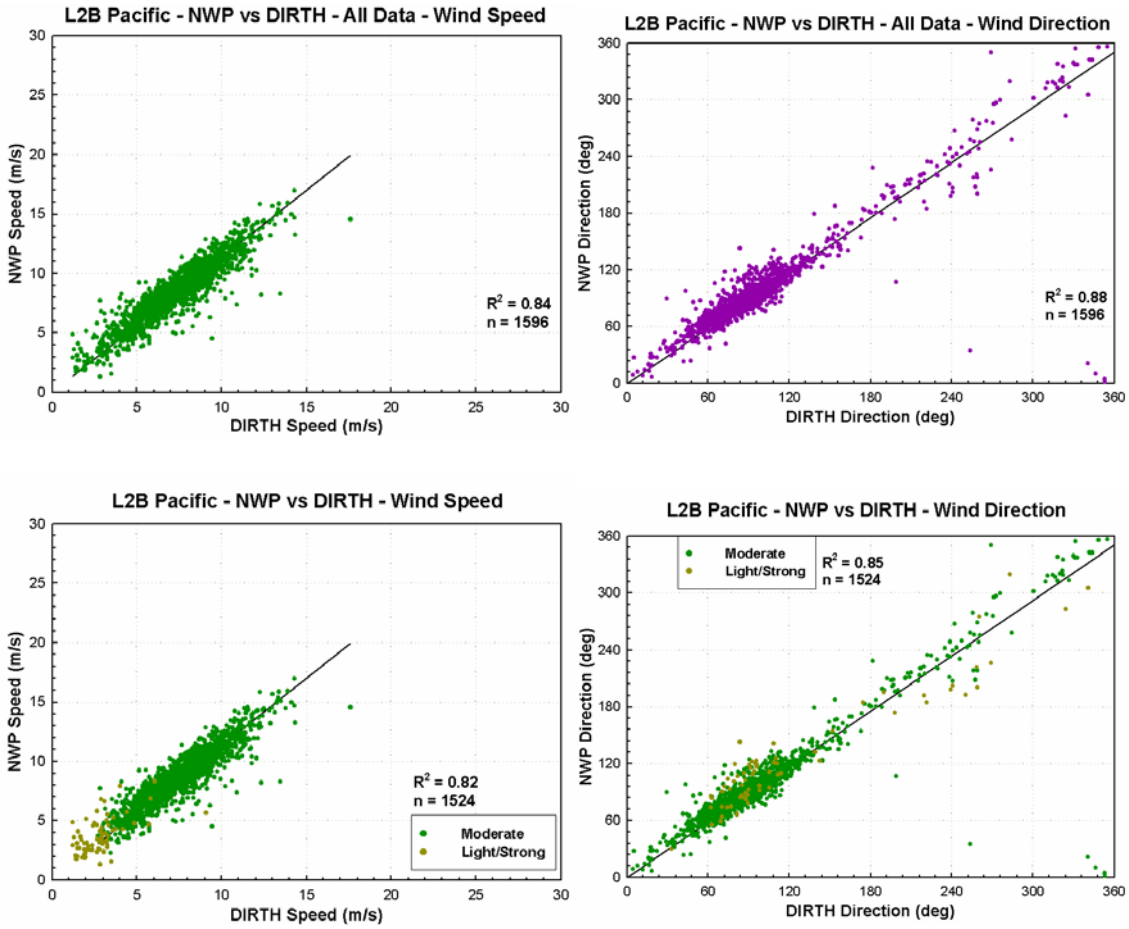

Figure 19. NWP vs. DIRTH measurements from the L2B dataset for wind speed (left panels) and direction (right panels). Upper panels depict all the data for all the buoys in the Pacific Ocean. Lower panels depict both moderate (3 to 20m/s) and light/strong winds. The R^2 corresponds only to the moderate winds. 'n' is the number of data points.

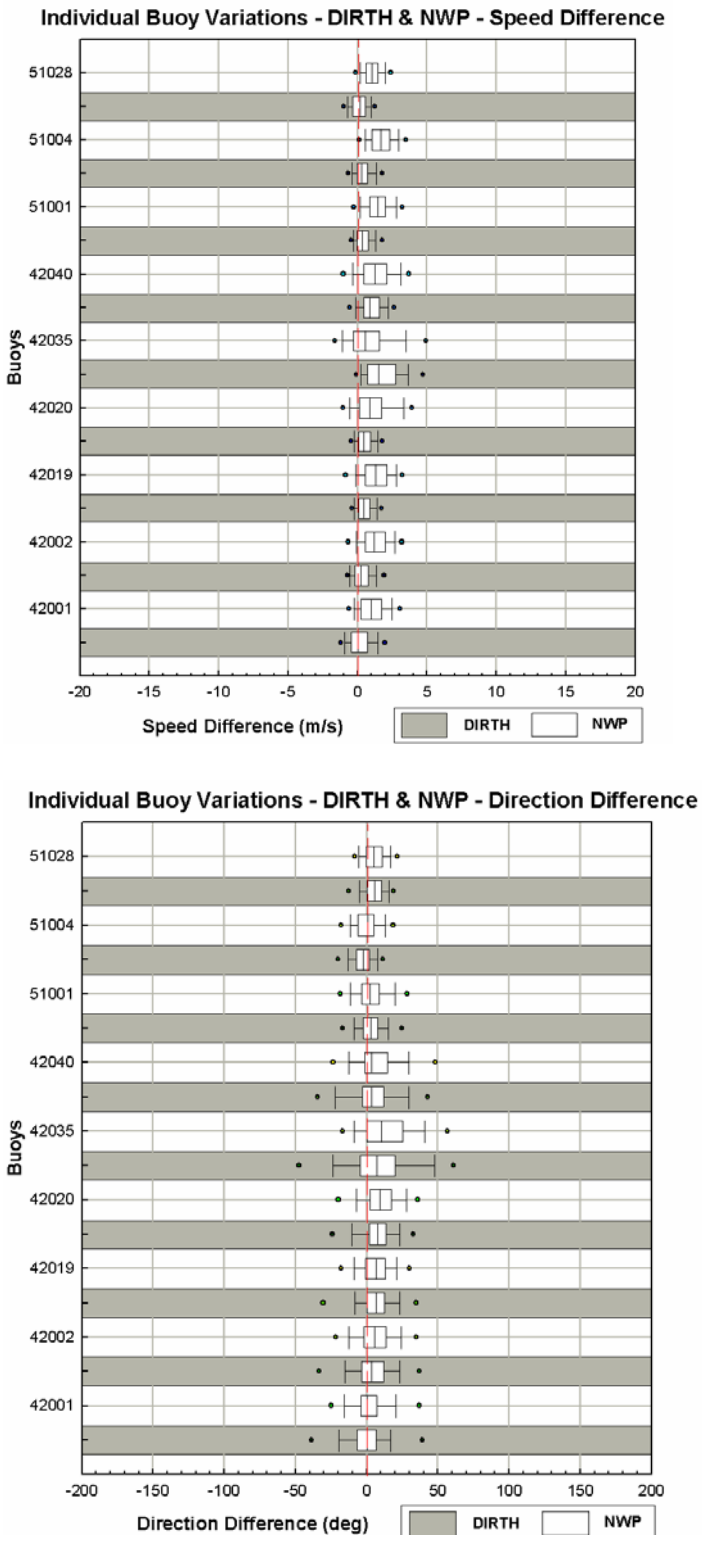

Figure 20. Individual buoy variations for all data for all the buoys under consideration (GOM and Pacific) are shown for both DIRTH and NWP. The x-axis is the difference between DIRTH/NWP and buoy measurements (QS-Buoy). The edges of the boxes depict the 25th and 75th percentile. The central line denotes the median. The error bars beyond the box depict the 10th and 90th percentile and the points depict the 5th and 95th percentile.

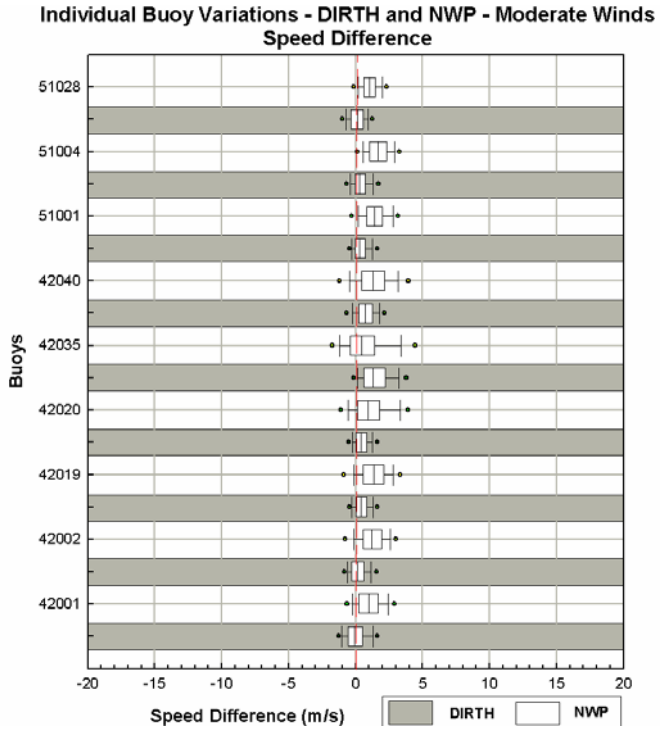

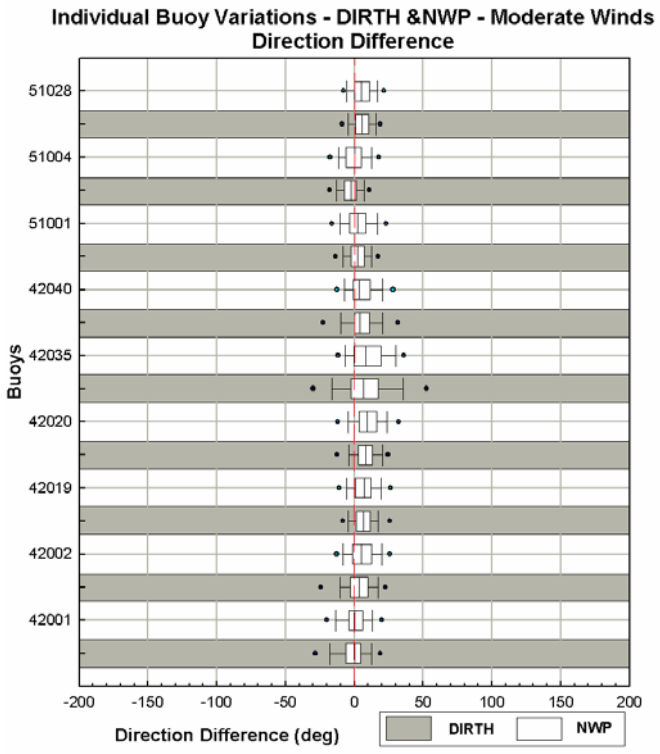

Figure 21. Individual buoy variations for moderate winds for all the buoys under consideration (GOM and Pacific) are shown for both DIRTH and NWP. The x-axis is the difference between DIRTH/NWP and buoy measurements (QS-Buoy). The edges of the boxes depict the 25th and 75th percentile. The central line denotes the median. The error bars beyond the box depict the 10th and 90th percentile and the points depict the 5th and 95th percentile.

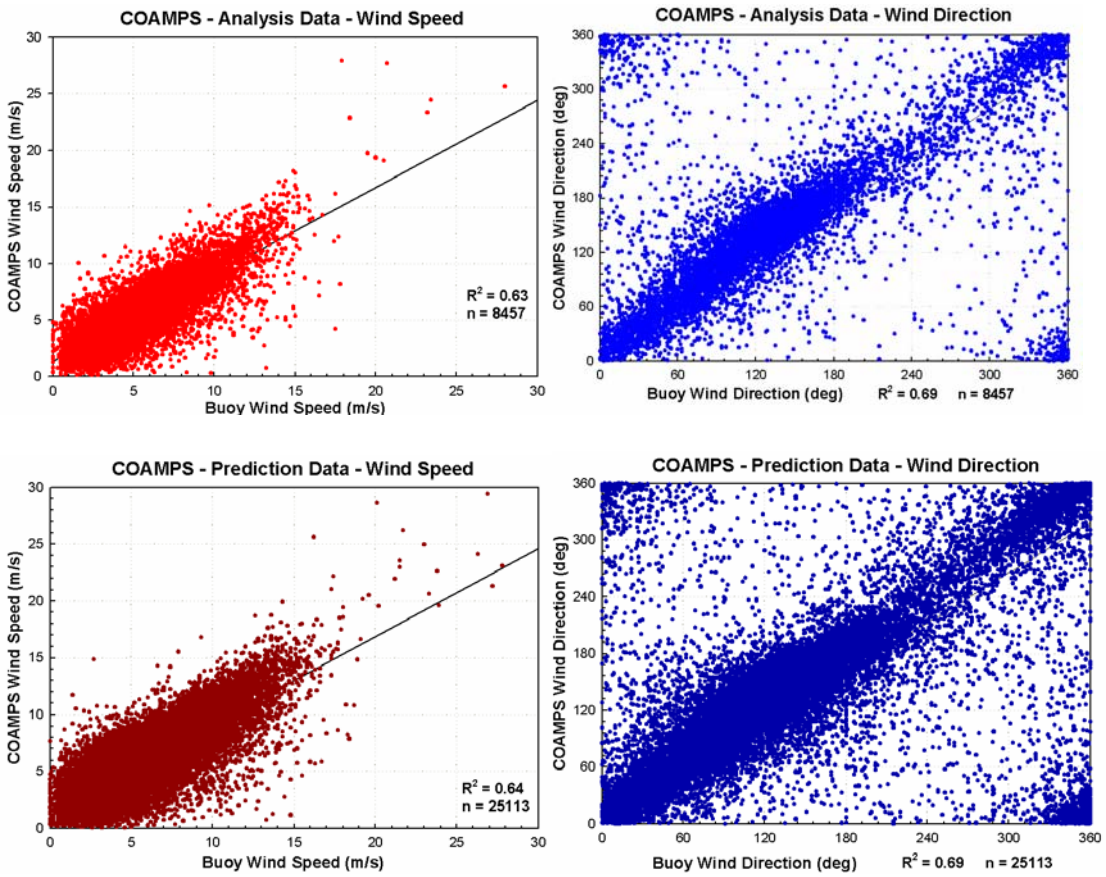

Figure 22. COAMPS vs. buoys for wind speed (left panels) and direction (right panels). Analysis data is shown in the upper panels and prediction data in the lower panels.

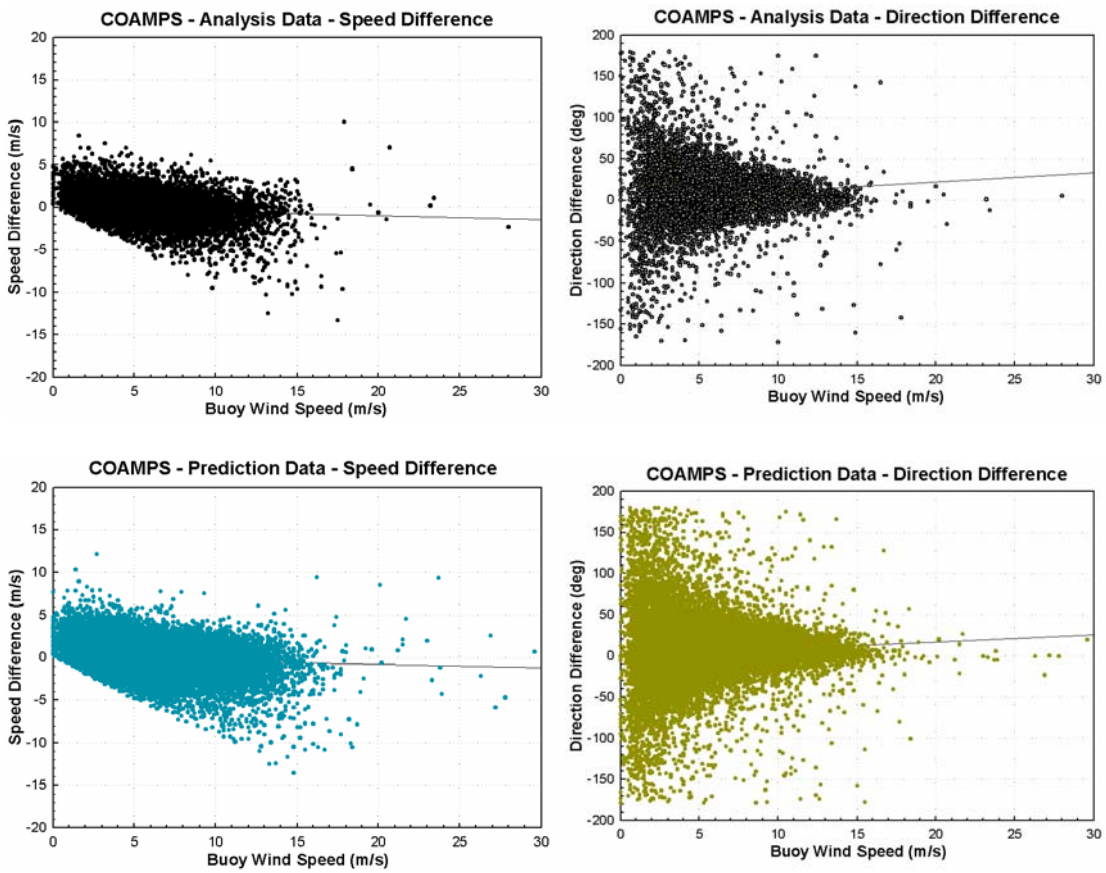

Figure 23. Difference in measurements by COAMPS and the buoys (CO-Buoys) for wind speed (left panels) and direction (right panels) are plotted against the buoy wind speed to illustrate the effect of increase in wind speed to accuracy of COAMPS measurement.

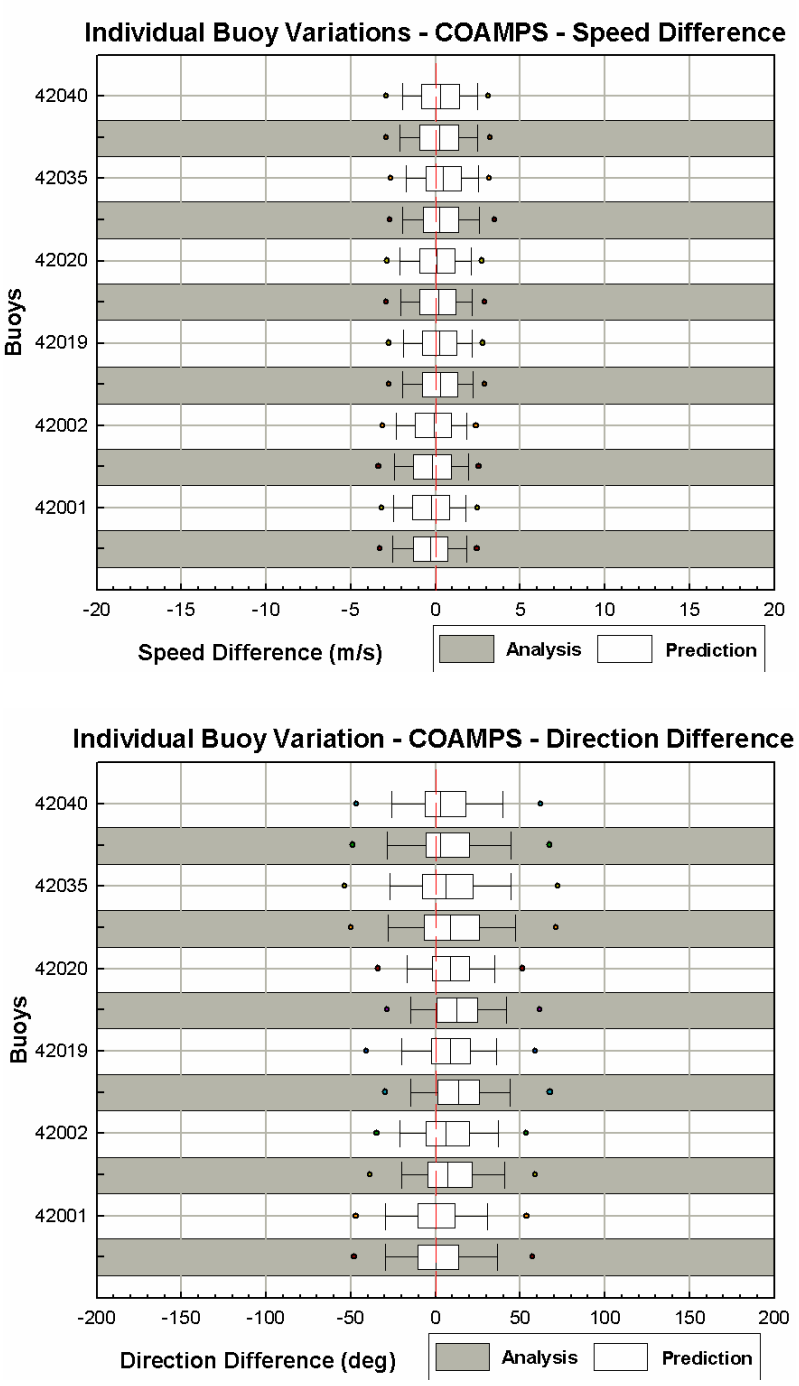

Figure 24. Individual buoy variations for difference in wind retrievals by COAMPS and buoys for all the buoys under consideration. Both analysis and prediction data are plotted together for comparison. The edges of the boxes depict the 25th and 75th percentile. The central line denotes the median. The error bars beyond the box depict the 10th and 90th percentile and the points depict the 5th and 95th percentile.

The important point to notice here is that the correlations for the analysis data and prediction data are the same which speaks well for the forecasting capabilities of COAMPS. Figure 23 displays the relationship between the buoy wind speed and the difference between the measurements by COAMPS and buoys. At low wind speeds, COAMPS is slightly positively biased, i.e. it overestimates the winds. As the wind speed increases, COAMPS tends to underestimate the intensity. This trend is displayed by both analysis and prediction data. Another observation that stands out is that the lower edge of the scattered datapoints appears to fall along a straight, downward-sloping line. This is seen for both analysis and prediction data. For wind direction, COAMPS shows greater discrepancy in measurement at low wind speeds with higher accuracy as the wind speed increases, very much like QuikSCAT. In Figure 24, differences in measurements at each buoy are plotted as box plots to study the variance with location of buoy. The results are fairly constant for all the buoys for both wind speed and direction.

2.4.5. Statistics

Regression analysis was performed on the datasets to obtain the values of coefficient of determination (R^2), root mean square error (RMSE), F-test significance and two-sample t-test significance (Table 2). The F-test and t-test are generally performed whenever two datasets are directly compared for similarity in variance and mean respectively. The regression procedure available in SAS was used to obtain the R^2 and RMSE values. The F-test was performed to determine if the difference in variances of the two datasets under consideration was significant and t-test was performed to determine if the difference in means of the same datasets was significant.

Table 2. Regression analysis and statistics tests results.

Dataset	Speed				Direction			
	R^2	RMSE	F-test p-value	t-test p-value	R^2	RMSE	F-test p-value	t-test p-value
QS Level 3								
All Data	0.72	1.69	0.0595	<0.0001	0.82	40.52	0.5452	0.0001
Moderate Winds	0.67	1.66	0.0002	<0.0001	0.86	34.08	0.4356	0.0004
Moderate Winds/Select Buoys	0.75	1.48	<0.0001	<0.0001	0.89	29.53	0.7552	0.0028
QS Level 2B – DIRTH								
All Data	0.83	1.24	<0.0001	<0.0001	0.86	33.77	0.6574	0.0493
Moderate Winds	0.80	1.22	0.5005	<0.0001	0.91	27.09	0.7237	0.0910
Moderate Winds/Select Buoys	0.88	0.94	0.0094	<0.0001	0.93	23.31	0.7046	0.1408
QS Level 2B – NWP								
All Data	0.79	1.55	0.0008	<0.0001	0.89	30.24	0.6840	0.0058
Moderate Winds	0.74	1.55	<0.0001	<0.0001	0.95	20.70	0.7874	0.0160
Moderate Winds/Select Buoys	0.79	1.37	<0.0001	<0.0001	0.97	14.99	0.8860	0.0357
QS NWP vs. DIRTH								
All Data	0.78	1.60	<0.0001	<0.0001	0.95	19.93	0.4340	0.1817
Moderate Winds	0.74	1.55	<0.0001	<0.0001	0.94	20.57	0.2818	0.1424
Moderate Winds/Select Buoys	0.73	1.56	<0.0001	<0.0001	0.90	26.98	0.4508	0.0898
COAMPS								
Analysis Data	0.64	1.75	<0.0001	0.7545	0.76	43.42	0.0002	<0.0001
Prediction Data	0.66	1.70	<0.0001	0.0502	0.77	42.85	0.0051	<0.0001

If the variances could be considered to be equal from the F-test, pooled t-test was performed assuming equal variances, else Satterwaithe t-test was performed assuming unequal variances. The significance used in the study was 0.05, i.e. a 95% confidence interval. Results from these tests are presented in Table 2.

2.5. Conclusion

The regressions for Level 3 winds are fairly good for both wind speed and direction. The effect of light and strong winds is quite apparent especially for wind direction. QuikSCAT is unable to accurately determine the direction of the wind if it is too low in magnitude. Since the number of data points for higher wind speeds is very low, no definite conclusion can be made. For the evaluation of any measurement method, it is important to ensure that the reference being used for comparison is accurate and reliable. Two buoys in the study, i.e. 42046 and 42362, are half-hourly and hourly respectively with lower levels of measurement accuracy. Such discrepancy can lead to reductions in correlation. From the monthly time series analysis of the QuikSCAT winds and their differences from the buoy winds, it can be observed that these buoys are inappropriate for evaluation of another method of measurement. The best regressions were obtained using moderate winds. From the plots of speed and direction differences against buoy wind speed, the QuikSCAT speed measurements are more or less evenly distributed about zero. For direction differences, there is greater variance for low wind speeds and the accuracy increases with speed. The Pacific buoys, provided for referencing and comparison, show very good correlations, however, the measurements are not much different from the GOM measurements, especially for wind direction. Hence, it can be concluded that QuikSCAT retrievals are fairly reliable in coastal regions. Measurements

at individual buoys show that distance from the coast does make a big impact on measurement accuracy.

Level 2B DIRTH winds gave the best results among all the datasets. NWP winds also show good results, but slightly lower than DIRTH winds. The variations in correlations with the entire dataset and moderate winds are the same as in Level 3. The coefficient of determination for NWP wind direction is higher than that for DIRTH indicating that the ambiguities used to obtain the selected wind solution were not very accurate and the NWP measurements are much closer to reality. For the Pacific buoys, correlations are expectedly good, being only slightly better than GOM correlations. Comparing NWP and DIRTH winds, correlations obtained were fairly good, though not as good as their individual comparisons with buoy data. Once again, the distance of the buoy from shore has an effect on the accuracy of QuikSCAT winds due to land contamination.

COAMPS winds were not as well correlated as QuikSCAT winds; however, the results are fairly good. The Pacific reference buoys were not considered for the model. The important point to note here is that the regressions for analysis data and prediction data are similar. Hence, the accuracy of COAMPS is quite good for predictions. However, both analysis and prediction datasets show that COAMPS overestimates low wind speeds and significantly underestimates high wind speeds. The lower edge of the scattered datapoints appears to fall along a straight, downward-sloping line. The reason for this cannot be understood from the present study and further investigation on the working of the model has to be made. Also, similar to QuikSCAT, variance in wind direction measurements is higher at low wind speeds and the accuracy increases with

speed. For individual buoy variations, no significant difference can be seen among all the buoys.

Overall, it can be concluded that the Level 2B (DIRTH) winds from QuikSCAT are the most accurate among all the datasets. Because the Level 3 data is at a lower resolution and is averaged over the grid, its accuracy is found to be lower than the Level 2B dataset. The effect of land contamination is a major problem with QuikSCAT retrievals as the accuracy of measurement decreases with proximity to the coast. COAMPS also showed good results for both analysis and prediction data.

Chapter 3. Hurricanes

3.1. Introduction

With the advent of erratic global climatic changes, extreme weather conditions are becoming more frequent and sudden (Kossin et al., 2007). The devastation caused to an entire city by Hurricane Katrina in 2005, alone indicates the necessity for accurate and real-time climatic information. Many agencies are working towards developing better and faster storm and hurricane warning systems. Although there are many tools from which physical conditions of the atmosphere and the ocean can be obtained, satellites remain one of the most important as they are not affected by extreme turbulence, as opposed to in situ observations, and are capable of providing near-real-time, large-scale accurate information for forecasting and emergency preparedness.

NASA's QuikSCAT is one of the most important of these satellites because of its capability to measure winds in most weather conditions and also because it is not affected by the atmosphere and clouds. QuikSCAT data is readily and routinely available. Many studies have been conducted to determine the accuracy and effectiveness of QuikSCAT during extreme weather (Bao et al., 2000; Hennon et al., 2006; Yueh et al., 2003; Adams et al., 2005; Brennan et al.; Morey et al., 2006; Xie et al., 2006; Kossin et al., 2007). Most of these studies, however, have focused on comparing the performance of QuikSCAT to various models. Here, a relatively straightforward approach is taken to compare QuikSCAT wind retrievals with those of buoys in the Gulf of Mexico. COAMPS model data was available for the years 2005 and 2006, hence the regression analysis for it has been shown for the hurricanes that took place during those seasons. Seven hurricanes and

one tropical storm that took place from 2002 to 2006 are considered here. Table 2 below gives details of these storms along with the maximum intensity as reported by the best track analysis of the National Hurricane Center (NHC). The latest product from QuikSCAT, distributed by JPL, is used to ascertain the product's accuracy. This is the Level 2B (L2B) swath data with a resolution of 12.5km, double of its predecessors. From the correlation and evaluation chapter presented previously, it has been determined that L2B (DIRTH) winds are the most accurate with greatest correlation with buoy data, hence this is the dataset that is used here. Correlation studies were performed on these datasets for the specific days in which the hurricanes were present over the Gulf of Mexico. The results of the same are presented.

Table 3. Occurrences of hurricanes and their maximum intensities as reported by the NHC.

Hurricane	Dates of Occurrence in GOM	Maximum Intensity – NHC	
		m/s	knots
Lili	2-3 October 2002	64.3	125
Claudette	12-15 July 2003	38.58	75
Ivan	14-15 September 2004	72.016	140
Dennis	5-7 July 2005	64.3	125
Emily	15-17 July 2005	72.016	140
Katrina	26-29 August 2005	77.16	150
Rita	20-25 September 2005	79.732	155
Alberto (TS)	10-13 June 2006	30.864	60

3.2. Data

As mentioned above, the QuikSCAT product used is L2B 12.5 km swath data. This dataset was directly compared with ten buoys, well spread out in the Gulf of Mexico. Due to the conservativeness of the rain flag present in the data, it was not considered for this study. This is because most of the time, rain flagged data during hurricanes and storms

gives valid wind measurements as the attenuation and scattering caused by rain is overshadowed by the extremely strong winds. Chelton et al. (2006) established that for buoy wind speeds higher than 13 m/s, the accuracy of rain-flagged QuikSCAT measurements are not significantly better than rain-free measurements. Details of such conditions and their effects on the measurements are discussed in detail in Section 4. For understanding the impact of sea surface temperature (SST) on the intensity of the hurricanes, MODIS Aqua and GOES-12 SST maps (Walker et al., 2005; Walker et al., 2006) were studied.

Even though a direct relationship between the two does not exist, an increase in SST can lead to a substantial increase in the intensity of the hurricane. Changes in SST as small as 1˚C, near the inner core of the hurricane, can lead to almost 40% increase in the total enthalpy (sensible and latent heat) flux (Cione and Uhlhorn, 2003) in the high wind hurricane environment. Hence, the presence of the Loop Current or warm core rings can provide a large reservoir of heat that can extend down to about 150 meters in the case of the Loop Current. However, the stability of the troposphere can reduce the effect of increase in SST. If the troposphere is stable and if there is not much difference between the SST and the temperature of the marine atmospheric boundary layer (MABL), the effect of intensification of the storm is reduced (Chelton et al., 2004). Also, at the low latitudes of the Gulf of Mexico, even weak storms that are moving fast will be more likely to intensify as opposed to stronger and slower storms at higher latitudes (Cione and Uhlhorn, 2003). Although a strong relationship exists between intensity and SST, as mentioned above, it is not very direct. Atmospheric shear is another very important factor that can dramatically impact the strengthening of the hurricane (Emanuel, 2005), along

with atmospheric stability and cloud-top temperature, however, all these factors are beyond the scope of this study.

The geographical locations of the buoys and the tracks of all the storms are displayed in Figure 25. For comparison of QuikSCAT and buoy measurements, the maximum time difference between the measurements was maintained at 5min and the maximum spatial difference was maintained at 0.1° (~10km).

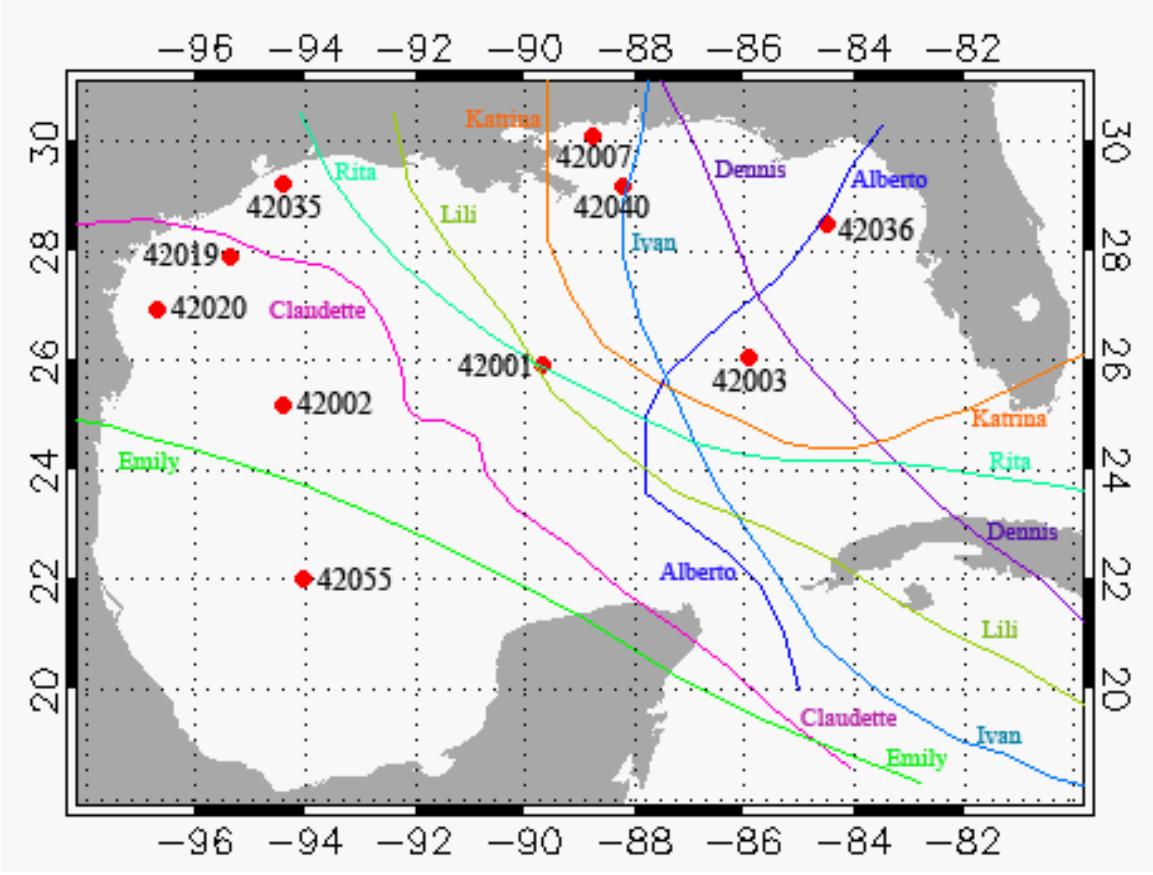

Figure 25. Map of the Gulf of Mexico showing all the buoys along with the tracks of all the storms examined in the present study.

3.3. Results

3.3.1. Regressions

The correlation between corresponding QuikSCAT and buoy speed and direction measurements are plotted below in Figures 26-28. For all the cases, the results are considerably encouraging. Hurricanes Dennis, Emily, Katrina, Rita and tropical storm Alberto also display COAMPS data for the same time period.

As is very obviously inferred from the graphs, all correlations are extremely good for all the hurricanes with the exception of Hurricane Ivan. The data is more scattered with reasonable correlation for wind speed but no correlation for wind direction. Various factors could have influenced such discrepancy. In order to understand those, three buoys were considered individually. As Hurricane Ivan traveled north, 42003, 42040 and 42007 lay directly in its path. The time series for these buoys were examined to see how the buoy wind measurements varied. The plots for 11th – 19th September 2004 are shown in Figures 29-31. Buoy 42003 measured a maximum wind speed of 28 m/s early on 15th September with the wind blowing towards west and then southwest. Buoy 42040 came closest to the eye of the hurricane and also measured a maximum wind speed of 28 m/s late on 15th September with the wind blowing towards the west. Just a few hours after this measurement, the buoy lost its mooring and went adrift due to the extreme turbulence and very high wave heights. Buoy 42007 measured a maximum wind speed of 26 m/s early on 16th September with the wind blowing towards the west and then changing direction on the 16th to blow to the north and subsequently northeast. The few (2 to 6) QuikSCAT measurements during the same time period are also shown. Because only one measurement is made every day, the continuous changes in wind measurements cannot

be seen. In Figures 29-31, due to lack of continuity, QuikSCAT measurements had to be depicted by a dotted line.

The COAMPS data for the 2005 and 2006 seasons also shows good correlation with a little more variance as compared to QuikSCAT. This can be explained by the fact that COAMPS provides analysis data, obtained by the integration of various sources, at 00:00 and 12:00 and provides predicted data for every 3 hours in between those times based on the previous analysis data. In which case, it can be observed that even the prediction data of COAMPS correlates reasonably well with actual buoy data at that time.

3.3.2. SSHA and SST

The L2B winds from QuikSCAT were plotted as wind vectors to create vector maps overlaid upon sea surface height anomaly (SSHA) measurements from Jason-1 for the Gulf of Mexico. This program was developed and mapped in IDL. The wind vectors are averaged and gridded along a 0.4˚ x 0.4˚ grid for clarity. Although this is a lower resolution than the actual resolution of the data, we believe the accuracy of the data was not compromised as the averaging of accurate data will give an accurate estimation for that area. From these maps, it could be observed that on certain occasions, there was a noticeable increase in intensity of the hurricanes as they traveled across the GOM. To understand the reason of this, these maps were then compared with MODIS Aqua SST nighttime maps using data obtained from the website http://oceancolor.gsfc.nasa.gov/ and the GOES-12 SST maps obtained from Walker et al. (2005) and Walker et al. (2006a,b). The SSHA measurements are in 10-day cycles. The vector winds plotted using the L2B dataset from QuikSCAT are satisfactorily able to depict the closed circulation of the storms and the exact location of the eye.

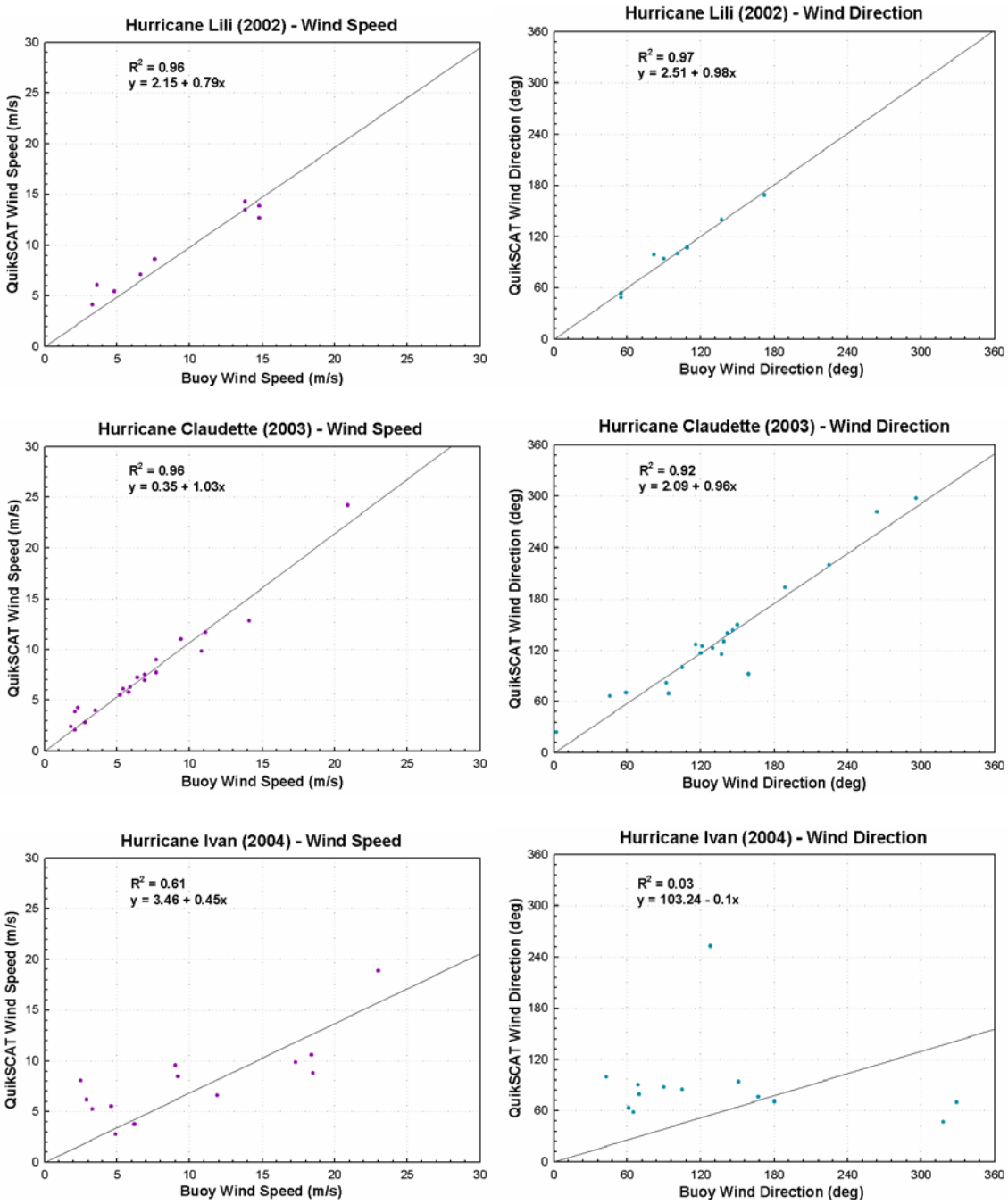

Figure 26. Regression plots for Hurricanes Lili (upper), Claudette (middle) and Ivan (lower) for wind speed (left) and direction (right).

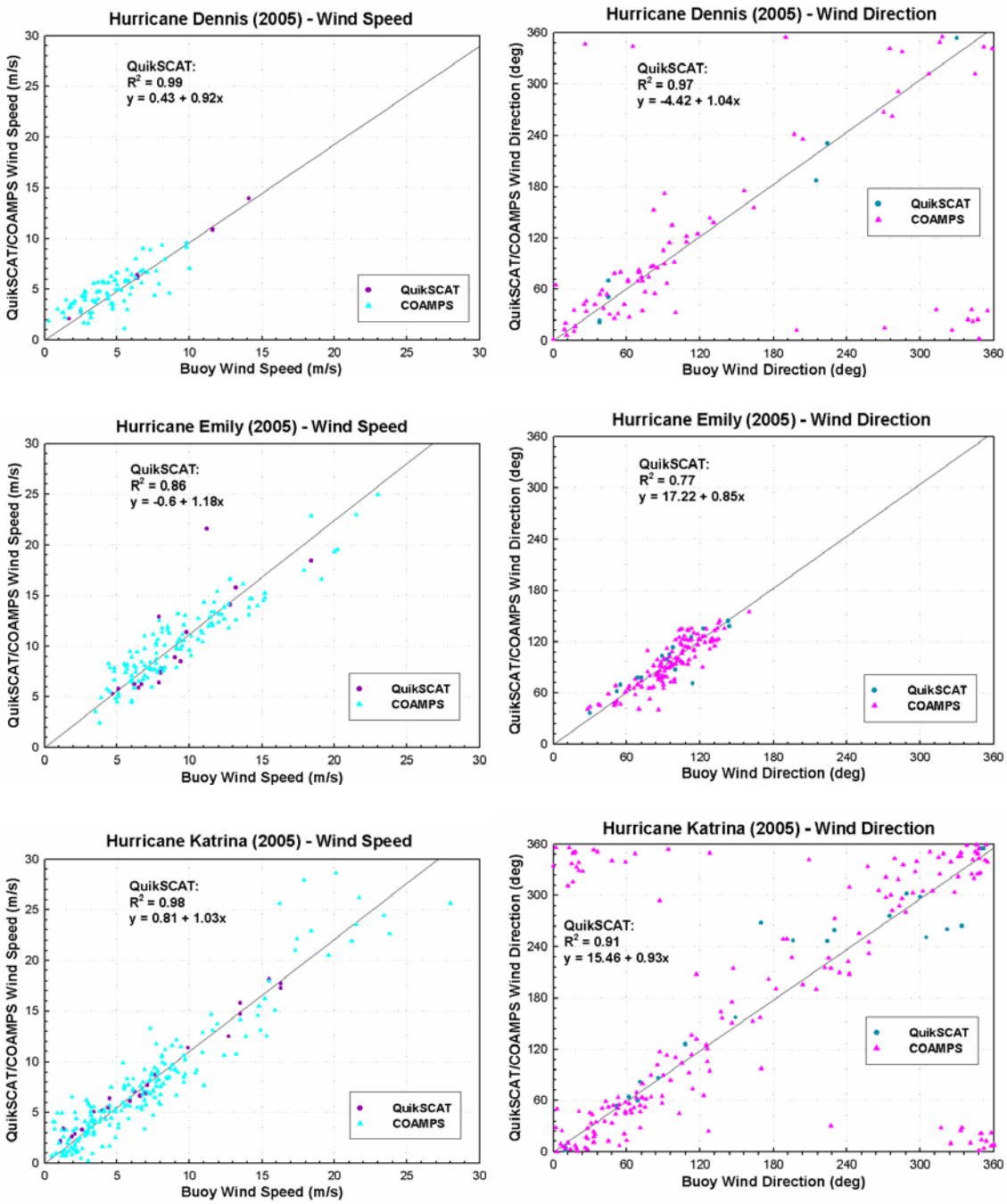

Figure 27. Regression plots for Hurricanes Dennis (upper), Emily (middle) and Katrina (lower) for wind speed (left) and direction (right). The R-square value and equation correspond to the regression between QuikSCAT and the buoys.

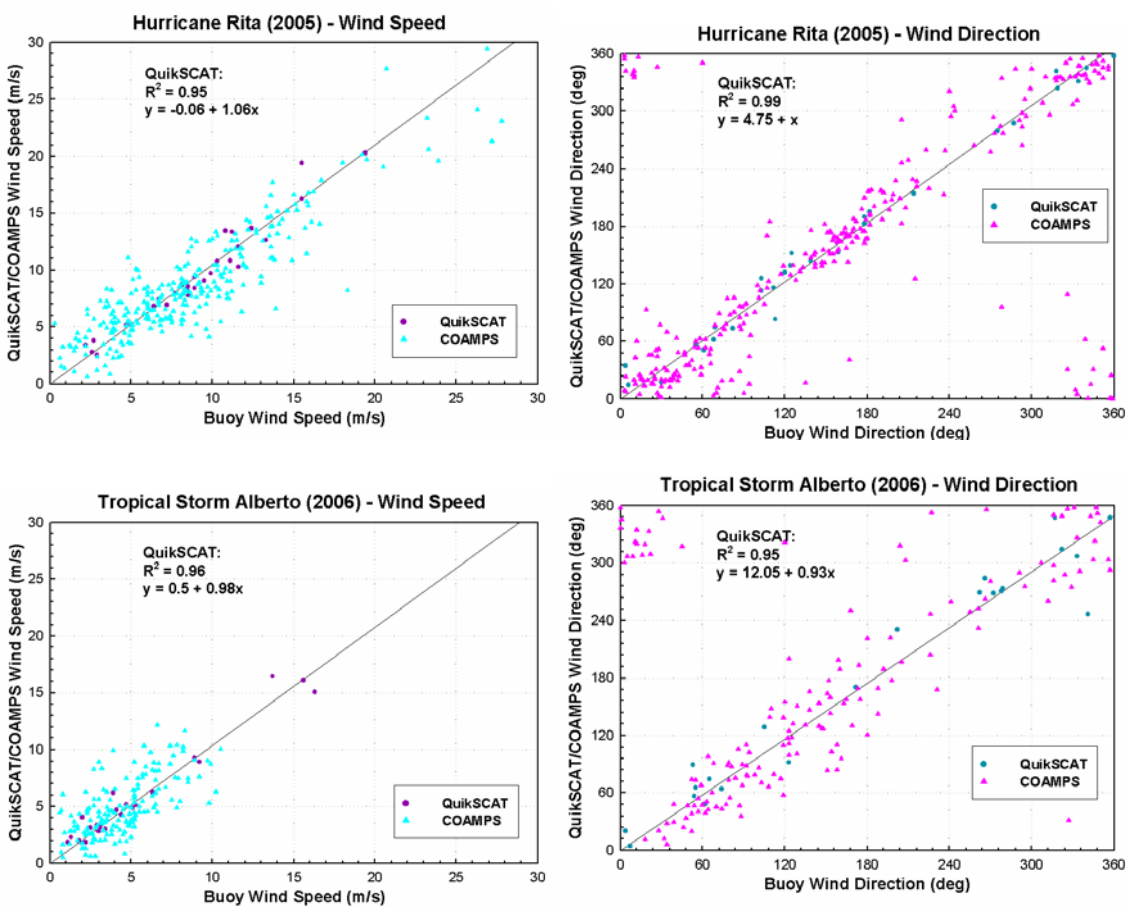

Figure 28. Regression plots for Hurricane Rita and Tropical Storm Alberto for wind speed (left) and direction (right). The R-square value and equation correspond to the regression between QuikSCAT and the buoys.

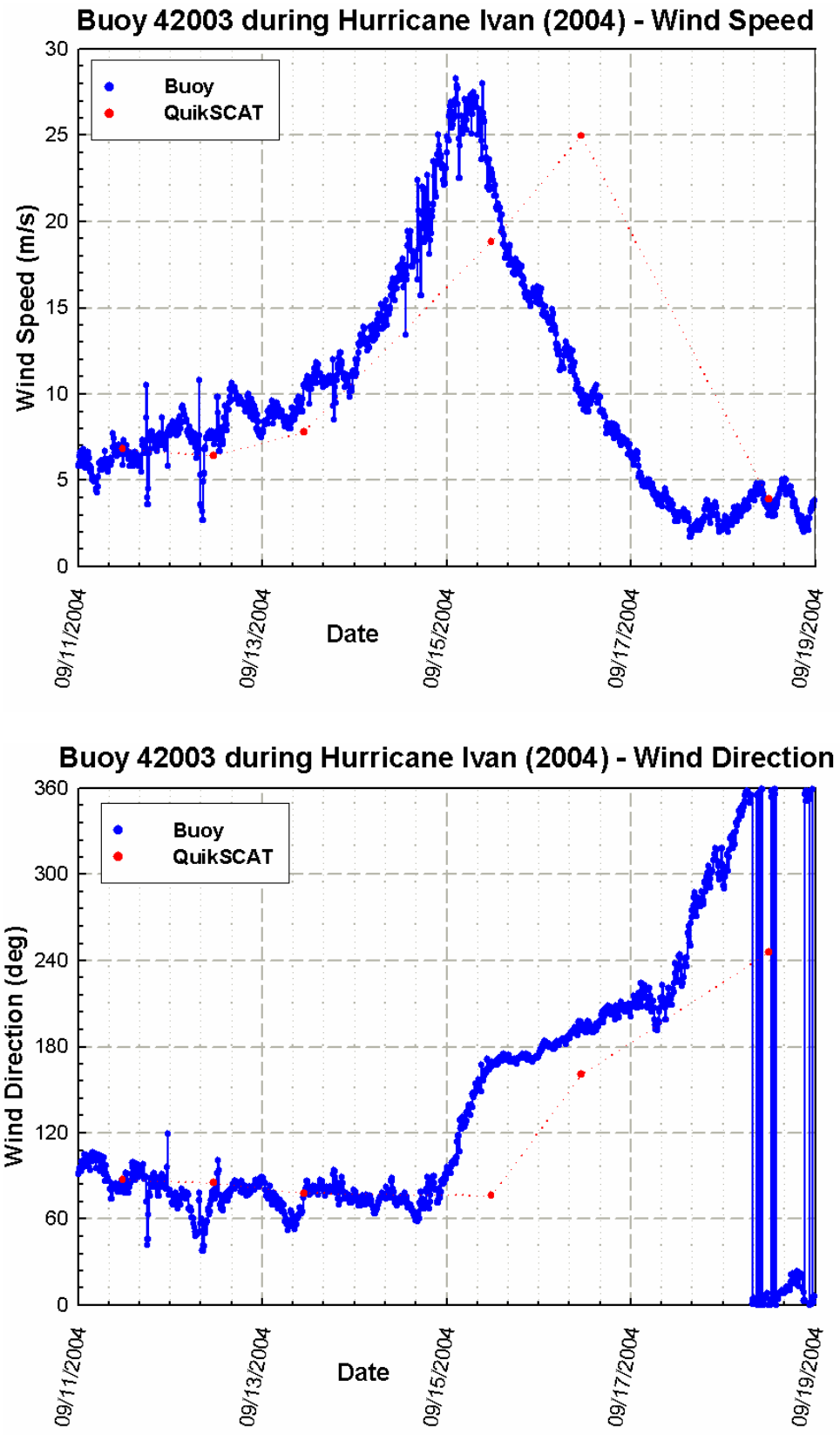

Figure 29. Time series analysis for buoy 42003 during Hurricane Ivan for wind speed (above) and wind direction (below).

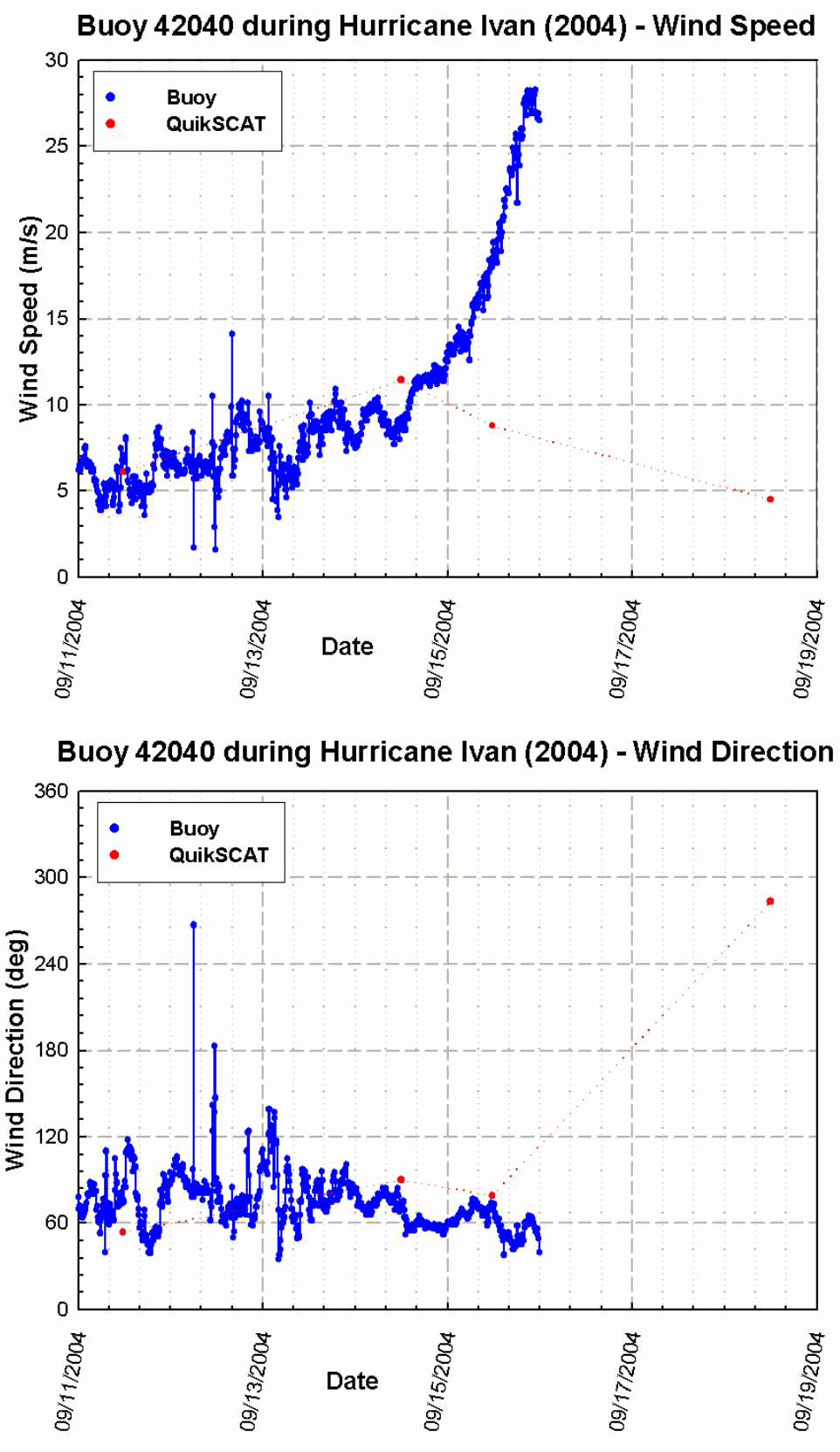

Figure 30. Time series analysis for buoy 42040 during Hurricane Ivan for wind speed (above) and wind direction (below).

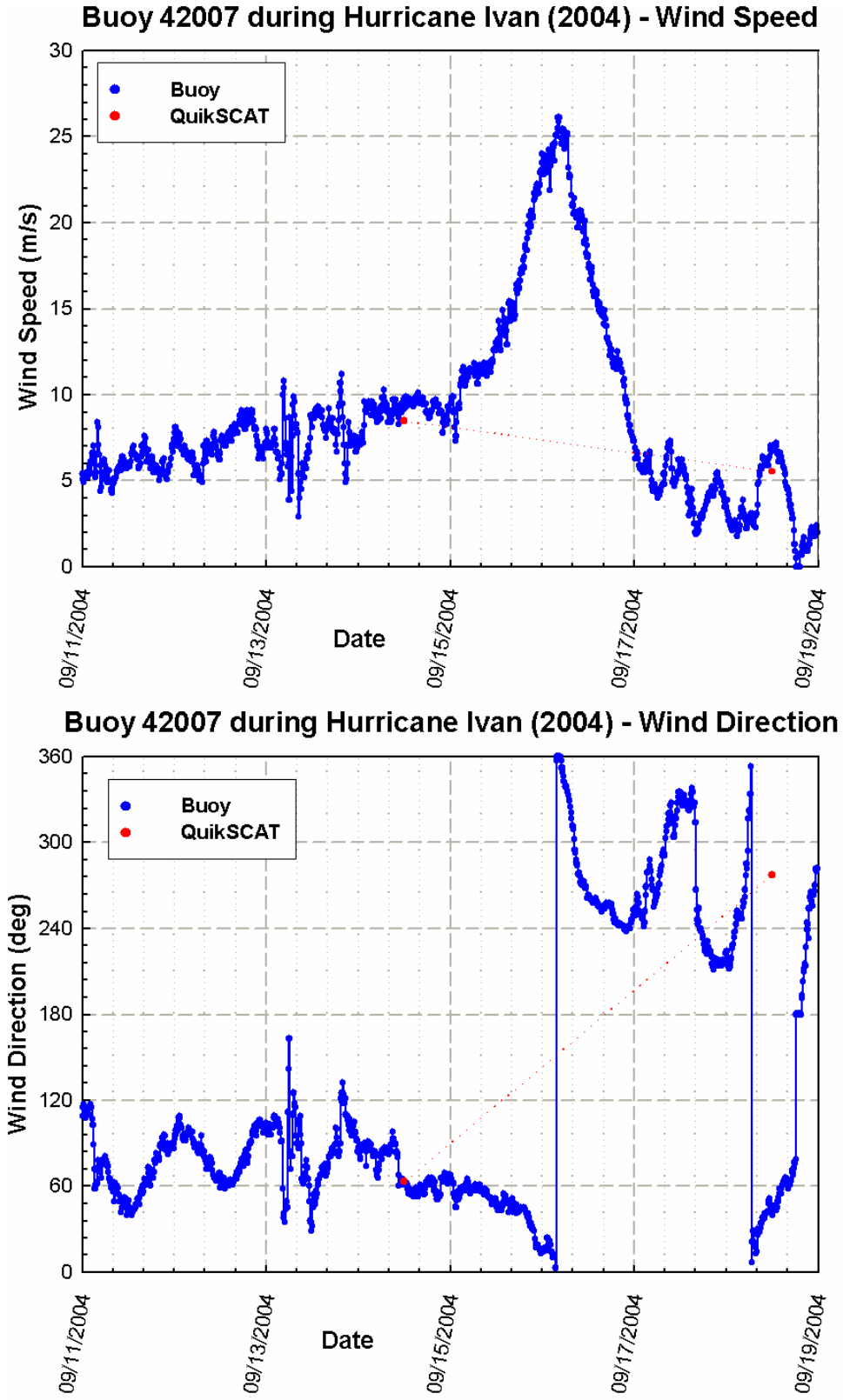

Figure 31. Time series analysis of buoy 42007 during Hurricane Ivan for wind speed (above) and wind direction (below).

One drawback with the vector fields from QuikSCAT is that many times a part of the GOM is not covered because it didn't fall in the swath. This leads to substantial loss of data which may be at a very critical time as can be seen in many of the maps below. It can be observed from the maps that SSHA and SST have many similarities and tend to mirror some features. It has been previously observed (Cione and Uhlhorn, 2003; Chelton et al., 2004; Emanuel, 2005) that winds increase in magnitude over areas of higher SST and decrease in magnitude over areas of lower SST. This trend is seen very clearly when the SST gradient is high. Thus, the intensity of a hurricane is likely to increase if higher SST is available in its path and more so if the gradient of SST increase is large. The wind, SSHA and SST fields for Hurricanes Ivan and Katrina are shown as an example of this process (Figures 32 – 37).

Figure 32 displays the wind and SSHA fields for Hurricane Ivan. The entry of the hurricane into the GOM is captured on the first map. On the second map, i.e. 15th Sept, the hurricane can be seen nearing the coast just below the Mississippi River delta. It was at the end of this day that buoy 42040 was set adrift by the high seas caused by Hurricane Ivan (Walker et al., 2005). A definite increase in intensity can be observed from the wind fields. The SST conditions, from MODIS Aqua (Figure 33), before the hurricane came into the GOM are relatively high and spread throughout, which means that the hurricane had a significant supply of heat. This is further verified by the trail of cold water that the hurricane left in its wake. The GOES-12 nighttime composite SST image (Figure 34) displayed higher accuracy with respect to mesoscale variations in SST conditions. The SSHA measurements from Jason-1 (Figure 32) are from a cycle that occurred before the passage of the storm, while in Figure 34, the SSH measurements (referred to as 'SSH-W' from now on) are performed immediately after the passage of the storm. From the SSHA

measurements, it can be observed that the Loop Current (LC) was at an elevation slightly lower than the mean. Also, the presence of an eddy, probably a warm core ring (WCR) from the elevated sea level, is seen north of the LC. From Figure 34, the LC can be seen clearly by SSH-W and it appears to be connected to a WCR (indicated by a positive SSH). This may be the same WCR as observed from the SSHA. Areas of upwelling, after the passage of the storm, can be seen on the north and south of the WCR in Figure 34 in areas of cyclonic circulation as discussed by Walker et al. (2005). Due to the coarseness of the data, these features cannot be seen in the SSHA fields, however, as indicated by Walker et al. (2005), the cyclonic features were already present before the passage of the hurricane. The same regions of cooling can be seen in Figure 33. Thus, the hurricane passed directly over the LC and the WCR as it traversed the GOM.

The wind fields of Hurricane Katrina are quite visible in the vector maps (Figure 35). Once again, a definite increase in intensity of the hurricane is seen in the second map as compared to the first map. Hurricane Katrina had the highest SST fields (MODIS) compared to the previous hurricanes (not shown). This would explain the higher intensities experienced during the passage of this storm. Much of the heat is fluxed out from the seawater during the lifetime of the hurricane. The MODIS images depict a cold wake all along the track of the hurricane after its passage (Figure 36). The SSHA fields reveal regions of elevated sea level in central GOM. The SSH-W fields (Figure 37) depict these regions as the LC and its eddy (formation of a WCR). Two areas of cooling are observed, one directly north of the LC eddy and the other (less intense) on the southern portion west of the LC. Both these regions depict the presence of cyclonic circulation. There is overall cooling to the east of the hurricane track.

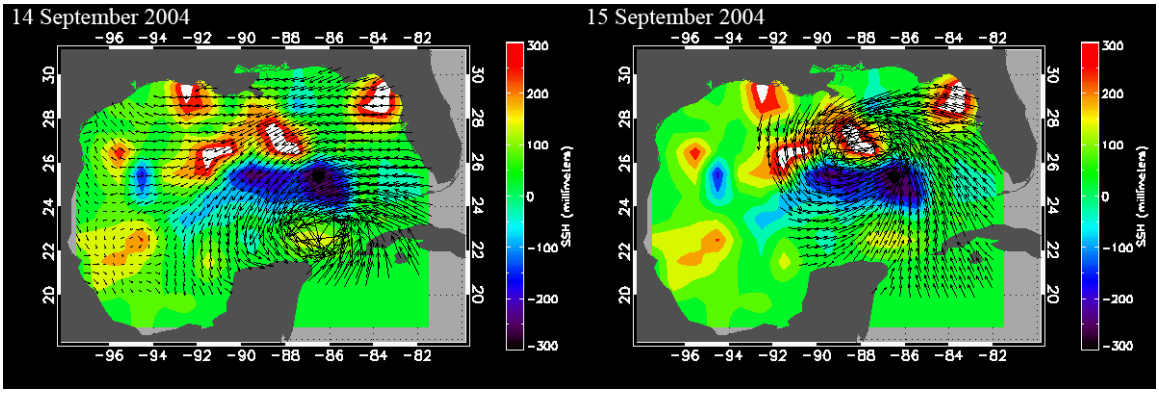

Figure 32. Vector winds overlaid on top of SSHA measurements during Hurricane Ivan during 14th (left) and 15th (right) Sept, 2004.

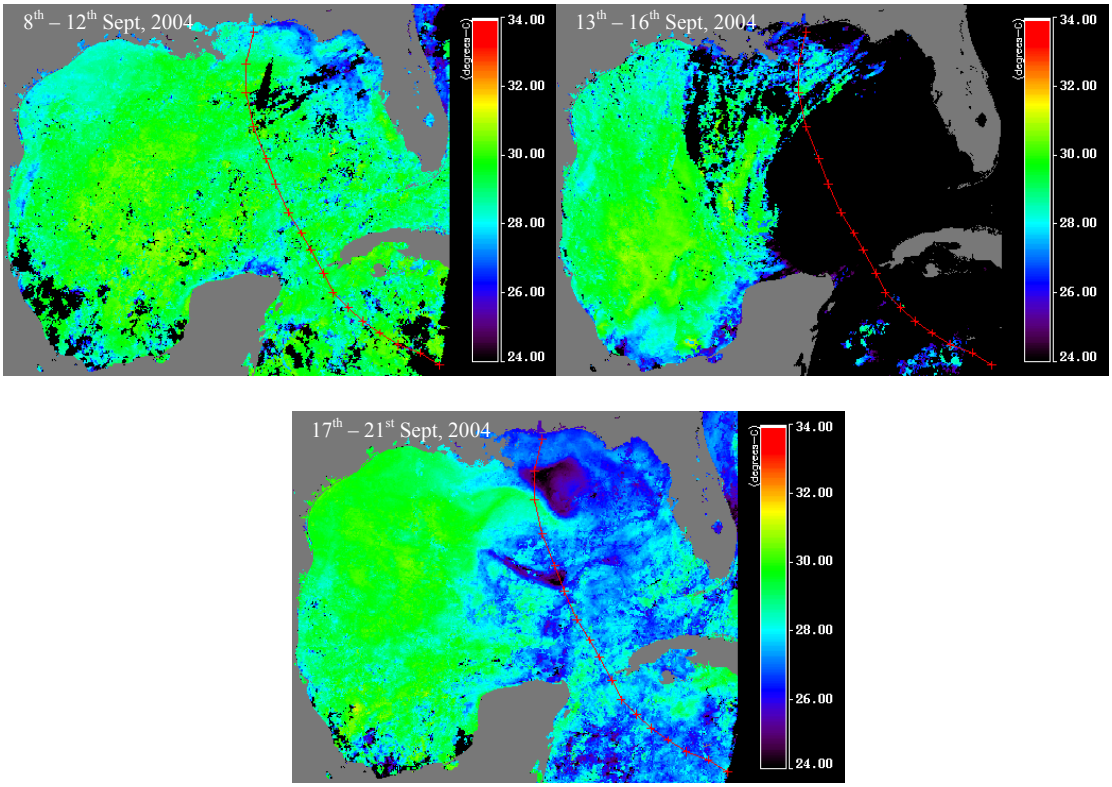

Figure 33. MODIS SST nighttime measurements during Hurricane Ivan. Top, left map represents a 5-day composite before the hurricane came into the GOM (8th – 12th Sept, 2004). Top, right map represents a composite for the days when the hurricane was in the GOM (13th – 16th Sept, 2004). Lower map represents a 5-day composite after the hurricane made landfall (17th – 21st Sept, 2004).

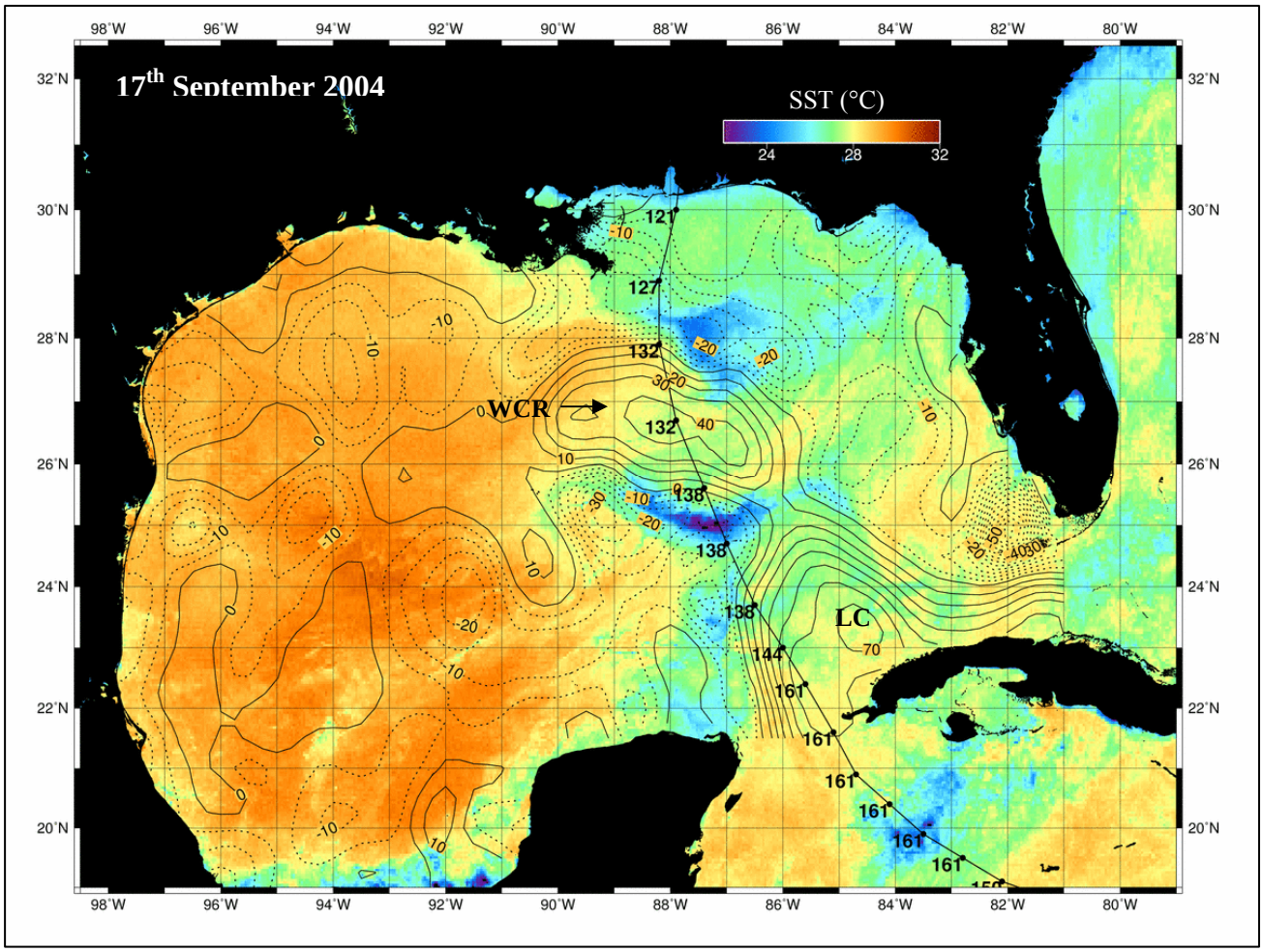

Figure 34. GOES-12 SST nighttime composite image for 17th Sept, 2004 showing sea surface cooling from Hurricane Ivan. SSH (in cm) are superimposed to reveal the location of the LC and eddies. Solid lines depict positive SSH and dashed depict negative SSH. The LC is a region of high SSH. Image obtained from Walker et al. (2005).

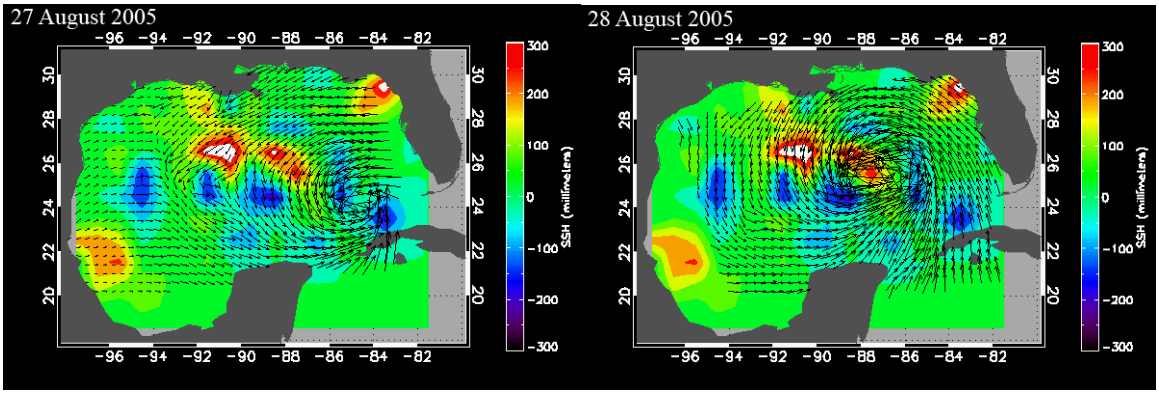

Figure 35. Vector winds overlaid on top of SSH measurements during Hurricane Katrina during 27th (left) and 28th (right) Aug, 2005.

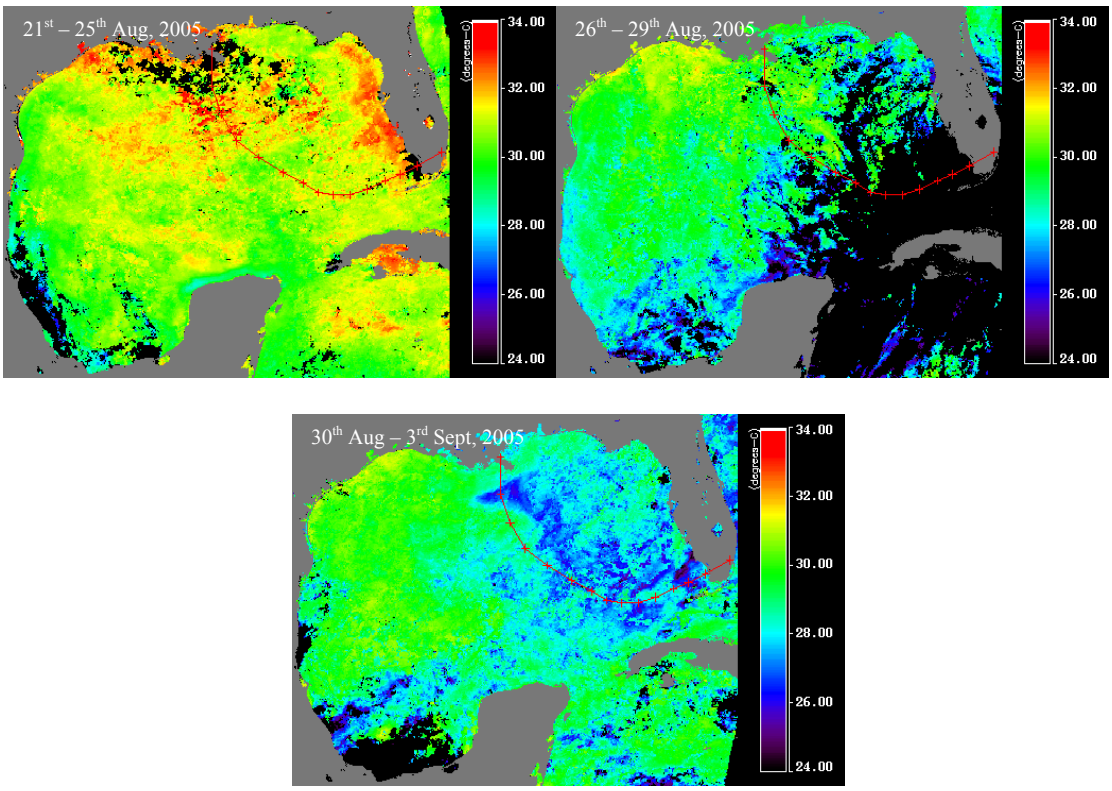

Figure 36. MODIS SST nighttime measurements during Hurricane Katrina. Top, left map represents a 5-day composite before the hurricane came into the GOM (21st – 25th Aug, 2005). Top, right map represents a composite for the days when the hurricane was in the GOM (26th – 29th Aug, 2005). Lower map represents a 5-day composite after the hurricane made landfall (30th Aug – 3rd Sept, 2005).

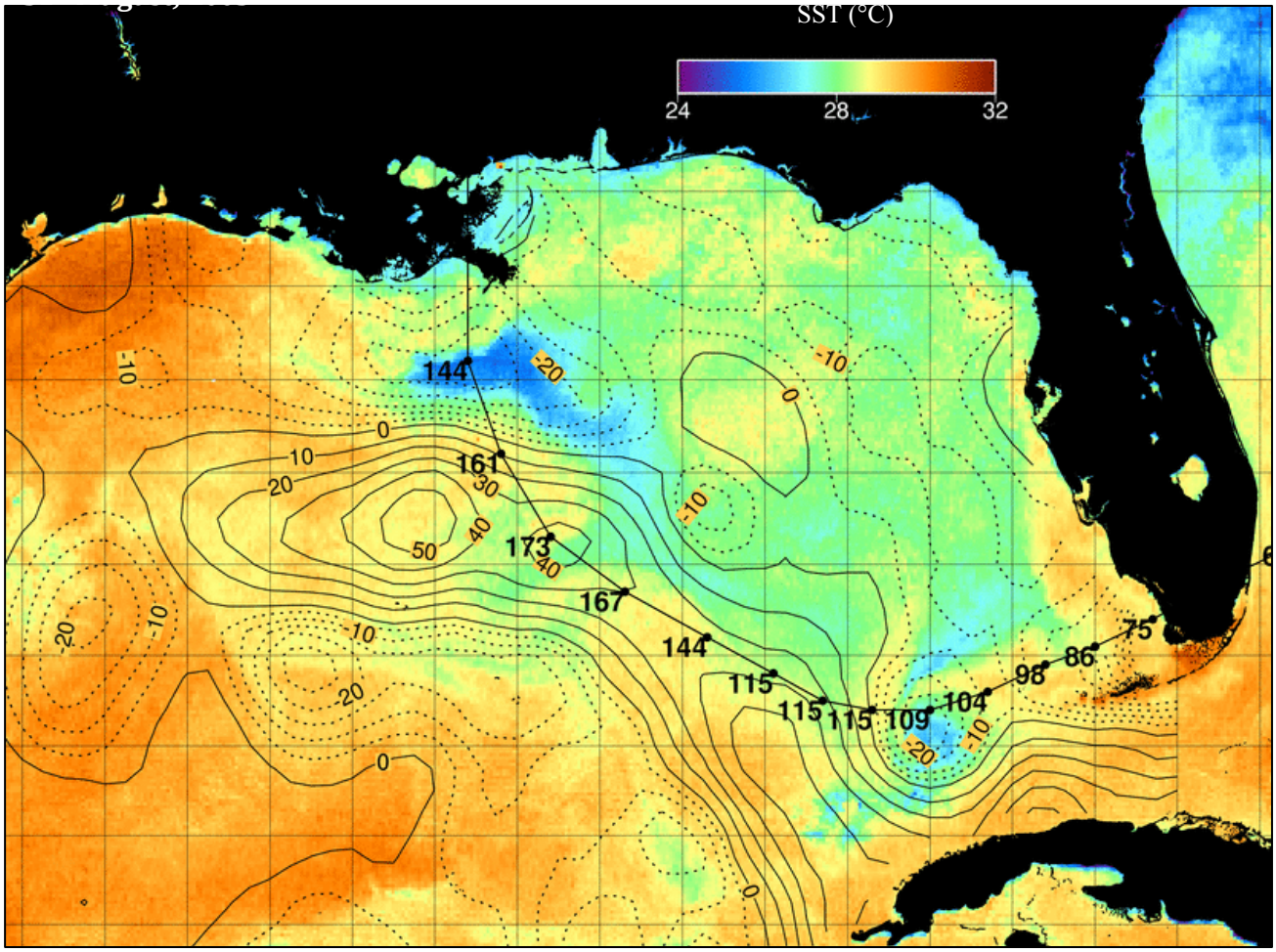

Figure 37. GOES-12 SST nighttime composite image for 31st Aug, 2005 showing sea surface cooling from Katrina. SSH (in cm) are superimposed to reveal the location of the LC and eddies. Solid lines depict positive SSH and dashed depict negative SSH. The LC is a region of high SSH. Image obtained from Walker et al. (2006a) and Walker et al. (2006b).

Table 4. Variations of QuikSCAT winds before and after passage over the LC and WCR.

Hurricanes	Before Date	Maximum QS Winds (m/s)	After Date	Maximum QS Winds (m/s)
Ivan	9/14/2004	18.78	9/15/2004	24.69
Katrina	8/27/2005	33.38	8/27/2005	48.63

The variations of hurricane intensities for both the hurricanes, as measured by QuikSCAT L2B, are given in Table 4. The actual measurements indicate an increase in intensity from Day 1 to Day 2 for both the hurricanes (Figures 32 and 35). These observations of QuikSCAT winds support the argument that the strength of a hurricane is affected by presence of the LC and WCRs.

3.3.3. Enhanced Wind Region

In the previous sections, we have seen how QuikSCAT has been able to accurately depict intensity changes due to variations in other physical parameters like SSH and SST. Although, with the current JPL GMF, QuikSCAT is unable to give accurate wind speed measurements during hurricanes, it is still an important tool for estimating the extent or region covered by enhanced wind speeds and the radius of maximum wind. Previous work (Hsu et al., 2000; Hsu and Babin, 2005; Kossin et al., 2007) has been done for the estimation of critical wind radii (i.e. 34-kt, 50-kt and 64-kt wind radii) and radius of maximum wind. Hsu et al. (2000) and Hsu and Babin (2005) used the method of cloud-top temperature detection for estimating the radius of maximum wind and compared it to estimations obtained using buoy data and aircraft reconnaissance. Kossin et al. (2007) described three different methods to obtain estimations of the radius of maximum wind and critical wind radii. None of the above studies used satellite microwave scatterometers for their estimations because, as we have seen in the previous sections, microwave scatterometers, like QuikSCAT, work best in moderate winds and low-precipitation regions. Hence, these are most useful only for obtaining approximate measurements of the outer core wind data. Aircraft reconnaissance, buoy data and now satellite IR-imagery are the preferred methods for estimating the inner core wind data. However, QuikSCAT

is used by the Tropical Prediction Center at NHC for estimation of wind radii, using their own GMF. It can be quite useful, especially for tropical cyclones, out in the open ocean where buoy and aircraft reconnaissance data is difficult to come by. According to the NHC, it is able to depict 34-kt and occasionally 50-kt wind radii for most storms and hurricanes whenever these radii extend beyond the region of high precipitation.

In the present study, a preliminary analysis on the region of enhanced winds is conducted. The estimation of the radius of maximum wind and the critical wind radii require many complex calculations in which many parameters have to be considered, like ability to discern the eye of the storm, the radius of the eye, the temperature in the eye and in the surrounding eyewall, the temperature at the region of maximum convection, wind shear, etc. Here, longitudinal (vertical) and latitudinal (horizontal) transects of the QS wind speeds were taken across the eyes of the Hurricanes Ivan and Katrina. These transects were plotted and aided in the estimation of the region of enhanced wind. These plots are presented below in Figures 38 and 39.

Hurricane Ivan (Figure 38) displays the region of enhanced wind to be to the southeast of the eye of the hurricane (denoted by the red line), as can be deciphered from the plots of vertical and horizontal transects. The rate of decrease in wind speed is observed to be greater towards the north and west. Hurricane Katrina was definitely a much stronger hurricane and this can be observed from the maximum QS winds (Figure 39). Unlike Hurricane Ivan, the wind field for Hurricane Katrina appears to be a little more symmetric about the eye of the hurricane. The convection appears to be slightly greater to the northeast of the hurricane eye. The rate of decrease in wind speed is greater to the south and west.

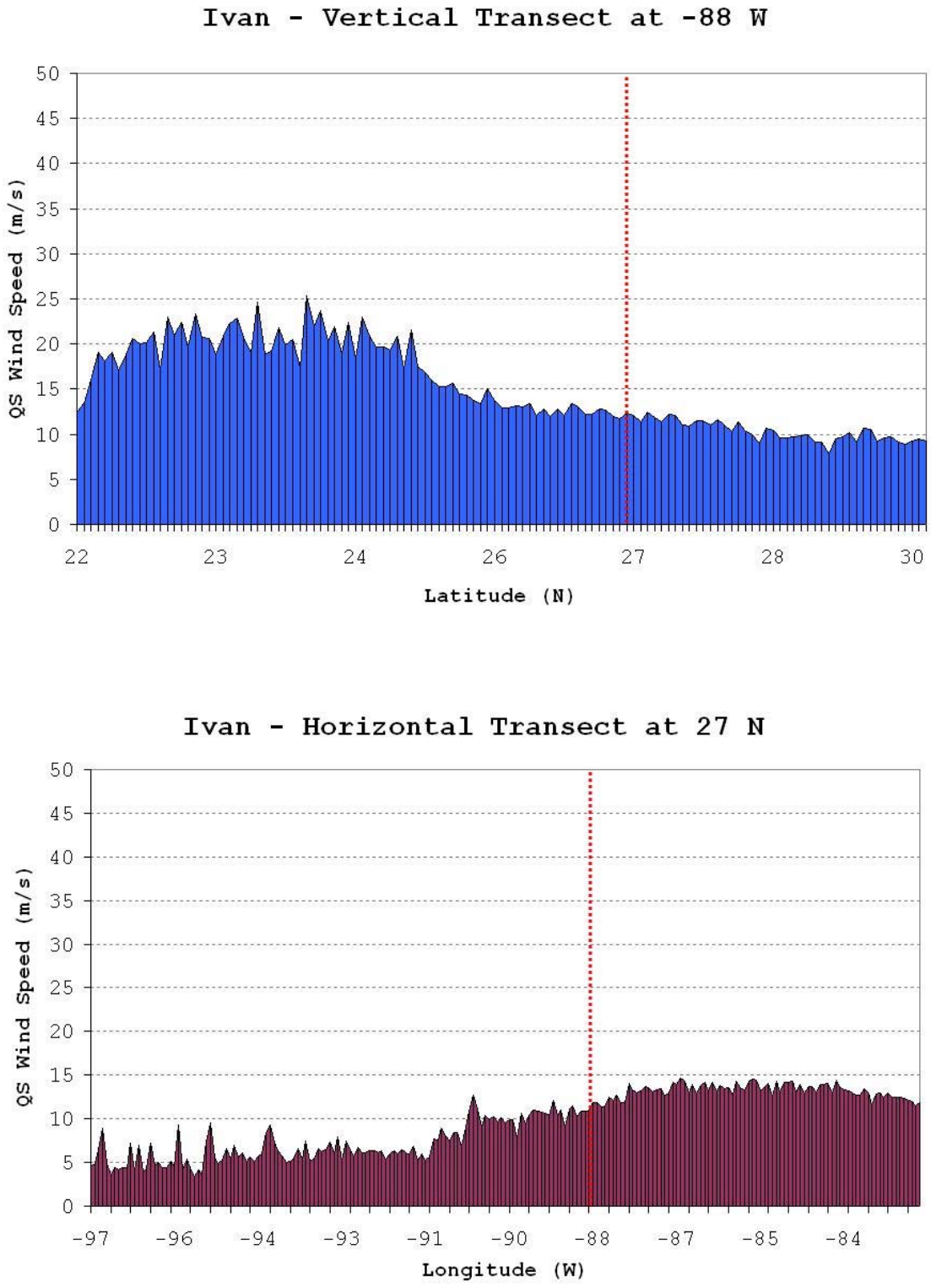

Figure 38. Vertical (longitudinal) and horizontal (latitudinal) transects across the eye of the Hurricane Ivan on 15th Sept, 2004. The red line depicts the location of the eye.

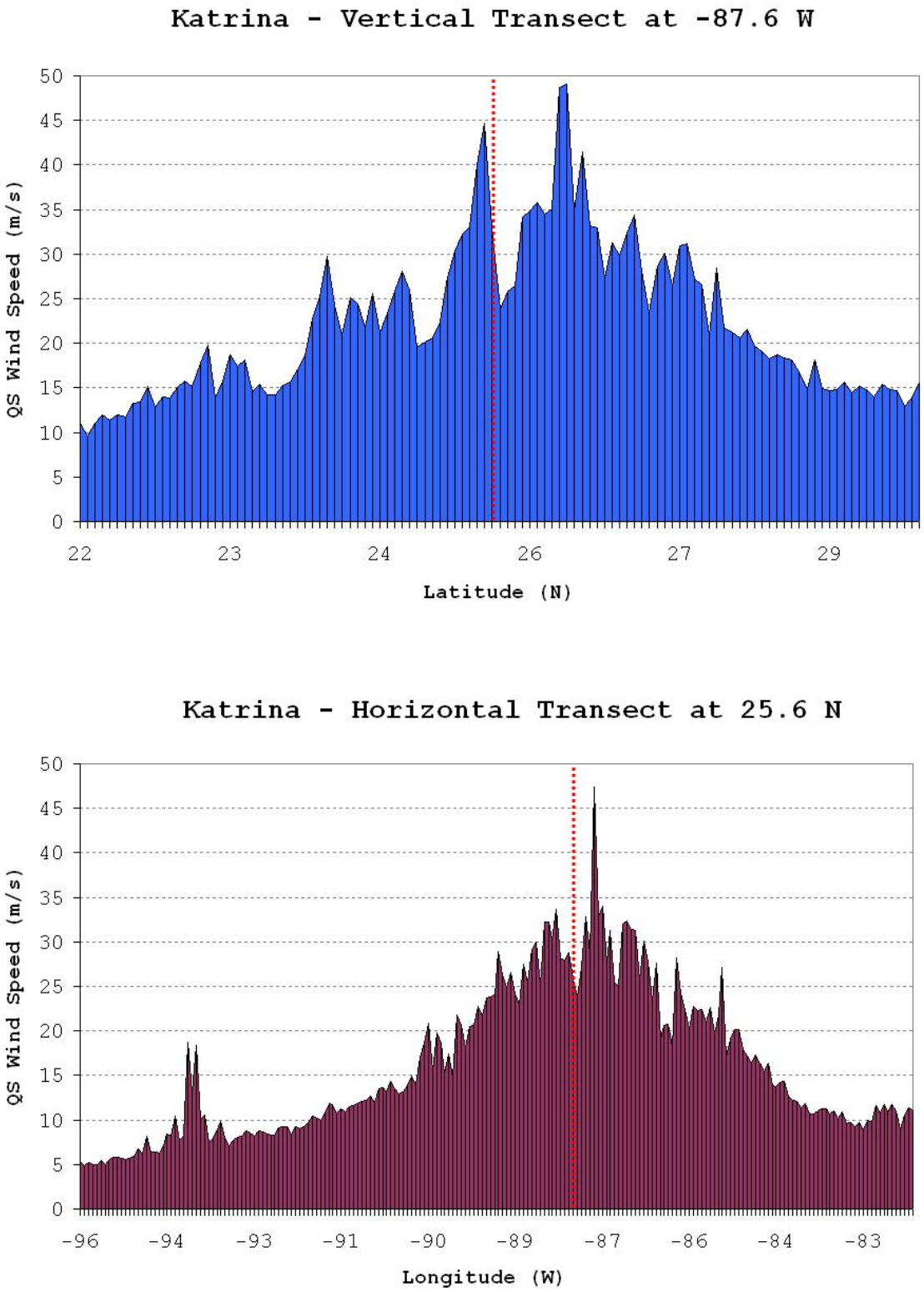

Figure 39. Vertical (longitudinal) and horizontal (latitudinal) transects across the eye of the Hurricane Katrina on 28th Aug, 2005. The red line depicts the location of the eye.

3.4. Conclusion and Discussion

All regression plots show very good results indicating that QuikSCAT data follows the accuracy of buoy data closely during hurricanes. Interestingly, Hurricane Ivan was an exception to this. Wind speed correlation is very small and wind direction is quite uncorrelated. Three buoys that lay directly in the path of the hurricane were considered separately to visualize the time series of the wind retrievals by the buoys and QuikSCAT. QuikSCAT data was not very abundant and, hence, is not very representative. Research of this discrepancy for Hurricane Ivan brings forth many intriguing facts. The maximum sustained winds measured by the buoys were less than half the value specified by the NHC best track analysis. The reason why the measurements done by the buoys get affected so much is mainly the extreme wave heights experienced as the hurricane passes by. The highest wave height measured at buoy 42003 was 36 ft. Buoy 42040 measured seas as high as 52 ft and at buoy 42007 the highest wave height measured was 20 ft. Such unusually high wave heights created tremendous damage to various structures, including buoys, located in the gulf, although the storm surge was not as high as that by Hurricane Katrina in the following year (Stone et al., 2005). According to the NHC report, "Ivan was the most destructive hurricane to affect this area in more than 100 years."

Buoys experience all the turbulence and violence of nature at the time of measurement. Readings taken by a buoy are averaged over 8-minute periods and if the buoy is spending a significant portion of this time in the trough of a wave, the wind is likely to be diminished. Also, the tipping over of the buoy prevents it from being perpendicular to the surface at all times. Hence, it becomes necessary to use a tool that is remote and unaffected. Many studies show the buoys have under reported the actual wind speeds despite their proximity to the hurricane. This explains the scales on the above

plots. Throughout the lifetime of the hurricanes, the wind speeds didn't increase beyond 30 m/s, although the NHC reported maximum sustained winds more than twice as high.

However, the hurricanes do not affect the buoys alone as QuikSCAT wind vectors also suffer from a substantial loss in accuracy. The excessive amount of rain tends to make the atmosphere opaque at the scatterometer frequency by drowning out radar echo by excessive backscatter. Being a Ku-band scatterometer, atmospheric effects to raindrops are very significant in the measurements of QuikSCAT. In addition to this, the geophysical model function (GMF) is also limited in its functionality. The design limit of the GMF is 30 m/s which is far too low for measuring hurricane winds. Hence, it is likely to give misleading measurements for such strong winds. Hennon et al. (2006) evaluated the performance of the present GMFs (25 km and 12.5 km) provided by QuikSCAT and concluded that beyond 15 m/s QuikSCAT's wind retrievals are extremely diminished. Yueh et al. (2003) performed an analysis on QuikSCAT wind retrievals during tropical cyclones. They compared a radiative transfer model derived from the collocated QuikSCAT and Special Sensor Microwave/Imager (SSM/I) dataset with that of a published parametric model developed for rain radars. Yueh et al. (2003) conducted the study to correct for the attenuation and scattering caused by rain. Their results displayed the reduction in wind direction sensitivity with increase in rain rates. When compared to the National Hurricane Center (NHC) best track analysis, they obtained very good results when using an improved QuikSCAT GMF with rain model corrections. Without these rain model corrections, the QuikSCAT measurements were almost half of the measurements by the NHC best track analysis. They concluded that QuikSCAT's performance is unreliable for wind speeds higher than 20 m/s. Their results are confirmed in the results obtained during this study. The ambiguity removal algorithm used to

determine the most accurate wind measurement at every wind vector cell is also not very efficient. It is very likely to make the wrong choice and give erroneous measurements.

The underlying issue is then that both sources of wind measurements are limited and cannot be completely relied upon. In order to overcome this drawback of QuikSCAT, new geophysical model functions have been suggested which have higher design limits to accommodate hurricane winds as well (e.g. Adams et al., 2005) with some success. NOAA Ocean Prediction Center (OPC) routinely makes use of QuikSCAT for their analysis and forecasting procedures. The OPC has its own function for deriving the wind measurements from the backscatter obtained by QuikSCAT, thereby enhancing its performance considerably. They are able to measure winds well in excess of the threshold of hurricane force winds (32.6 m/s), making QuikSCAT an extremely important tool in their forecasts.

The Tropical Prediction Center / NHC also uses QuikSCAT for most of its forecasts. This is because of QuikSCAT's ability for early detection of storms and hurricanes. QuikSCAT has a record of detecting a storm up to 45 hours before NHC declares it as one. It can detect a closed circulation even before it is declared as a depression by the NHC. This is because the system has to have a significant amount of convection and apparent circulation before it can be designated to be a tropical depression. QuikSCAT is an extremely important tool in the analysis done by NHC forecasters; however, they generally ignore the rain flag due to its conservativeness and calculate the ambiguities themselves as the standard ambiguity removal algorithm used by JPL tends to limit the ability of QuikSCAT to locate definite circulations (Brennan and Knabb, 2007). QuikSCAT also gives a very reliable estimate of the wind radii.

Vector wind and SSHA maps compared with SST fields provided a lot of information about the intensity changes of the hurricanes and relationships between SSHA, SST and winds. Though these relationships are not very direct and more or less implicit, the variations of one are likely to affect the other in some way. The SSHA measurements by Jason-1 are quite sparse with a low temporal resolution of 10 days. The SSH-W measurements, however, had a higher resolution and greater clarity. With the help of vector winds, the location of the eye of the hurricane can be accurately determined. However, one major problem being faced is the lack of complete coverage at all times. Due to this, many times crucial information about the onset of a storm or its progress and intensity variations is not available. MODIS SST images suffered from the effect of cloud coverage. During the storms, SST information is unclear due to the opaque barrier formed by the excess cloud formation. The GOES-12 nighttime, composite images using the mid-infrared channel, were able to provide better information regarding temporal changes in SST. These were less affected by cloud and water vapor because of effective cloud and atmospheric effect corrections in the processing algorithm (Walker et al., 2003). The position of the LC can be seen clearly as well as the presence of WCRs and cyclonic circulations using the gridded SSH data. The wind fields depict an increase in wind speeds between the QS measurements made on two consequent days for both Hurricanes Ivan and Katrina. From the SSHA and SSH-W fields, the LC and its eddies from before and after the storm, can be observed. In previous studies, the effect of the Loop Current and warm core rings on the intensification of hurricanes has been observed (Shay et al., 2000; Ritchie et al., 2003; Emanuel, 2005b; Walker et al., 2005; Walker et al., 2006a; Walker et al., 2006b). From the results seen in the present study, this has been verified. QuikSCAT winds indicated a definite increase in intensity after

passage of the hurricane over the Loop Current and any warm core rings that may be present in its path. The LC and WCRs, with surface mixed layers extending to depths of >100m (Walker et al., 2006b), act as large reservoirs of heat to hurricanes. Although QuikSCAT wind vectors are able to depict the subsequent effects and provide precise locations of the hurricane eye, the measurements are still diminished as compared to NHC reports.

QuikSCAT is still used by the NHC to obtain estimates of the radius of maximum wind and the critical wind radii whenever they are not obscured by heavy precipitation. In the present study, longitudinal and latitudinal transects about the eyes of the Hurricanes Ivan and Katrina were obtained to estimate the locations of the regions of enhanced wind. For Hurricane Ivan, the results depicted maximum convection to the southeast of the hurricane eye and for Hurricane Katrina, the maximum convection was seen to be to the northeast of the hurricane eye. This is a very preliminary study and further work on the calculation of the radius of maximum wind using other methods has to be conducted. Cloud-top and brightness temperatures in and around the eye-wall have to be taken into account and integrated with wind intensity measurements by QuikSCAT.

Chapter 4. Conclusion and Future Scope

In this study, the evaluation of QuikSCAT and COAMPS wind retrievals is compared with buoy wind measurements in the Gulf of Mexico. The study period is from January 2005 to February 2007. During the evaluation of any measurement method, it becomes important to ensure that accurate reference data are being used. For this reason, two buoys (42046 and 42362) with a higher temporal resolution than 10 min and with their measurements rounded off to the integer values were removed. Thus, overall my analysis contained two permutations of the dataset: all wind data and moderate wind data. For the evaluation of QuikSCAT, regression analyses were performed on the datasets obtained from QuikSCAT, namely, the Level 3 and Level 2B datasets. Although rain can adversely affect QuikSCAT measurements, the rain flagging technique adopted by QuikSCAT appears to be too conservative. This causes the loss of good data, hence rain flagging was not taken into consideration in this study. As QuikSCAT is known for its inaccuracy at low and high wind speeds (<3m/s and >20m/s), these conditions were eliminated from my analysis.

For L3 data, the comparisons between buoys and QuikSCAT were good; with the correlations increasing when light and strong winds were removed. The increases in correlations were strongest for the wind direction measurements indicating that these measurements are more sensitive to variations in wind speed. This is likely because it is difficult for the scatterometer to distinguish the direction of the wind when the backscatter is very low. This conclusion is corroborated in the plots where the difference in wind direction measurements from QuikSCAT and the buoys is plotted against buoy

wind speed. Maximum deviation from the zero line occurs at the low wind speeds with accuracy increasing with wind speed. The discrepancy in measurement accuracy with distance from shore is shown when the individual buoy measurements are considered. The QuikSCAT data has highest variations for buoys that are closest to land.

The L2B dataset from QuikSCAT has two different sub datasets, namely DIRTH and NWP measurements. The DIRTH winds are obtained by enhancing the ambiguity removal algorithm by reducing direction errors at nadir and far-swath measurements. The ambiguity removal algorithm has to have an initial direction measurement to choose the best wind solution among the ambiguities. For this purpose, NWP (NCEP global data analyses, 2.5˚ resolution, 1000mb) model winds are used. The wind solution closest to the NWP wind measurement nearest the wind vector cell at that time is chosen as the selected wind solution. Both these datasets are provided in the L2B product. The correlations obtained for the L2B winds are higher than those for L3. In fact, the best results were obtained for this dataset. Again, the results get better when light and strong winds are removed. The comparison between DIRTH and NWP is good, but not as good as would be expected since DIRTH winds are obtained after using NWP winds in the ambiguity removal. This is because NWP wind measurements are at 1000mb, i.e. 100m above the sea surface, not 10m. Also, the effect of land contamination is evident for nearshore measurements from the individual buoy results. Pacific reference buoys used for L3 and L2B evaluations displayed very good correlations but the results were not much better than those for the Gulf of Mexico, especially for wind direction measurements.

The COAMPS regional model displayed fairly good correlations with buoy wind measurements for the Gulf of Mexico. Although the results for COAMPS were not as

good as QuikSCAT, it is apparent that the forecasting capability of COAMPS is very good. The correlations were not different for analysis and prediction data. One observation made during the evaluation was that COAMPS tends to overestimate for low wind speeds and underestimates for high wind speeds for both analysis and prediction.

The most important analysis is the reliability of QuikSCAT measurements during extreme weather conditions. The Gulf of Mexico is one of the most hurricane prone regions in the North Atlantic with severe hurricanes and tropical storms occurring every year. The latest calamities caused by Hurricanes Katrina and Rita are only too fresh in our minds and supportive of the fact. It is of significant importance to ascertain the accuracy of QuikSCAT at such vulnerable times. The hurricanes under consideration occurred during the period 2002 – 2006. The regression analysis of QuikSCAT measurement specifically during the days that the hurricanes were in the Gulf of Mexico was performed against buoy measurements. For this purpose, the L2B DIRTH winds were considered. COAMPS measurements were present for the years 2005 and 2006, hence, this dataset was also considered for those hurricane seasons. The correlations are very good between QuikSCAT and the buoys. This indicates that the performance of QuikSCAT is at par with that of buoys during extreme weather. This may not be a good sign as the buoys themselves are quite limited in their measurement accuracies in such turbulence. The best track analyses by the National Hurricane Center demonstrate this point. The maximum intensities recorded by QuikSCAT are almost half the maximum sustained winds recorded in the best track analyses. This is because QuikSCAT tends to underestimate wind speeds during such harsh weather due to the presence of rain. Rain alters the backscatter drastically and attenuates the signal by making the atmosphere almost opaque to the QuikSCAT frequency of operation. Overall, QuikSCAT

measurements are unreliable above 20 m/s. The problem lies with the design limitations of the geophysical model function. However, QuikSCAT is still a very important tool for forecasting purposes, used by NHC themselves. This is due to QuikSCAT's capability to detect a closed circulation up to 45 hours in advance of the NHC analyses. By plotting the vector winds, the initial stages of formation of a storm can be easily distinguished. The NHC on the other hand requires much more stringent conditions to be present before declaring it to be of potential danger. During this study, it was seen the results for Hurricane Ivan were very different from those for all the others. Hurricane Ivan had caused very high seas so as to cause severe damage to many structures including buoys leading to many erroneous measurements.

Jason -1 sea surface height anomaly overlaid with QuikSCAT vector winds were compared with MODIS Aqua and GOES-12 sea surface temperature measurements to understand the relationship between these parameters and how they can affect each other. Many drawbacks were observed in this study. The SSH measurements were very coarse and had a very low temporal resolution of 10 days. The problem faced with QuikSCAT winds was that many times a complete coverage of the data was not available due to which there was loss of crucial information about the progression or intensity variations of the storm. MODIS SST images were highly affected by cloud coverage leading to loss of data during the passage of the storm through the GOM. For many of the hurricanes, the wind fields reflected an increase in intensity over about 24 hours as the hurricanes traversed the GOM. Air-sea fluxes cause significant variations in upper ocean thermodynamics leading to changes in hurricane intensities. The initial warming of the GOM has a noticeable effect on the intensity increase of the hurricanes. The cold wake of denser water is seen after the hurricane pass. The SSH contours in the GOES-12 SST

maps provided a considerable amount of information regarding the position and extent of the Loop Current and warm core rings. From the SSHA measurements before the passage of the hurricane, the SSH-W measurements after the passage of the hurricane and the SST measurements, it can be concluded that the increase in intensity of the hurricane occurred after its passage over the LC and the WCR. Thus, from these results, QuikSCAT is observed to be capable of depicting such variations with satisfactory results.

QuikSCAT has also been observed to be capable of depicting estimates of the wind radii about the eye of the hurricane (Kossin et al., 2007). Although, it can only be used in the outer wall environment where precipitation is low, it is an important tool for the estimation of wind fields in the hurricane. In this study, longitudinal and latitudinal transects across the eyes of the Hurricane Ivan and Katrina displayed the regions of enhanced wind speeds. Albeit the wind measurements are diminished from their actual values (NHC best tract analysis), the region covered by the hurricane can be observed and a reasonable estimate on the region of enhanced winds can be made.

Future scope for this project would be to perform in depth analysis of wind stress and its variations with SST. The curl and divergence of the wind stress should be compared with the downwind and crosswind components of SST fronts. Another aspect that can be considered is to perform principal component analysis (PCA) of wind stress and SST to get more accurate correlation results. Estimation of critical wind radii using cloud-top and brightness temperatures in the hurricane environment should be made and compared with conventional methods for such measurements. QuikSCAT would benefit greatly if a better GMF is designed to not only increase the accuracy of retrievals at low and high wind speeds but also to increase the resolution. With the complexity of

nearshore winds, many small scale features go unnoticed due to the coarseness of the swath. Improvement of measurement during rain can significantly impact the reliability and accuracy of QuikSCAT during hurricanes which would be of immense help for forecasting and emergency preparedness.

References

Adams, Ian S., Jones, W. Linwood, Vasudevan, Santhosh, and Soisuvarn, Seubson, 2005: Hurricane Wind Retrievals Using the SeaWinds Scatterometer on QuikSCAT, *OCEANS, 2005. Proceedings of MTS/IEEE*, Vol. 3, pp 2148-2150.

Atlas, R., Bloom, S.C., Ho_man, R.N., Brin, E., Ardizzone, J., Terry, J., Bungato, D. and Jusem, J.C., 1999: Geophysical Validation of NSCAT Winds Using Atmosheric Data and Analyses, Journal of Geophysical Research, 104(C5), pp 11405-11424.

Bao, J.-W., Wilczak, J.M., Choi, J.-K. and Kantha, L.H., 2000: Numerical Simulations of Air-Sea Interaction Under High Wind Conditions Using a Coupled Model: A Study of Hurricane Development, *Monthly Weather Review*, Vol. 128, pp 2190-2210.

Beckley, B.D., Zelensky, N.P., Luthcke, S.B. and Callahan, P.S., 2004: Towards a Seamless Transition from TOPEX/Poseidon to Jason-1, *Marine Geodesy*, Vol. 27, pp 373-389.

Bhatt, Vihang, Kumar, Raj, Basu, Sujit and Agarwal, Vijay K., 2005: Assimilation of Altimeter Significant Wave Height into a Third-Generation Global Spectral Wave Model, *IEEE Transactions on Geoscience and Remote Sensing*, Vol. 43, No. 1, pp 110-116.

Brennan, Michael J. and Knabb, Richard D.: Operational Evaluation of QuikSCAT Ocean Surface Vector Winds in Tropical Cyclones at the Tropical Prediction Center/National Hurricane Center, 10.5.

Buyers, H.R., 1974: General Meteorology, *McGraw-Hill*, New York, pp 314.

Callahan, Philip S., 2006: QuikSCAT Science Data Product User's Manual, Overview and Geophysical Data Products, V3.0, *D-18053-RevA, JPL*, ftp://podaac.jpl.nasa.gov/pub/ocean_wind/quikscat/doc/QSUG_v3.pdf.

Chambers, D.P., Ries, J.C. and Urban, T.J., 2003: Calibration and Verification of Jason-1 Using Global Along-Track Residuals with TOPEX, *Marine Geodesy*, Vol. 26, pp 305-317.

Chao, Yi, Li, Zhijin, Kindle, John C., Paduan, Jeffery D., and Chavez, Fancisco P., 2003: A High-Resolution Surface Vector Wind Product for Coastal Oceans: Blending Satellite Scatterometer Measurements with Regional Mesoscale Atmospheric Model Simulations, *Geophysical Research Letters*, Vol. 30, No. 1, pp 13.1-13.4.

Chelton, Dudley B., Esbensen, Steven K., Schlax, Michael G., Thum, Nicolai and Freilich, Michael H., 2001: Observations of Coupling Between Surface Wind Stress and Sea Surface Temperature in the Eastern Tropical Pacific, *Journal of Climate*, Vol. 14, pp 1479-1497.

Chelton, Dudley B., Schlax, Michael G., Freilich, Michael H., Milliff, Ralph F., 2004: Satellite Measurements Reveal Persistent Small-Scale Features in Ocean Winds, *Science*, Vol. 303, pp 978-982.

Chelton, Dudley B., Freilich, Michael H., Sienkiewicz, Joseph M., and Von Ahn, Joan M., 2006: On the Use of QuikSCAT Scatterometer Measurements of Surface Winds for Marine Weather Prediction, *Monthly Weather Review*, Vol. 134, pp 2055-2070.

Cione, Joseph J. and Uhlhorn, Eric W., 2003: Sea Surface Temperature Variability in Hurricanes: Implications with Respect to Intensity Change, *Monthly Weather Review*, Vol. 131, pp 1784-1796.

Cummins, Patrick F. and Lagerloef, Gary S.E., 2004: Wind-Driven Interannual Variability Over the Northeast Pacific Ocean, *Deep-Sea Research*, I 51, pp 2105-2112.

Desai, Shailen D. and Haines, Bruce J., 2003: Near-Real-Time GPS-Based Orbit Determination and Sea Surface Height Observations from the Jason-1 Mission, *Marine Geodesy*, Vol. 26, pp 383-397.

Desai, Shailen D. and Vincent, Patrick, 2003: Statistical Evaluation of the Jason-1 Operational Sensor Data Record, *Marine Geodesy*, Vol. 26, pp 187-199.

Desai, Shailen D. and Haines, Bruce J., 2004: Monitoring Measurements from the Jason-1 Microwave Radiometer and Independent Validation with GPS, *Marine Geodesy*, Vol. 27, pp 221-240.

Dunbar, R. Scott and Perry, Kelly L., 2001: SeaWinds on QuikSCAT Level 3 Daily, Gridded Ocean Wind Vectors, *JPL SeaWinds Project*, Version 1.1, ftp://podaac.jpl.nasa.gov/pub/ocean_wind/quikscat/L3/doc/qscat_L3.pdf.

Dunbar, R. Scott, Hsiao, Vincent S., Kim, Young-Joon, Pak, Kyung S., Weiss, Barry H. and Zhang, Angela, 2001: SeaWinds Algorithm Specifications, *JPL D-21978*, ftp://podaac.jpl.nasa.gov/ocean_wind/quikscat/doc/SWS_Algorithm_SpecsL1.pdf.

Dunbar, R. Scott, 2006: Level 2B Data Software Interface Specification (SIS-2), SeaWinds Processing and Analysis Center, JPL, ftp://podaac.jpl.nasa.gov/pub/ocean_wind/quikscat/L2B/doc/L2B_SIS_200609.pdf.

Ebuchi, Naoto, Graber, Hans C., and Caruso, Michael J., 2002: Evaluation of Wind Vectors Observed by QuikSCAT/SeaWinds Using Ocean Buoy Data, *Journal of Atmospheric and Oceanic Technology*, Vol. 19, pp 2049-2061.

Elsner, James B., Tsonis, Anastasios A., and Jagger, Thomas H., 2006: High Frequency Variability in Hurricane Power Dissipation and its Relationship to Global Temperature, Bulletin of American Meteorological Society, Vol. 87, 6, pp 763-768.

Emanuel, Kerry A., 2005a: Increasing Destructiveness of Tropical Cyclones over the Past 30 years, *Nature*, Vol. 436, pp 686-688.

Emanuel, Kerry A., 2005b: Divine Wind: The History and Science of Hurricanes, *Oxford University Press. Inc.*, New York, NY, pp 285.

Fairell, C., Bradley, E.F., Rogers, D.P., Edson, J.B. and Young, G.S., 1994: The Toga Coare Bulk Flux Algorithm (Draft).

Feng, Hui, Vandemark, Doug, Quilfen, Yves, Chapron, Bertrand and Beckley, Brian, 2006: Assessment of Wind-Forcing Impact on a Global Wind-Wave Model Using the Topex Altimeter, *Ocean Engineering*, Vol. 33, pp 1431-1461.

Freilich, Michael H. and Vanhoff, Barry A., 2006: The Accuracy of Preliminary WindSat Vector Wind Measurements: Comparisons with NDBC Buoys and QuikSCAT, *IEEE Transactions on Geoscience and Remote Sensing*, Vol. 44, No. 3, pp 622-636.

Freilich, Michail H.: SeaWinds Algorithm Theoretical Basis Document, NASA, ftp://podaac.jpl.nasa.gov/pub/ocean_wind/quikscat/doc/atbd-sws-01.pdf.

Hennon, Christopher C., Long, David G., and Wentz, Frank J., 2006: Validation of QuikSCAT Wind Retrievals in Tropical Cyclone Environments, JP1.1, *Joint Poster Session 1, Marine Meteorological Applications of Real and Synthetic Aperture Radar* (Joint between the 14th Conference on Interaction of the Sea and Atmosphere and 14th Conference on Satellite Meteorology and Oceanography).

Hoffman, Ross N. and Leidner, S. Mark, 2005: An Introduction to the Near-Real-Time QuikSCAT Data, *Weather and Forecasting*, Vol. 20, pp 476-492.

Hsu, S.A, Martin, M.F. Jr., Blanchard, B.W., 2000: An Evaluation of the USACE's Deep Water Wave Prediction Techniques Under Hurricane Conditions During Georges in 1998, *Journal of Coastal Research*, Vol. 16, No. 3, pp 823-829.

Hsu, S.A. and Babin, Adele, 2005: Estimation of Radius of Maximum Winds via Satellite During Hurricane Lili (2002) Over the Gulf of Mexico, *NWA Electronic Journal of Operational Meteorology*, 2005-EJ3.

JPL, 2001: Catch the Wind: The QuikSCAT Story, California Institute of Technology, EV-2001-05-003-JPL, http://winds.jpl.nasa.gov/education/Video_Resource_Guide.pdf.

Katsaros, Kristina B. and Forde, Evan B., 2001: QuikSCAT's SeaWinds facilitates Early Identification of Tropical Depressions in 1999 Hurricane Season, *Geophysical Research Letters*, Vol. 28, No. 6, pp 1043-1046.

Kochanski, Adam and Koracin, Darko, 2005: Analysis of Wind Stress Algorithms and Computation of the Wind Stress Curl in Bodega Bay, California, *Sixth Conference on Coastal Atmospheric and Oceanic Prediction and Processes* (Poster Presentation).

Kossin, James P., 2002: Daily Hurricane Variability Inferred from GOES Infrared Imagery, *Monthly Weather Review*, Vol. 130, pp 2260-2270.

Kossin, J.P., Knapp, K.R., Vimont, D.J., Murnane, R.J., and Harper, B.A., 2007: A Globally Consistent Reanalysis of Hurricane Variability and Trends, *Geophysical Research Letters*, Vol. 34, L04815, pp 1-6.

Kossin, James P., Knaff, John A., Berger, Howard I., Herndon, Derrick C., 2007: Estimating Hurricane Wind Structure in the Absence of Aircraft Reconnaissance, *Weather and Forecasting*, Vol. 22, pp 89-100.

Kozai Katsutoshi, 2003: Satellite-Derived Sea Surface Height and Sea Surface Wind Data Fusion for Spilled Oil Tracking, *Adv. Space Res.*, Vol. 32, No. 11, pp 2287-2293.

Large, W.G. and Pond, S., 1981: Open Ocean Momentum Flux Measurements in Moderate to Strong Winds, *Journal of Physical Oceanography*, Vol. 11, pp 324-336.

Leben, Robert R., Born, G.H. and Engebreth, B.R., 2002: Operational Altimeter Data Processing for Mesoscale Monitoring, *Marine Geodesy*, Vol. 25, pp 3-18.

Leben, Robert R. and Powell, Brian S., 2003: Accuracy Assessment of Jason-1 and TOPEX/POSEIDON Along-Track Sea Surface Slope, *Marine Geodesy*, Vol. 26, pp 355-366.

Legler, David M., 1983: Empirical Orthogonal Function Analysis of Wind Vectors Over the Tropical Pacific Region, *Bulletin of the American Meteorological Society*, Vol. 64, No. 3, pp 234-241.

Lentz, Steven J. and Largier, John, 2006: The Influence of Wind Forcing on the Chesapeake Bay Buoyant Coastal Current, *Journal of Physical Oceanography*, Vol. 36, pp 1305-1315.

Long, David G., Luke, Jeremy B., and Plant, William, 2003: Ultra High Resolution Wind Retrieval for SeaWinds, *Geoscience and Remote Sensing Symposium, 2003, IGARSS '03. Proceedings, 2003 IEEE International*, Vol. 2, pp 1264-1266.

Luis, Alvarinho J., Isoguchi, Osamu and Kawamura, H., 2006: Characteristic Patterns of QuikSCAT-based Wind Stress and Turbulent Heat Flux in the Tropical Indian Ocean, *Remote Sensing of Environment*, 103, pp 398-407.

Monaldo, Frank M., Thompson, Donald R., Pichel, William G. and Colon, Pablo C-., 2004: A Systematic Comparison of QuikSCAT and SAR Ocean Surface Wind Speeds, *IEEE Transactions of Geoscience and Remote Sensing*, Vol. 42, No. 2, pp 283-290.

Morey, Steven L., Bourassa, Mark A., Dukhovskoy, Dmitry S. and O'Brien, James J., 2006: Modeling Studies of the Upper Ocean Response to a Tropical Cyclone, *Ocean Dynamics*, Vol. 56, pp 594-606.

O'Neill, Larry W., Chelton, Dudley B. and Esbensen, Steven K., 2003: Observations of SST-Induced Perturbations of the Wind Stress Field over the Southern Ocean on Seasonal Timescales, *Journal of Climate*, Vol. 16, pp 2340-2353.

Perez, Renellys C., Chelton, Dudley B. and Miller, Robert N., 2005: The Effects of Wind Forcing and Background Mean Currents on the Latitudinal Structure of Equatorial Rossby Waves, *Journal of Physical Oceanography*, Vol. 35, pp 666-681.

Pickett, Mark H., Tang, Wenqing, Rosenfeld, Leslie K., and Wash, Carlyle H., 2003: QuikSCAT Satellite Comparisons with Nearshore Buoy Wind Data off the U.S. West Coast, *Journal of Atmospheric and Oceanic Technology*, Vol. 20, pp 1869-1878.

Portabella, Marcos and Stoffelen, Ad, 2002: Characterization of Residual Information for SeaWinds Quality Control, *IEEE Transactions of Geoscience and Remote Sensing*, Vol. 40, No. 12, pp 2747-2758.

Ritchie, E.A., Simpson, J., Liu, W.T., Halverson, J., Veldon, C., Brueske, K.F. and Pierce, H., 2003: Hurricanes! Coping with Disaster, R. Simpson, ed. *American Geophysical Union*, Washington, D.C., 10.1029.055SP02.

Samelson, R.M., Skyllingstad, E.D., Chelton, D.B., Esbensen, S.K., O'Neill, L.W. and Thum, N., 2006: On the Coupling of Wind Stress and Sea Surface Temperature, *Journal of Climate*, Vol. 19, pp 1557-1565.

Shay, L.K., Goni, G.J. and Black, P.G., 2000: Effects of a Warm Oceanic Feature on Hurricane Opal, *Monthly Weather Review*, Vol. 128, pp 1366-1383.

Sienkiewicz, Joseph M., Von Ahn, Joan M.: The Application of QuikSCAT Winds in the NOAA Ocean Prediction Center.

Spencer, Michael W., Wu, Chialin, and Long, David G., 2000: Improved Resolution Backscatter Measurements with the SeaWinds Pencil-Beam Scatterometer, *IEEE Transactions on Geoscience and Remote Sensing*, Vol. 38, No. 1, pp 89-103.

Stiles, Bryan W. (JPL), 1999: Special Wind Vector Data Product: Direction Interval Retrieval with Threshold Nudging (DIRTH), Product Description, Version 1.1.

Stone, G.W., Walker, N.D., Hsu, S.A., Babin, A., Liu, B., Keim, B.D., Teague, W., Mitchell, D., and Leben, R., 2005: Hurricane Ivan's Impact Along The Northern Gulf of Mexico, *EOS*, Vol. 86, No. 48, pp 497-508.

Strong, B., Brumley, B., Stone, Gregory W. and Zhang, Xiongping, 2003: The Application of the Doppler Shifted Dispersion Relationship to Hurricane Wave Data from an ADCP Directional Wave Gauge and Co-Located Pressure Sensor, *Proceedings of IEEE 7th Working Conference on Current Measurement Technology*, San Diego, CA.

Tang, Wenqing, Liu, W. Timothy and Stiles, Bryan W., 2004: Evaluation of High-Resolution Ocean Surface Vector Winds Measured by QuikSCAT Scatterometer in Coastal Regions, *IEEE Transactions on Geoscience and Remote Sensing*, Vol. 42, No. 8, pp 1762-1769.

Tolman, Hendrik L., Alves, Jose-Henrique G.M. and Chao, Yung Y., 2005: Operational Forecasting of Wind-Generated Waves by Hurricane Isabel at NCEP, *Weather and Forecasting*, Vol. 20, pp 544-557.

Touboul, J., Giovanangeli, J.P., Kharif, C. and Pelinovsky, E., 2006: Freak Waves Under the Action of Wind: Experiments and Simulations, *European Journal of Mechanics B/Fluids*, 25, pp 662-676.

Walker, Nan D., Myint, S., Babin, Adele and Haag, Alaric, 2003: Advances in Satellite Radiometry for the Surveillance of Surface Temperatures, Ocean Eddies and Upwelling Processes in the Gulf of Mexico using GOES-8 Measurements During Summer, *Geophysical Research Letters*, Vol. 30, No. 16, 1854, doi:10.1029/2003GL017555.

Walker, Nan D., Leben, Robert R. and Balasubramanian, S., 2005: Hurricane-Forced Upwelling and Chlorophyll a Enhancement Within Cold-Core Cyclones in the Gulf of Mexico, *Geophysical Research Letters*, Vol. 22, L18610, doi:10.1029/2005GL023716.

Walker, Nan D., Leben, Robert R., Hsu, S.A., Haag, Alaric S., Balasubramanian, S., Blanchard, B. and Weeks, E., 2006a: Potential Role of Real-Time Satellite Infrared Radiometry and Altimetry in Hurricane Intensity Prediction, *AGU Ocean Sciences Meeting*, Honolulu Hawaii, February 2006 (Poster presentation).

Walker, Nan D., Haag, Alaric, Balasubramanian, S., Leben, Robert R., Van Heerden, Ivor, Kemp, Paul and Mashriqui, Hassan, 2006b: Hurricane Prediction: A Century of Advances, *Oceanography*, Vol. 19, No. 2, pp 24-36.

Wang, Ping, Kirby, James H., Haber, Joseph D., Horwitz, Mark H., Knorr, Paul O., and Krock, Jennifer R., 2006: Morphological and Sedimentological Impacts of Hurricane Ivan and Immediate Poststorm Beach Recovery Along the Northwestern Florida Barrier-Island Coasts, *Journal of Coastal Research*, Vol. 22, No. 6, pp 1382-1402.

Xie, Shang-Ping, Ishiwatari, Masaki, Hashizume, Hiroshi and Takeuchi, Kensuke, 1998: Coupled Ocean-Atmospheric Waves on the Equatorial Front, *Geophysical Research Letters*, Vol. 25, No. 20, pp 3863-3866.

Xie, Lian, Bao, Shaowu, Pietrafesa, Leonard J., Foley, Kristen and Fuentes, Montserrat, 2006: A Real-Time Hurricane Surface Wind Forecasting Model: Formulation and Verification, *Monthly Weather Review*, Vol. 134, pp 1355-1370.

Yueh, Simon H., Stiles, Bryan W., and Liu, W. Timothy, 2003: QuikSCAT Wind Retrievals for Tropical Cyclones, *IEEE Transactions on Geoscience and Remote Sensing*, Vol. 41, No. 11, pp 2616-2627.

Zingone, Eddie, 2004: Buoy Wind Performance in Hurricane Ivan and How Findings Relate to Buoy Verification in the Anchorage Area of Responsibility, Alaska Region Headquarters, National Weather Service, http://pafc.arh.noaa.gov/papers/IvanBuoyReport.pdf.

Appendix: Acronyms

Acronyms	Full Forms
COAMPS	Coupled Ocean/Atmospheric Mesoscale Prediction System
DIRTH	Direction Interval Retrieval and Threshold Nudging
DIR	Direction Interval Retrieval
ESL	Earth Scan Laboratory
GMF	Geophysical Model Function
GOM	Gulf of Mexico
HDF	Hierarchical Data Format
IDL	Interface Description Language
JPL	Jet Propulsion Laboratory
L2B	Level 2B
L3	Level 3
LC	Loop Current
MABL	Marine Atmospheric Boundary Layer
MLE	Maximum Likelihood Estimator
MMD	Marine Meteorology Division
MM5	Mesoscale Model 5
MODIS	Moderate Resolution Imaging Spectroradiometer
NCEP	National Centers of Environmental Prediction
NDBC	National Data Buoy Center
NHC	National Hurricane Center
NOGAPS	Navy Operational Global Atmospheric Prediction System
NRL	Naval Research Laboratory
NWP	Numerical Weather Product
OPC	Ocean Prediction Center
PO.DAAC	Physical Oceanography Distributed Active Archive Center
QuikSCAT/QS	Quick Scatterometer
RMSE	Root Mean Square Error
SAS	Statistical Analysis System
SSH(A)	Sea Surface Height (Anomaly)
SSM/I	Special Sensor Microwave/Imager

Acronyms	Full Forms
SST	Sea Surface Temperature
TOPEX/POSEIDON	Ocean Topography Experiment/Poseidon
TN	Threshold Nudging
WCR	Warm Core Ring
WVC	Wind Vector Cell

Vita

Neha Sharma was born in Dhanbad, India. She is the daughter of Mr. V. K. Sharma and Mrs. Sudha Sharma and the sister of Mr. Ritesh Sharma. Neha graduated as Bachelor in Engineering from Maharashtra Institute of Technology Women Engineering College, Pune University, India in 2005. The same year she started graduate studies with Dr. Eurico J. D'Sa in the Department of Oceanography and Coastal Sciences at Louisiana State University. Her master's research was the evaluation of performance of NASA's QuikSCAT and COAMPS regional model wind products, conducting a long-term and event-based evaluation concentrating on hurricane conditions and subsequent comparison with other physical parameters of the ocean, namely SSH and SST. Her career interests lie in meteorology, weather forecasting, remote sensing, air-sea interaction and physical oceanography.